การจำลองพฤติกรรมไม่เชิงเส้นในระบบถังกวนแบบต่อเนื่อง
ที่มีเครื่องแยกและนำกลับมาใช้ใหม่ สำหรับการผลิต
พอลีเอทิลีนความหนาแน่นต่ำ

นายนิคม กลมเกลี้ยง

MODELING OF NON-LINEAR BEHAVIOR IN A

CSTR-SEPARATOR-RECYCLE SYSTEM

PRODUCING LDPE

Nikom Klomkliang

A Thesis Submitted in Partial Fulfillment of the Requirements for the

Degree of Master of Engineering in Chemical Engineering

Suranaree University of Technology

Academic Year 2007

MODELING OF NON-LINEAR BEHAVIOR IN A

CSTR-SEPARATOR-RECYCLE SYSTEM

PRODUCING LDPE

Suranaree University of Technology has approved this thesis submitted in partial fulfillment of the requirements for a Master's Degree.

Thesis Examining Committee

_____

(Assoc. Prof. Dr. Chaiyot Tangsathitkulchai)

Chairperson

_____

(Dr. Terasut Sookkumnerd)

Member (Thesis Advisor)

_____

(Dr. Panarat Tomanee)

Member

_____   _____

(Prof. Dr. Pairote Sattayatham)   (Assoc. Prof. Dr. Vorapot Khompis)

Vice Rector for Academic Affairs   Dean of Institute of engineering

นิคม กลมเกลี้ยง : การจำลองพฤติกรรมไม่เชิงเส้นในระบบถังกวนแบบต่อเนื่องที่มีเครื่อง
แยกและการนำกลับมาใช้ใหม่ สำหรับการผลิตพอลีเอทิลีนความหนาแน่นต่ำ
(MODELING OF NON-LINEAR BEHAVIOR IN A CSTR-SEPARATOR-RECYCLE
SYSTEM PRODUCING LDPE) อาจารย์ที่ปรึกษา : อ. ดร.ธีระสุต สุขกำเนิด, 129 หน้า

วิทยานิพนธ์นี้ได้สร้างแบบจำลองทางคณิตศาสตร์ของกระบวนการผลิตพอลีเอทิลีนความ
หนาแน่นต่ำที่ความดันสูงในระบบปฏิกิริยาพอลิเมอไรเซชันของถังกวนแบบต่อเนื่องที่มีการแยก
และนำกลับมาใช้ใหม่ มีวัตถุประสงค์เพื่อวิเคราะห์พฤติกรรมความไม่เป็นเชิงเส้น เมื่อรวมปฏิกิริยา
การย่อยสลายของเอทิลีนและอะเซทิลีนเข้าในแบบจำลอง แบบจำลองทางคณิตศาสตร์ทั้งหมดได้ถูก
พัฒนาขึ้นในระดับโรงงานอุตสาหกรรม ผลกระทบของตัวแปรการปฏิบัติการต่าง ๆ เช่น อุณหภูมิ
ขาเข้าระบบ เวลาในการเกิดปฏิกิริยา และความเข้มข้นขาเข้าระบบของตัวก่อเกิดปฏิกิริยา (initiator)
ที่มีผลต่ออุณหภูมิของถังปฏิกรณ์พอลิเมอไรเซชัน การเปลี่ยนแปลงมวลสารทั้งหมด และความ
เสถียรภาพได้มีการวิเคราะห์ด้วยเช่นกัน แบบจำลองทางคณิตศาสตร์ทั้งหมดประกอบด้วย สมการ
อนุพันธ์และสมการพีชคณิต แบบจำลอง ณ สภาวะคงที่นั้นได้ถูกแก้โดยวิธีเชิงตัวเลขด้วยวิธีของ
นิวตัน ในขณะที่แบบจำลองที่สภาวะไม่คงที่ได้ถูกใช้ในการวิเคราะห์เสถียรภาพเปรียบเทียบกับค่า
เจาะจง (eigenvalue) ของระบบ จากผลเฉลยที่สภาวะคงที่ และการวิเคราะห์ค่าเจาะจง นำไปสร้าง
แผนผังตัวแปร

เมื่อพิจารณาผลกระทบของปฏิกิริยาการย่อยของเอทิลีนและอะเซทิลีน พบว่า มีความสำคัญ
ในการรวมปฏิกิริยาการย่อยสลายในแบบจำลอง โดยเฉพาะผลกระทบของปฏิกิริยาการย่อยสลาย
ของอะเซทิลีนนั้น ทำให้เกิดความไม่เสถียรที่สภาวะที่ต้องการ นั่นคือ สภาวะคงที่ที่ส่วนกลางที่มี
เสถียรภาพหายไปโดยสิ้นเชิง แม้กระทั่งที่อัตราการนำมวลกลับมาใช้ใหม่ต่ำ ๆ (20%) เนื่องจากมี
อะเซทิลีนที่ขาเข้าของถังปฏิกรณ์เคมี ยิ่งไปกว่านั้น การแยกอะเซทิลีนประสิทธิภาพสูง (100%) ทำ
ให้เกิดเสถียรภาพของสภาวะคงที่ที่ส่วนกลางได้ โดยพิจารณาจากแผนผังตัวแปร (bifurcation)
อย่างไรก็ตาม การแยกอะเซทิลีนที่ประสิทธิภาพต่ำกว่าเล็กน้อย (95%) ก็ทำให้สภาวะคงที่ที่ส่วน
กลางที่มีความเสถียรหายไปได้

ในระหว่างการผลิตพอลีเอทิลีนนั้น มีความจำเป็นในการเปลี่ยนเงื่อนไขการปฏิบัติการของ
ถังปฏิกรณ์เคมี เพื่อผลิตพอลิเมอร์ที่มีคุณสมบัติแตกต่างกันโดยที่อุณหภูมิของถังปฏิกรณ์เคมีมีผล
ต่อคุณสมบัติของพอลิเมอร์ทั้งทางด้านโครงสร้าง และทางกายภาพ เมื่ออัตราการนำมวลกลับมาใช้
ใหม่เพิ่มขึ้น ทำให้ช่วงของอุณหภูมิถังปฏิกรณ์เคมีที่มีความเสถียรมีช่วงกว้างขึ้นบนช่วงของตัวแปร
การปฏิบัติการที่กว้างขึ้นด้วย ดังนั้น ถ้าปฏิบัติการที่อัตราการนำมวลกลับมาใช้ใหม่ที่สูง ๆ สามารถ

ผลิตพอลีเมอร์ที่มีคุณสมบัติแตกต่างกันได้หลากหลายขึ้นด้วย และสามารถยอมรับการเปลี่ยนแปลงมวลสารทั้งหมดที่เกิดขึ้นได้ อย่างไรก็ตาม ที่อัตราการนำมวลกลับมาใช้ใหม่ที่สูงกว่านั้น ปริมาณของอะเซทิลีนสามารถผลิตได้มากกว่า ซึ่งนำไปสู่การหายไปของสภาวะคงที่ส่วนกลางที่มีความเสถียร และได้รับการเปลี่ยนแปลงมวลสารที่ค่าต่ำกว่าแทน แต่กระนั้น ปัญหาข้างต้นจะไม่เกิด ถ้าเครื่องแยกสามารถแยกอะเซทิลีนออกจากสายการนำกลับมาใช้ใหม่ได้ทั้งหมด ทั้งนี้ การวิเคราะห์เสถียรภาพและแผนผังตัวแปรเชิงตัวเลข (nurmerical bifurcation) ได้ถูกใช้เพื่อคาดเดาช่วงของการปฏิบัติการที่มีความเสถียร อนึ่ง แบบจำลองนี้มีประโยชน์สำหรับการออกแบบถังปฏิกรณ์เคมีที่เหมาะสม การเลือกเงื่อนไขการปฏิบัติการที่ดีที่สุด และการควบคุมระบบเพื่อได้รับการผลิตพอลีเมอร์ในปริมาณมากที่สุดด้วย

สาขาวิชา <u>วิศวกรรมเคมี</u>   ลายมือชื่อนักศึกษา_____

ปีการศึกษา 2550   ลายมือชื่ออาจารย์ที่ปรึกษา_____

NIKOM KLOMKLIANG : MODELING OF NON-LINEAR BEHAVIOR IN

A CSTR-SEPARATOR-RECYCLE SYSTEM PRODUCING LDPE. THESIS

ADVISOR : TERASUT SOOKKUMNERD, Ph.D. 129 PP.

LOW-DENSITY POLYETHYLENE (LDPE)/RECYCLE/DECOMPOSITION/

BIFURCATION

The simulation of low-density polyethylene (LDPE) in high pressure CSTR-separator-recycle polymerization systems was investigated in this thesis. In order to analyze the non-linear behavior when ethylene and acetylene decomposition kinetics were included in the model, a comprehensive mathematical model of an industrial LDPE plant was developed. The effect of bifurcation parameters such as feed temperature, residence time, and inlet initiator concentration on reactor temperature and its stability and overall conversion were also investigated. The overall mathematical model comprises both differential and algebraic equations. The steady-state model was solved numerically with Newton methods while the unstable steady-state was identified from the evaluation of eigenvalues and validated by the simulation of unsteady-state models. From steady state solution and eigenvalue analysis, the bifurcation diagram was constructed.

When both ethylene and acetylene decomposition was considered, the effect becomes more significant. The acetylene decomposition would unstabilize the reactor and yield the undersirable results because the middle stable steady state disappeared completely even at low recycle ratio (0.20) due to acetylene presence in the inlet of an autoclave reactor. From further investigation, it was found that the high efficiency

(100%) of acetylene separation yields the much improved bifurcation in which middle stable steady states resurfaced. However, the lower efficiency acetylene separation (even at 95%) could not remediate the problems.

During LDPE production, it is often necessary to change the reactor operating conditions to produce a different grade polymer since reactor temperature can significantly affect the polymer molecular structure and subsequently the physical properties. When the recycle ratio is increased, the range of reactor temperature at stable is wider over the longer operating parameters range. Consequently, if ones operate at high recycle ratio, they could produce a variety of different-grade polymers with acceptable overall conversion. However, at the higher recycle ratio, a larger amount of acetylene can be produced and these phenomena could lead to disappearance of middle stable branch and lower overall conversion. Nevertheless, if all of acetylene could be separated from the recycle stream, there would not pose a problem. A numerical bifurcation and stability analysis were performed in order to predict the region of stable operation. The models are useful for the design of optimal reactor, selecting the best operating conditions, and tuning the feedback controls of the LDPE plant in order to obtain the maximum polymer productivity.

School of <u>Chemical Engineering</u>   Student's Signature_____

Academic Year 2007   Advisor's Signature_____

ACKNOWLEDGEMENTS

TABLE OF CONTENTS

Page

TABLE OF CONTENTS (Continued)

Page

TABLE OF CONTENTS (Continued)

Page

TABLE OF CONTENTS (Continued)

Page

LIST OF TABLES

LIST OF FIGURES

Figure   **Page**

LIST OF FIGURES (Continued)

Figure   **Page**

LIST OF FIGURES (Continued)

LIST OF FIGURES (Continued)

LIST OF FIGURES (Continued)

LIST OF FIGURES (Continued)

Figure   **Page**

LIST OF FIGURES (Continued)

Figure   **Page**

LIST OF FIGURES (Continued)

Figure   **Page**

LIST OF FIGURES (Continued)

Figure   **Page**

SYMBOLS AND ABBREVIATIONS

C_p = Total specific heat, $\text{cal·g}^{-1}\text{·K}^{-1}$

E_a = Activation energy of the generalized Arrhenius equation, cal·mol^{-1}

f = Initiator decomposition efficiency

g = acetylene decomposition efficiency

$[I]$ = Initiator concentration, mol·L^{-1}

k_{d_I} = Initiator I decomposition rate constant, s^{-1}

k_p = Propagation rate constant, $\text{L·mol}^{-1}\text{·s}^{-1}$

k_{tc} = Termination by combination rate constant, $\text{L·mol}^{-1}\text{·s}^{-1}$

k_{tt} = Total termination rate constant, $\text{L·mol}^{-1}\text{·s}^{-1}$

k_{tx} = Termination by inhibition rate constant, $\text{L·mol}^{-1}\text{·s}^{-1}$

$[M]$ = Monomer concentration, mol·L^{-1}

MW_M = Molecular weight of monomer, g·mol^{-1}

P = Reactor pressure, atm

$[P]$ = Polymer concentration, mol·L^{-1}

Q_{out} = Outlet volumetric flow rate, $\text{cm}^{-3}\text{·s}^{-1}$

$[R]$ = Free radical concentration, mol·L^{-1}

R_i = Species i kinetic rate change, $\text{L·mol}^{-1}\text{·s}^{-1}$

$R_{W_{D_i}}^{k}$ = Kinetic rate of change of decomposition product i, $\text{L·mol}^{-1}\text{·s}^{-1}$

T = Temperature, K

SYMBOLS AND ABBREVIATIONS (Continued)

V	=	Volume of reaction mixture, cm^3
V_a	=	Activation volume of the generalized Arrhenius equation, $cal \cdot atm^{-1} \cdot mol^{-1}$
W_i	=	Weight fraction of species i in the reaction mixture
ΔH_{decomp}	=	Heat of ethylene decomposition, $cal \cdot mol^{-1}$
ΔH_{polym}	=	Heat of polymerization, $cal \cdot mol^{-1}$
ρ_i	=	Species j density, $g \cdot cm^{-3}$
d	=	Decomposition
D_i	=	Decomposition product i
I	=	Initiator
M	=	Monomer
P	=	Polymerization
X	=	Inhibitor species

CHAPTER I

INTRODUCTION

1.1 Significance of the Problem

In the beginning of the commercial production of low-density polyethylene (LDPE), polymerization reaction was initiated only by using free radical initiators resulting to partially crystalline polymers. The degree of the crystalline structure was determined by measuring product's density. The polymerization process was carried out at high pressure and high temperatures. At high temperatures one has to deal with side reactions, which lead to a branched polymer, and thus the densities were lower than the expected values of a completely amorphous and crystalline polyethylene (Whiteley et al., 1998).

Later developments led to a process involving catalysts. Such a process could be carried out at lower pressure and lower temperatures and hence the densities were higher (high-density polyethylene or HDPE). High-density polyethylene has a density ranging from 0.94 to 0.97 kg/m^3. Its molecules have an extremely long carbon backbone with no side groups. As a result, these molecules align into more compact arrangements, accounting for the higher density. High-density polyethylene is stiffer, stronger, and less translucent than low-density polyethylene.

The original process for the LDPE production was based on an autoclave reactor. There, the hot reactants mixed with the cold incoming ethylene and keep the process stable. Later on, the process involving the tubular reactor was developed. This

process produced LDPE with a consistent molecular weight. Nowadays, both production processes are commercially used. Although they are operated at very high pressures, some of these reactors have been in service for many years. Not only LDPE, but LLDPE (Linear LDPE) can also be produced in the high-pressure process.

The physical properties of LDPE produced in autoclave reactors differ significantly from those produced in the tubular reactors. The products from autoclave reactors are suitable for extrusion coating applications. On the other hand, LDPE resins produced from tubular reactors are more suitable for extruded foam applications. Hence, the reactor type has to be chosen, depending on the application (Auger and Nguyen, 2001). If the application allows both types, then one advantage of autoclave reactors is that they have lower investment costs, based on the cost of the reactor system. On the other hand, the variable costs for tubular reactors are slightly lower (Whiteley et al., 1998).

Since LDPE can be produced within a very broad range of different grades and different manufacturing processes, polyethylene has now become one of the major plastic worldwide. Summing up the most important types of polyethylene, in particular low-density, linear low-density and high-density polyethylene, the annual production rate is $\approx 45 \times 10^6$ ton in 1995, as shown in Table 1.1. Such a high production rate also implies that any failures in the production process are very costly. Failure includes both upstream or downstream processing.

Table 1.1 Low-density, linear low-density, and high-density polyethylene production

capacities in $10^3 t$ per year in 1995 (Whiteley et al., 1998)

	N. America	Europe	Japan	Rest	Total
LDPE	3891	7701	1444	4210	17246
LLDPE	4422	1948	1059	3728	11157
HDPE	6198	4881	1024	4715	16891
Total	14511	14530	3527	12653	45221

In both reactors, a free radical mechanism using initiators such as peroxides or oxygen takes place at temperatures ranging from 150 to 300°C and pressures ranging from 1,000 to 3,000 atm. The conversion of ethylene is normally in the ranges of 10 and 30%wt while the mean residence time in reactors varies from 15 to 120 seconds (Gemassmer, 1978; Zhang et al., 1996). Because of low conversion of ethylene, recycling of monomer is a common procedure for LDPE production. Runaway reaction, or uncontrollable increases of temperature and pressure, happens more frequently in autoclave reactors than in tubular ones because of the existence of multiple steady states in autoclave reactors. Polymerization reaction can exhibit highly non-linear behavior, such as multiple steady states, sustained oscillations, and chaos (Ray & Villa, 2000). As a result, an analysis of the non-linear dynamics of polymerization reactors has been one of important research areas. In particular, polymerization reactions are of great interest because of complicated steady-state non-linear bifurcation behavior. This knowledge is important because the non-linear behavior of chemical reactors causes many operational difficulties. Furthermore, the knowledge of this behavior can be used in optimization through elimination of

non-linearities. Although the reaction systems involving material recycles are common in industrial practice, a few results concerning its non-linear behavior are available in literature. Therefore, multiple steady states in CSTR-separator-recycle polymerization systems for production of LDPE are investigated in this research.

In polymerization reactors, both heat effects and autocatalytic kinetics are presented; hence, non-linear phenomena are common. Freitas et al. (1994) considered a generic model of the free radical homopolymerization, which up to five steady states may exist. They concluded that steady state multiplicity should occur for most polymerization systems. Topalis et al. (1996) and Zhang et al. (1996) demonstrated that multiple steady states could occur in a LDPE CSTR polymerization reactor. Furthermore, a coupling between a reactor and a separator through the recycle of reactant-rich stream due to the low conversion of ethylene is the other source of multiplicities. Pushpavanam and Kienle (2001) considered an exothermic first-order reaction in a CSTR-separator-recycle system. Twenty-four different bifurcation diagrams which include a maximum of two steady states, isolated solution branches and limit cycle were presented. Although the units were decoupled energetically via heat exchangers, energy feedback was still present. Kiss et al. (2002) studied a case of complex reactions, including polymerization in isothermal CSTR-separator-recycle systems and a sharp separation between reactants and products was assumed with constant product compositions. It was shown that LDPE polymerization systems can have multiple steady states.

Several authors (Marini and Georgakis, 1984; Chan et al., 1993; Topalis et al., 1996; Zhang et al., 1996) have studied LDPE polymerization reactors and have proposed the reactor model. They reported that the steady state of a continuous

autoclave polyethylene reactor was often open-loop unstable at typical industrial process operating conditions. Therefore, an appropriate control system of polymerization reactor is required for both startup and steady-state operations. One of the well-known phenomena in high-pressure polyethylene reactors is a rapid ethylene decomposition reaction when the reaction heat is not dissipated effectively. In such cases, the reactor temperature rises rapidly (starting at 300 to $320^\circ C$) at which reaction mixture decomposes explosively to lower molecular weight species such as carbon, methane, hydrogen, acetylene, and ethane. It is worthwhile to point out that the decomposition reaction often occurs unexpectedly even after a long period of stable reactor operation with no clearly detectable abnormal symptoms in reactors. When the decomposition reaction takes place, the reactor pressure and temperature build up quickly and reactor must be vented, shut down, and flushed for a long period of time before a new startup is initiated. Quite obviously, the resulting economic loss both from raw material and idle time is significant (Kwag et al., 1994). Because of these difficulties, the simulation technique is usually preferred over the experimental ones. Consequently, ethylene decomposition kinetics, proposed in the literature, would be included in the model studied in this thesis. Acetylene is one of the major products of ethylene decomposition and it was known reported that acetylene could decompose into free-radical and induced runaway reactions (Zhang et al., 1996). Because the recycling consists of unreacted monomer and ethylene decomposition products including acetylene, the recycling should affect the behavior of LDPE polymerization reactors. From these reasons, multiple steady states in CSTR-separator-recycle polymerization systems for production of LDPE in the presence of ethylene and acetylene decomposition are numerically investigated in this research.

1.2 Research Objectives

The overall objective of this research is to study the bifurcation behavior of LDPE in CSTR-separator-recycle polymerization systems at typical industrial process operating conditions. The specific objectives of this research are:

1) To estimate rate constants of ethylene decomposition reactions from kinetics and experimental results available in the literature.

2) To study multiple steady-state of a stand-alone CSTR for production of LDPE in the presence of decomposition in order to compare with the simulation results from Zhang and coworkers (1996) on bifurcation diagrams.

3) To study the effect of both ethylene and acetylene decomposition on the reactor temperature in the presence of recycles.

4) To study bifurcation behavior of LDPE in a CSTR-separator-recycle polymerization system in the presence of ethylene and acetylene decomposition with the effect of bifurcation parameters such as feed temperature and feed initiator concentration.

1.3 Scope and Limitations

The study will be separated into three parts. In the first part, the rate constants of ethylene decomposition as a function of temperature and pressure will be estimated from experimental observations available in the literature (Watanabe et al., 1972; Zhang et al., 1996).

In the second part, the analysis of bifurcation behavior of a LDPE stand-alone CSTR polymerization system as an adiabatic non-isothermal system including

ethylene decomposition kinetics is performed. The dynamic and steady-state simulation, such as the reactor temperature or conversion to polymer are predicted as a function of bifurcation parameters on the steady-state bifurcation diagrams. In this section, the bifurcation parameters are feed temperature and residence time. In addition, bifurcation behavior obtained in this thesis and those reported by Zhang et al. (1996) are compared. The studied reactor volume is constant value of 1,000 L. The pressure is assumed constant at 2,000 atm. The initiator is di-*tert*-butyl peroxide (DTBP).

In the third part, the analysis of bifurcation behavior of a LDPE CSTR-separator-recycle polymerization system as an adiabatic non-isothermal reactor in the presence of ethylene and acetylene decomposition kinetics in the model is performed as ethylene decomposes into carbon, methane, acetylene, and ethane and acetylene decompose into free-radical. The separation unit splits the products stream exiting a reactor into two streams with constant compositions. The recycling stream consists of monomer and decomposition products and the product stream consists only of LDPE. In this part, the dynamic and steady-state simulation, such as the reactor temperature, monomer conversion, conversion to polymer, and polymer selectivity are predicted as a function of bifurcation parameters on the steady-state bifurcation diagrams. The operating parameters used in this part are feed temperature and feed initiator concentration. In addition, the bifurcation behaviors of with and without mass recycle, with and without ethylene and acetylene decomposition are compared.

The steady-state model is solved numerically using Newton method through MATLAB and the stability for steady-state regions are identified with the evaluation

of eigenvalue and the eigenvalue technique was validated by solving the unsteady-state models with MATLAB.

1.4 Outcomes of the Research

It is well recognized that process modeling is useful for the design of optimal reactor operating conditions and reactor controls to obtain maximum polymer productivity and desired polymer properties. In developing a comprehensive process model for high-pressure ethylene polymerization, it is first required to develop a model that gives an accurate prediction of the first level reactor performance, such as temperature, polymer yield, and specific initiator consumption rate. Once these key reactor variables can be predicted by the model, one can further improve the process model to predict important polymer properties; for example, molecular weight, molecular weight distribution, degree of short chain and long chain branching, etc., and optimize the model to design a better LDPE CSTR-separator-recycle system.

CHAPTER II

LITERATURE REVIEW AND THEORY

A great number of papers have been published on the bifurcation behavior arising in a single CSTR and a CSTR-separator-recycle system. Bifurcation behaviors have been first observed in the first-order exothermic reactions and later in the more complex reactions, such as nth-order exothermic, consecutive first-order exothermic, and parallel first-order reactions. Polymerization reactions may be considered as complex series of consecutive and parallel reactions. Therefore, the bifurcation behavior is expected in polymerization reactors, especially in autoclave reactors.

2.1 Multiple Steady States and Bifurcation Analysis of

Polymerization Reactors

Continuous free-radical stirred tank polymerization reactors or CSTRs play an important role in the polymerization process industries. Most commercial free-radical polymerizations are carried out in stirred tank reactors and significant efforts have been concentrated on the development of efficient continuous processes. From this reason, the study on the non-linear behaviour of solution polymerization has been the subject of several investigations over the last two decades, both theoretically and experimentally. Many of the bifurcation behaviours of polymerization reactors have been found, including the existence of steady-state multiplicity, self-sustained and

thoroidal oscillations, and chaotic behaviour (Pinto, 1995). The purpose of this section is to review some of the relevant finding on the bifurcation behaviour of polymerization reactors in the literature.

Hamer et al. (1981) presented the first account of stable limit cycles for the polymerization of methyl methacrylate (MMA). They studied the homopolymerizations of MMA and vinyl acetate (VA), and their copolymerization. Schmidt et al. (1984) extended previous results for a case of non-isothermal reactor operation and confirmed the existence of isolated branches (isola) of steady-state solutions experimentally for MMA and VA polymerizations.

Teymour and Ray (1989) predicted the development of self-sustained oscillations for the VA polymerization and confirmed this behaviour with experiments. Pinto (1995) also showed through simulation that industrial scale reactors may present even more complex dynamic behaviour, including isolated branches of periodic solution and chaos.

Pinto and Ray (1995a) were the first to present a comprehensive mathematical model for copolymerization of MMA and VA in a lab-scale CSTR validated with experimental findings. The bifurcation behaviour of the system was examined using AUTO (Doedel, 1986) and the effect of perturbations in the heat transfer coefficient and the coolant temperature were studied. Experimental evidence for limit cycle behaviour demonstrated that decreasing the percentage of MMA monomer in the feed removed the stable limit cycle. Furthermore, they showed that copolymerization may present oscillatory responses in ranges of operation conditions where the homopolymerizations are stable. Pinto and Ray (1995b) studied the copolymerization of MMA and VA in a lab-scale CSTR. They showed that the system dynamics were

highly sensitive to small changes in the feed concentration, particularly, the initiator feed concentration. In an extremely small area of parameter spaces, two isolas were predicted.

Lee et al. (1999) analyzed the dynamics of LDPE compact autoclave reactors. Bifurcation diagrams were constructed by taking the initiator feed concentration as the bifurcation parameter. They showed that various multiplicity patterns and oscillatory behaviour such as the limit cycle and focus were found. The reactor behaviour even undergoes period doubling and gradually showed rise to a chaotic behaviour in certain ranges of the initiator feed concentration when the coolant temperature becomes low.

The steady-state multiplicity feature of styrene polymerization in a CSTR was studied by Russo and Bequette (1998). In their work, the cooling jacket capacity was included in the reactor model and process operability issues were addressed. More recently, Verazaluce-García et al. (2000) and López-Negrete de la Fuente et al. (2006) analyzed the high impact polystyrene (HIPS) CSTR stability. They showed that industrial HIPS reactors are operated in the vicinity of unstable steady states.

In order to study steady-state multiplicity of continuous free-radical solution and bulk polymerization reactors, Schmidt et al. (1984) studied the MMA polymerization in ethylacetate initiated by benzoyl peroxide and the VA polymerization in ter-butanol initiated by AIBN. The existence of five steady states was determined theoretically for MMA homopolymerization.

Freitas et al. (1994) studied the steady-state multiplicity of continuous free-radical solution and bulk polymerization CSTR. They approached the problem in the more general way. In their work, the reactor was described generically, without

defining a specific reaction system, in order to identify the operation conditions that give birth to the five-steady-state multiplicity.

Kiss et al. (2002) analyzed the multiple steady states behavior of six reaction systems of increasing complexity in isothermal CSTR-separator-recycle systems, from one-reactant, first-order reaction to chain-growth polymerization which corresponding to LDPE polymerization process. They found that one stable steady state was born for simple reaction (one and two reactants) systems. For consecutive-reaction systems, including polymerization, two steady states can be occurred.

Non-linear behavior of a low-density polyethylene tubular reactor-separator-recycle have been done by Häfele et al. (2005). A simplified dynamic version of the detailed model presented is shown similar to in the work of Häfele et al. (2006). As a result, both multiple steady states and oscillatory behavior have been found.

2.2 Kinetic of LDPE Polymerization

At high pressure, the polymerization of ethylene proceeds via a free-radical mechanism. Many reaction steps occur during the polymerization reaction resulting in polymer with a complex structure containing short and long chain branches. The industrial importance of polyethylene polymerization has led to extensive studies of its kinetics (Ehrlich & Mortimer, 1970; Zhang et al., 1997; Fogler H. S., 1999; Costas et al., 2002). In this section, a set of reaction mechanisms required to model the kinetics of free-radical homopolymerization of ethylene is described. The polymerization mechanism includes the following types of elementary reactions:
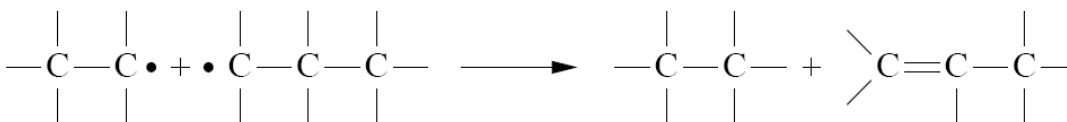
Figure 2.1 Symbolic scheme of a termination by disproportion (2.7)

2.2.1 Main Reactions

The main reactions, which are common to all free radical polymerizations, comprise initiation, propagation and termination. Therefore, free radical donators, such as oxygen or peroxides, in which decomposes into radicals, are used to initiate the polymerization. The next main step is the chain growth or chain propagation reaction. In the presence of radicals, new monomer molecules are added to the reactive end of the radical, forming longer radicals, so-called "living polymer". When the concentration of radicals is high enough, the chain growth reaction terminates resulting in "dead polymer" in the third step. Two different mechanisms lead to the termination, combination and disproportion. A schematic sketch of the termination by disproportion reaction is depicted in Figure 2.1. Since reaction (2.7) results in two dead polymer chains, one end of the one chain is unsaturated, meaning that there are double bonds in a polymer molecule.

The following reaction scheme summarizes the main reactions,

$$I \xrightarrow{k_I} 2R_I \qquad\qquad \text{initiator decomposition,} \qquad\qquad (2.1)$$

$$R_I + M \xrightarrow{k_{p,I}} R_1 \qquad\qquad \text{initiation,} \qquad\qquad (2.2)$$

$$R_X + M \xrightarrow{\ k_{p,X}\ } R_1 \qquad\qquad \text{initiation,} \qquad\qquad (2.3)$$

$$3M \xrightarrow{\ k_{t,h}\ } 2R_1 + M \qquad\qquad \text{thermal initiation,} \qquad\qquad (2.4)$$

$$R_i + M \xrightarrow{\ k_p\ } R_{i+1} \qquad\qquad \text{propagation,} \qquad\qquad (2.5)$$

$$R_i + R_j \xrightarrow{\ k_{t,c}\ } P_{i+j} \qquad\qquad \text{termination by combination and} \qquad (2.6)$$

$$R_i + R_j \xrightarrow{\ k_{t,d}\ } P_i + P_j + DB \qquad \text{termination by disproportion.} \qquad (2.7)$$
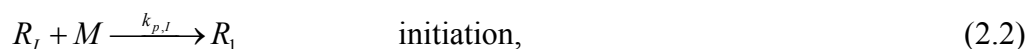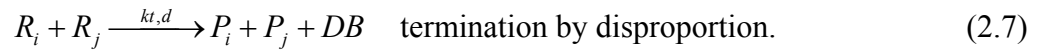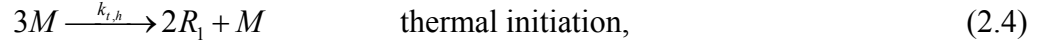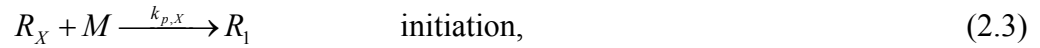
In this notation, R_I denote the corresponding initiator radicals. M is the monomer, ethylene. R_i in general is living polymer and P_i is a dead polymer of chain length i. From a chain growth point of view, there is no distinction between the radicals coming from an initiation by initiators (2.2), by modifier X (2.3) or by thermal initiation (2.4), since the main difference between the generated living polymer chains of chain length one is the terminating molecule. In order to account for the formation of double bonds by the termination reaction (2.7), the additional "species" DB is introduced. This species represents the concentration of molecules containing double bonds.

2.2.2 Side Reactions

In addition to the main reaction steps (2.1)-(2.7), which occur in all free radical polymerization processes, several side reactions are also present. These reactions lead to long-chain branching or short-chain branching and to an additional formation of double bonds. Both, long-chain and short-chain branching are crucial factors, which influence the physical properties of low-density polyethylene. In fact,

Hutchinson and Fuller (1998) reported that long-chain branching and β-scission have an important influence on the molecular weight distribution of the produced polymer. The reaction schemes for those reactions are
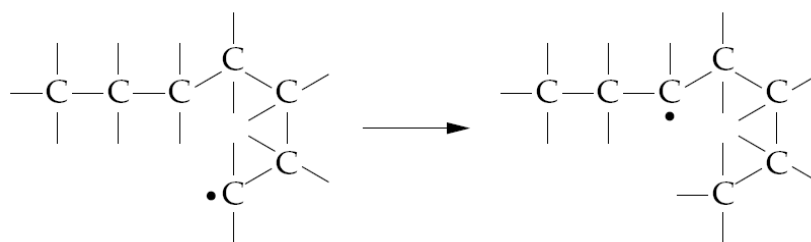
Figure 2.2 Reaction scheme for the back-biting reaction (2.12), that leads to short-chain branches (here with a butyl branch).

$$R_i + M \xrightarrow{k_{tr,M}} P_i + R_1 + DB \quad \text{chain transfer to monomer} \tag{2.8}$$

$$R_i + P_j \xrightarrow{k_{tr,P}} P_i + R_{sec,j} \qquad \text{chain transfer to polymer} \tag{2.9}$$

$$R_i + X \xrightarrow{k_{tr,X}} P_i + R_X \qquad \text{chain transfer to modifier} \tag{2.10}$$

$$R_{sec,i} + M \xrightarrow{k_{p,sec}} R_{i+1} + LCB \quad \text{propagation of sec. radicals} \tag{2.11}$$

$$R_i \xrightarrow{k_{bb}} R_i + SCB \qquad \text{back biting} \tag{2.12}$$

$$R_{sec,i} \xrightarrow{k_{\beta}} P_{i-k} + R_k + DB \qquad \beta\text{-scission} \tag{2.13}$$
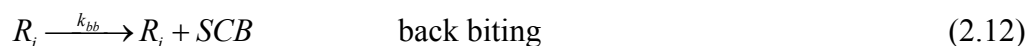
Reactions leading to long- and short-chain branching are (2.11) and (2.12). The back biting reaction is depicted in more detail in Figure 2.2. It is an

intramolecular transfer reaction, where the radical is transferred from the end to an intermediate position within the chain. This intramolecular transfer only happens within the first six to ten carbon atoms; hence, it is the origin of short-chain branches *SCB*. Figure 2.2 shows the formation of a butyl branch, but it is also possible that hexyl or amyl branches are established.

Long-chain branching is a result of the chain transfer reaction to polymer (Busch and van Boxtel, 1998), reaction (2.9)). There dead and living polymer are produced, where the reactive atom is not located at the end of the chain, but at an intermediate position (at least ten carbon atoms away from the end). Such a living
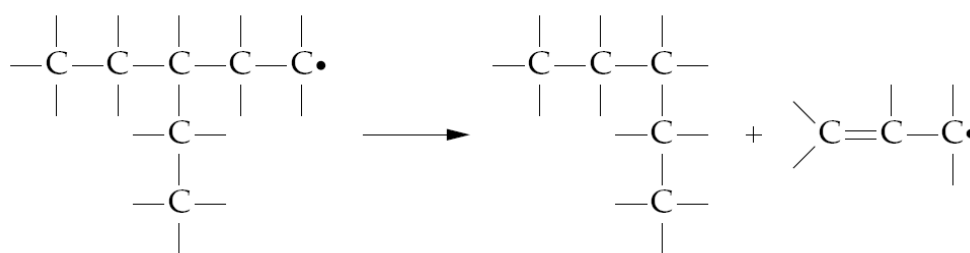
Figure 2.3 Reaction scheme for the *β*-scission (2.13) leading to an unsaturated end.

radical is denoted by the subscript *sec* for secondary living polymer. Secondary living polymer is then consumed by either a propagation reaction (2.5) leading to long-chain branching, or by the *β*-scission reaction (2.13). The propagation step of the secondary radicals is straightforward. New monomer adds to the branched molecule leading to longer branches. Hence, the additional enumerator *LCB* increases. The *β*-scission reaction is more sophisticated and hence depicted in detail in Figure 2.3. In the *β*-scission reaction, a carbon-carbon bond is split up, forming two shorter polymer chains. One dead polymer chain of length *i-k* and a primary living polymer chain of

chain length *k* with an unsaturated end. Such breakage might occur at any point *k* within the chain of the secondary living radical $R_{sec,i}$.

In addition to the main termination reactions and *β*-scission, dead polymer is produced by the chain transfer reactions (2.8)-(2.10). The difference between step growth in (2.5) and the transfer reaction in (2.8) is that in the later case a dead polymer with unsaturated end is produced. However, the probability that the first reaction takes place is much higher.

2.3 Kinetic of Ethylene Decomposition

The complexity of the chemistry of ethylene polymerization is further intensified by the existence of ethylene decomposition, which is a side reaction, especially at high temperature. In other word, it is necessary to include the decomposition reaction before evolving any criteria for the safe operation of LDPE reactors (Zhang et al., 1996; Albert et al., 1998). The mechanism includes important mechanisms; for example, initiation, propagation, and termination steps, to produce major decomposition products (C, CH_4, C_2H_2, and C_2H_6) as shown in equations (2.15) to (2.23). These reactions are highly exothermic and autoaccelerating; thereby, resulting in runaway reactions by developing high temperature and high pressure inside LDPE reactors. The decomposition reaction in LDPE reactors typically starts at around 300^oC when the operating pressure is higher than 1,500 atm and leads to explosion when temperatures are higher than 350^oC for autoclave reactors. However, the modeling of LDPE reactors in literature mainly deals with polymerization reaction and completely ignores ethylene decomposition reaction in spite of its importance in

the overall process (Chan et al., 1993; Chen et al., 1976; Marini and Georgakis, 1984; Topalis et al., 1996).

To demonstrate the complexity of the chemical reactions, the cracking of ethylene to carbon and methane are discussed in detail in Watanabe and coworkers' work (Watanabe et al., 1972). A simple overall reaction equation for ethylene cracking is:

$$C_2H_4 \longrightarrow C + CH_4 \qquad\qquad (2.14)$$

If this reaction were the only one occurred, the product at 100% conversion must consist solely of carbon and methane. At lower conversion, carbon, methane, acetylene, and ethane may be present. Practically, the decomposition product gas is consisted of propylene, propane, butanes, butenes, benzene, toluene, and heavier components. The above reaction (Eq. 2.14) is clearly not the elementary reaction.

Ethylene cracking represents the simplest application of the free-radical mechanism. Ethylene is divided into two ethyl radicals in the chain initiation step (Eq. 2.15). In the propagation step, the reversible reaction between ethyl radical and ethylene and hydrogen atom takes place (Eq. 2.16). The ethyl radical then reacts with an ethylene molecule to form ethane and a new ethyl radical (Eq. 2.17), which again decomposes to carbon and an ethyl radical (Eq. 2.19). The hydrogen atom reacts with ethylene molecule to yield a hydrogen gas and a new ethyl radical (Eq. 2.18). In addition, an ethyl radical reacts with an ethylene to give methane and an ethyl radical (Eq. 2.20).

Initiation: $\qquad 2C_2H_4 \xrightarrow{\ k_1\ } C_2H_3\cdot + C_2H_5\cdot \qquad$ (2.15)

Propagation: $\qquad C_2H_5\cdot \xleftrightarrow{\ k_2,k_2'\ } C_2H_4 + H\cdot \qquad$ (2.16)

$\qquad C_2H_5\cdot + C_2H_4 \xrightarrow{\ k_3\ } C_2H_6 + C_2H_3\cdot \qquad$ (2.17)

$\qquad H\cdot + C_2H_4 \xrightarrow{\ k_4\ } H_2 + C_2H_3\cdot \qquad$ (2.18)

$\qquad C_2H_3\cdot \xrightarrow{\ k_5\ } C + CH_3\cdot \qquad$ (2.19)

$\qquad CH_3\cdot + C_2H_4 \xrightarrow{\ k_6\ } CH_4 + C_2H_3\cdot \qquad$ (2.20)
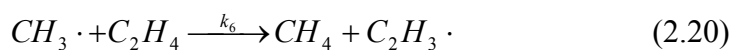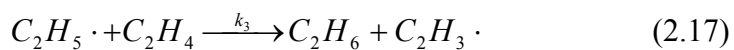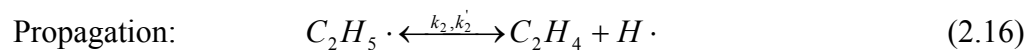
Free radicals formed in reactions (2.16) to (2.20) would be terminated if either a methyl radical or an ethyl radical reacts with the other radical by termination reactions to form a new ethane, methane, and ethylene and acetylene (Eqs. 2.21 to 2.23); for example,

Termination: $\qquad CH_3\cdot + CH_3\cdot \xrightarrow{\ k_7\ } C_2H_6 \qquad$ (2.21)

$\qquad C_2H_3\cdot + CH_3\cdot \xrightarrow{\ k_8\ } C_2H_2 + CH_4 \qquad$ (2.22)

$\qquad C_2H_3\cdot + C_2H_3\cdot \xrightarrow{\ k_9\ } C_2H_2 + C_2H_4 \qquad$ (2.23)
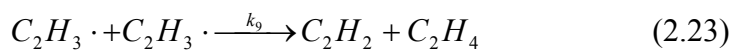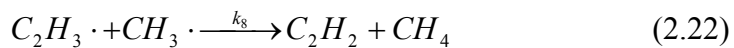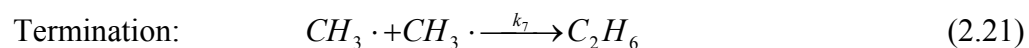
2.4 Decomposition and Polymerization of Ethylene

The relative magnitudes of the polymerization and decomposition rates are dependent on temperatures since ethylene is found to undergo polymerization at typical operating temperatures (below 300°C) but tends to decompose at elevated temperatures (Bonsel and Luft, 1995). Figure 2.4 shows the polymerization and decomposition rates of ethylene as a function of temperature that proposed by Zhang et al. (1996). Polymerization dominates in the low-temperature range and decomposition takes over at higher temperatures. The two reaction rates cross at about 310°C, it is generally accepted that above 300°C there is threat of decomposition (Marini and Georgakis, 1984; Bonsel and Luft, 1995) so the crossover of 310°C is reasonable. Therefore, if the reactor can be kept below a certain critical temperature, the decomposition can, in principle, be avoided. However, it is not easy to maintain a steady reaction temperature due to a fast reaction rate (about 0.1-1 sec at reactor conditions as shown in Figure 2.5), a short residence time, and no external cooling; hence, autoclave reactors are, in effect, adiabatic. Local areas of high temperature or hot spots can also be caused by imperfect mixing and can propagate through the reactor, which would result in global decomposition and runaway reactions (Zhang et al., 1996).
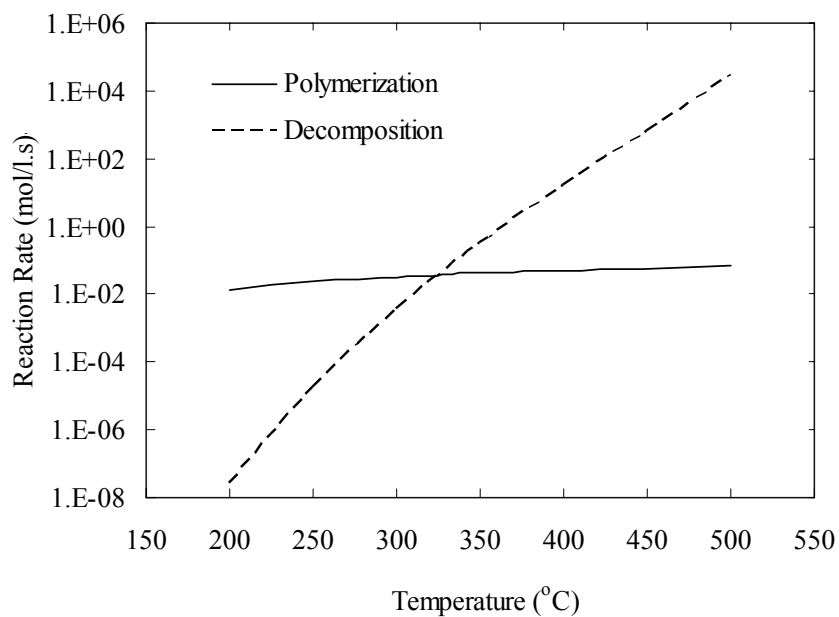
Figure 2.4 Polymerization and decomposition rates (Zhang et al., 1996).
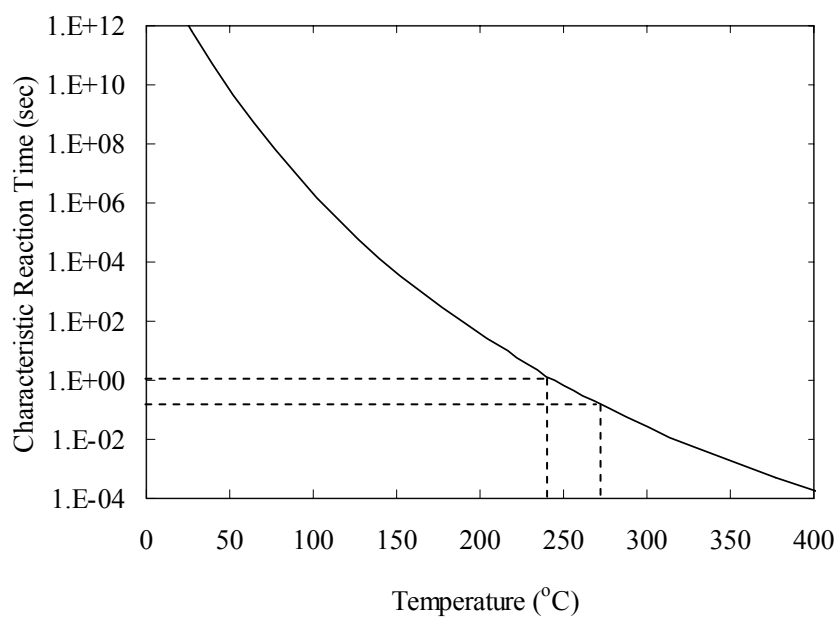
Figure 2.5 Characteristic reaction time for the decomposition of di-*tert*-butyl peroxide

peroxide (DTBP) vs. reactor temperature (Read et al., 1997).

2.5 Multiple Steady States and Bifurcation Analysis of LDPE CSTR

2.5.1 The Effect of Feed Initiator Concentration

Ethylene is the raw material for large scale production of LDPE at high pressure and high temperature. Because of these high pressures, high temperatures and very fast reaction, LDPE autoclave reactors are considered adiabatic and thermal runaway appears frequently. Above certain limits of pressure and temperature, ethylene decomposes into carbon, methane, hydrogen, acetylene, and ethane. Adiabatic autoclave reactors used for the production of LDPE were known to have serious runaway problems because of the onset of ethylene decomposition reactions; the phenomenon studied by Zhang et al. (1996) as shown in Figure 2.6. In Zhang and coworkers' work, the stability and runaway behavior for LDPE polymerization in a CSTR reactor was studied in the presence of ethylene decomposition by including the kinetics of ethylene decomposition in the model. In their model, the standard initiation, propagation, and termination reactions for polymerization were included along with the decomposition of ethylene. A simplified ethylene decomposition kinetic scheme was employed and the corresponding kinetics parameters were determined from experimental data (Watanabe et al., 1972; Bonsel and Luft, 1995). Dynamic simulation of this model was solved simultaneously by the differential-algebraic system solver DASSL for dynamic simulation and by a modified version of the general continuation package AUTO (Doedel, 1986). The simulation results indicated runaway behavior for the following conditions: residence time, feed temperature, excess initiator in feed, feed impurity, feed temperature disturbance, controller failure, and poorly tuned controller. They found that stability analysis ndicated safe operating limits for certain variables at typical conditions. This realistic and comprehensive

model is useful in the process design, control, and optimization of LDPE autoclaves. It was seen that three stable and two unstable branches appeared for the case of including ethylene decomposition in the model while, two stable and one unstable branches occurred in the case of without ethylene decomposition as shown in Figure 2.7. Unfortunately, the kinetic parameters of ethylene decomposition used in modeling were estimated from the inconsistent kinetics.

Zhang et al. (1996) used the ethylene decomposition reactions from the Watanabe et al. (1972) as shown in equations (2.15-2.23). The reaction rates of each component were also derived by Watanabe et al. (1972) and were taken as it was (Zhang et al., 1996). The rates of the individual reaction for species derived by Watanabe and coworkers (Watanabe et al., 1972) are shown in the following equations:

$$-\frac{d[C_2H_4]}{dt} = k_1[C_2H_4]^2 - k_2[C_2H_5\cdot] + k_2'[C_2H_4][H\cdot]$$

$$+ k_3[C_2H_4][H\cdot] + k_4[C_2H_4][H\cdot]$$

$$+ k_6[C_2H_4][CH_3\cdot] - k_9[C_2H_3\cdot]^2 \tag{2.24}$$

$$\frac{d[C_2H_5\cdot]}{dt} = k_1[C_2H_4]^2 - k_2[C_2H_5\cdot] + k_2'[C_2H_4][H\cdot]$$

$$- k_3[C_2H_4][C_2H_5\cdot] = 0 \tag{2.25}$$

$$\frac{d[C_2H_3\cdot]}{dt} = k_1[C_2H_4]^2 + k_3[C_2H_4][C_2H_5\cdot] + k_4[C_2H_4][H\cdot]$$

$$- k_5[C_2H_3\cdot] + k_6[C_2H_4][CH_3\cdot]$$

$$- k_8[C_2H_3\cdot][CH_3\cdot] - k_9[C_2H_3\cdot]^2 = 0 \tag{2.26}$$

$$\frac{d[CH_3\cdot]}{dt} = k_5[C_2H_3\cdot] - k_6[C_2H_4][CH_3\cdot]$$

$$- k_7[CH_3\cdot]^2 - k_8[C_2H_3\cdot][CH_3\cdot] = 0 \tag{2.27}$$

$$\frac{d[H\cdot]}{dt} = k_2[C_2H_5\cdot] - k_2'[C_2H_4][H\cdot] - k_4[C_2H_4][H\cdot] = 0 \tag{2.28}$$

However, the above reaction rates were derived is consistent with the relative rates of reaction. Relative rates of reaction which depends on the stoichiometric coefficients are shown by the following equation:

$$\frac{r_{ij}}{v_{ij}} = \frac{r_{ik}}{v_{ik}} \tag{2.29}$$

where

r_{ij} is reaction rate of species j for reaction i.

r_{ik} is reaction rate of species k for reaction i.

v_{ij} is stoichiometric coeffcients of species j for reaction i.

v_{ik} is stoichiometric coeffcients of species k for reaction i.

For example, the relative rates of the first reaction (Eq. 2.15) are shown by the following equation:

$$\frac{r_{1,C2H4}}{2} = \frac{r_{1,C2H3\cdot}}{1} = \frac{r_{1,C2H5\cdot}}{1} \tag{2.30}$$

The present study also takes ethylene decomposition reactions from the work of Watanabe et al. (1972). However, the new reaction rates of each component are derived by summing the rates of the individual reaction for a species and taken care correlation of relative rates of reaction that can be seen a detail in Chapter III.
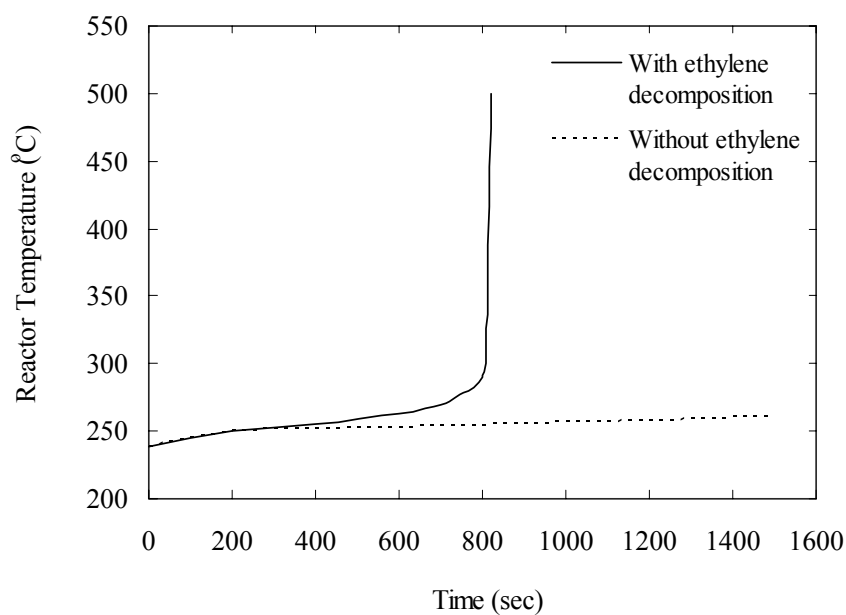
Figure 2.6 Dynamic responses of the LDPE CSTR to a feed disturbance with and without decomposition reaction (Zhang et al., 1996).
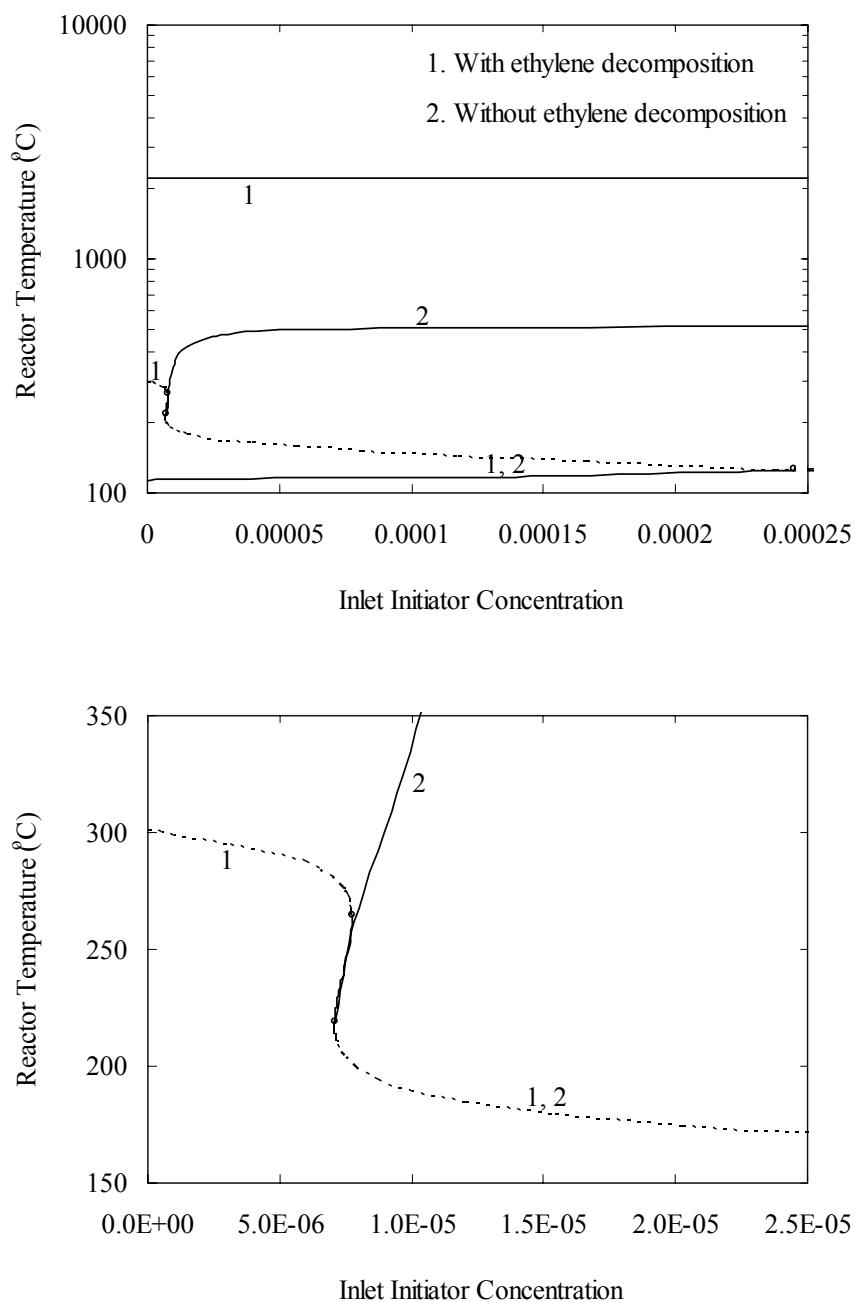
Figure 2.7 The steady-state reactor temperature is shown as a function of initiator

feed concentration with and without ethylene decomposition reactions

in the model (Zhang et al., 1996). Dash line refers to unstable branch

and solid line refers to stable branch.

2.5.2 The Effect of Residence Time

The stability analysis of an LDPE CSTR was presented by Topalis et al. (1996). A comprehensive kinetic mechanism describing the free-radical copolymerization of ethylene was considered. The reaction mechanism included: initiator decomposition, chain initiation and propagation, termination by combination and by disproportionation, chain transfer to monomer, solvent and polymer, intramolecular transfer and β-scission of *sec* and *tert* radicals. They considered only the monomer, initiator, energy and 'live' radical concentration balances for an adiabatic CSTR. In stability analysis of their reactor, an advanced numerical algorithm AUTO (Doedel, 1986) was employed. It can be seen that the reactor can exhibit up to three steady states (e.g. two stable and one unstable) over the range of variation of the residence time as shown in Figure 2.8. However, decomposition of ethylene is neglected in their models.

Due to high reaction rates and limited cooling capacity, the residence time in LDPE autoclaves is usually very short. Since the reactor operates in an adiabatic mode and the only heat removal is through sensible heat, it is important to study the effects of residence time on reactor stability. Zhang and coworkers presented the influence of residence time on steady-state reactor temperature with ethylene decomposition included in their model as shown in Figure 2.9. As description, dash line refers to unstable steady-state branch and solid line refers to stable steady-state branch. The highest steady state branch corresponded to conversion to polymer values below 14% as shown in Figure 2.10.
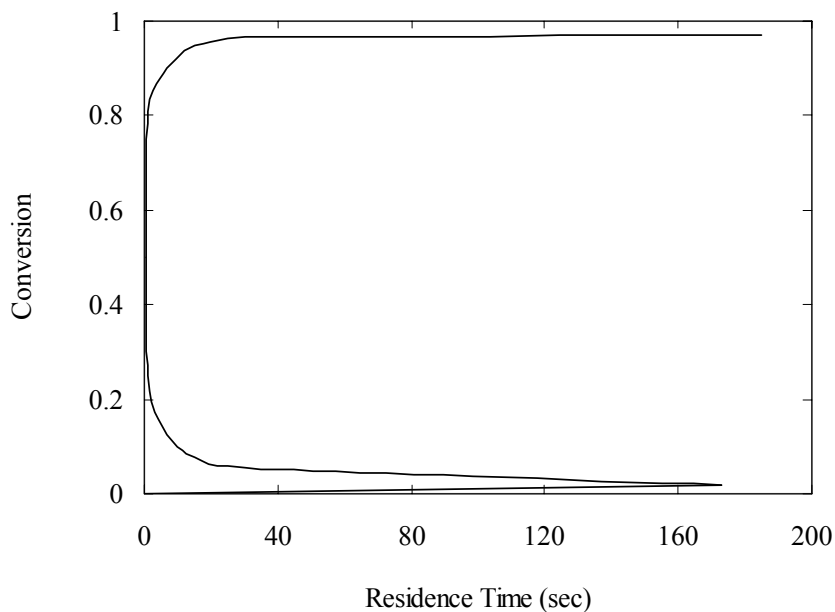
Figure 2.8 Steady-state multiplicity in a LDPE stand-alone CSTR without ethylene

decomposition in the model (Topalis et al., 1996).
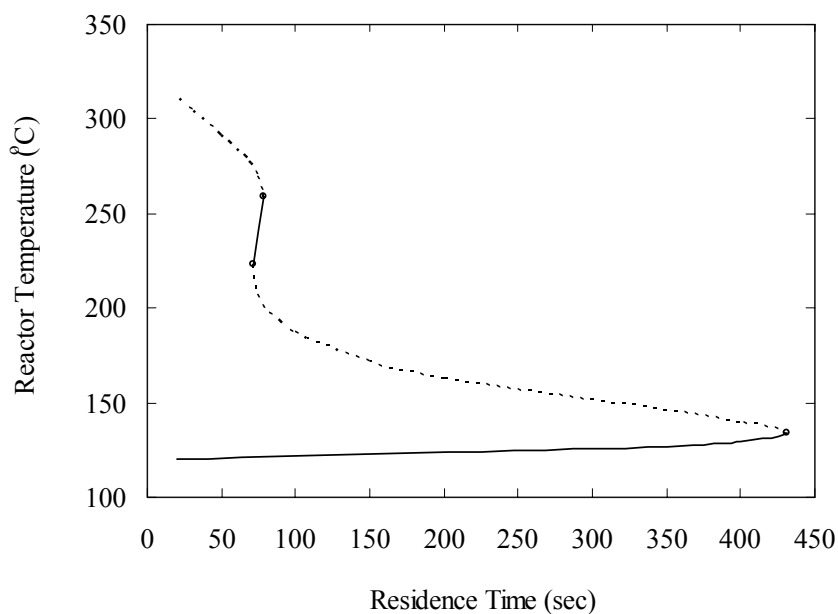
Figure 2.9 The steady-state reactor temperature shown as a function of residence time

with ethylene decomposition reactions included (Zhang et al., 1996).
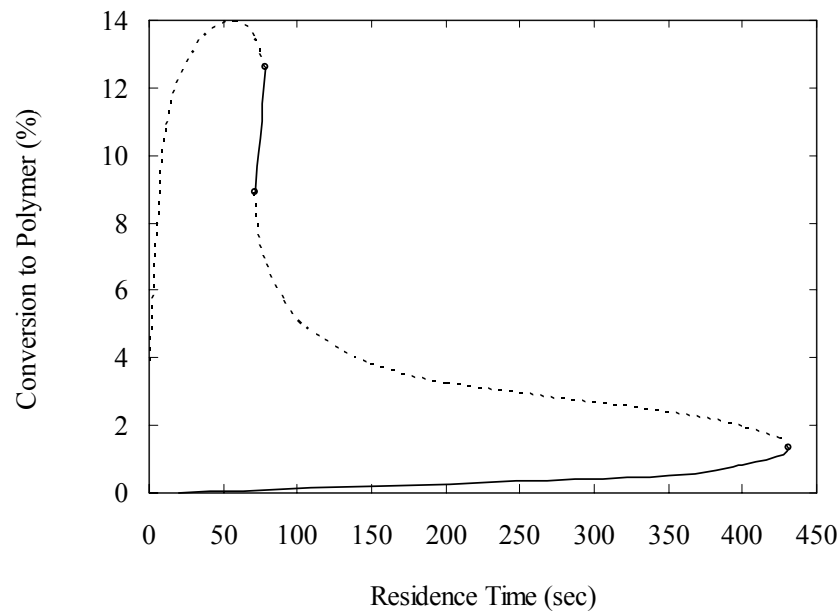
Figure 2.10 Effect of residence time on monomer conversion to polymer for LDPE

CSTR with ethylene decomposition reactions included. Dash line refers

to unstable branch and solid line refers to stable branch

(Zhang et el., 1996).

2.5.3 The Effect of Feed Temperature

Bifurcation behavior of feed temperature on reactor temperature was
similar to the behavior of feed initiator concentration and influence residence time on
reactor temperature and is presented by Zhang et al. (1996) as shown in Figure 2.11**.**
Zhang and coworkers reported that feed temperature is an important parameter in
LDPE autoclave operation since the reactor operates adiabatically. As a result, a small
variation in feed temperature may potentially cause a reactor runaway and their results
is shown in Figure 2.12 to confirm their conclusion
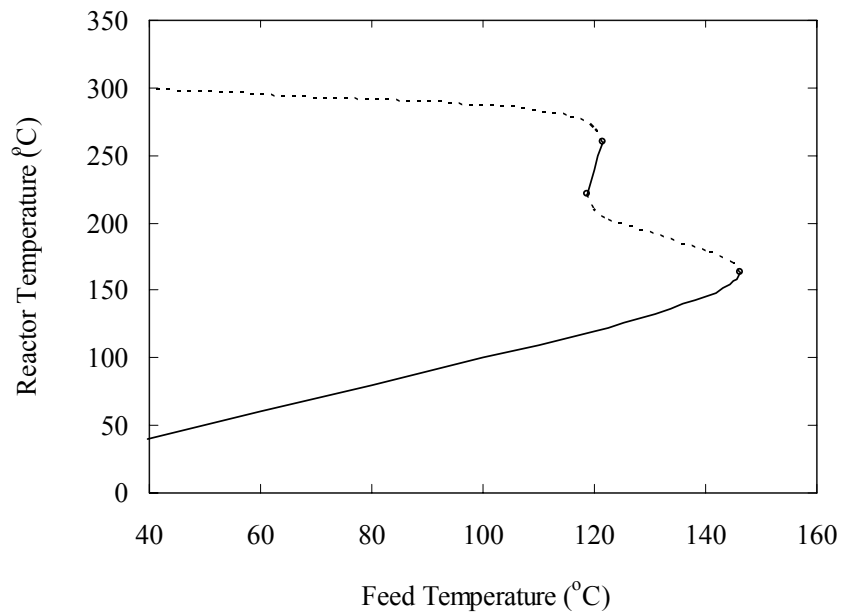
Figure 2.11 Steady-state reactor temperature is shown as a function of inlet temperature with ethylene decomposition reactions included (Zhang et al., 1996).
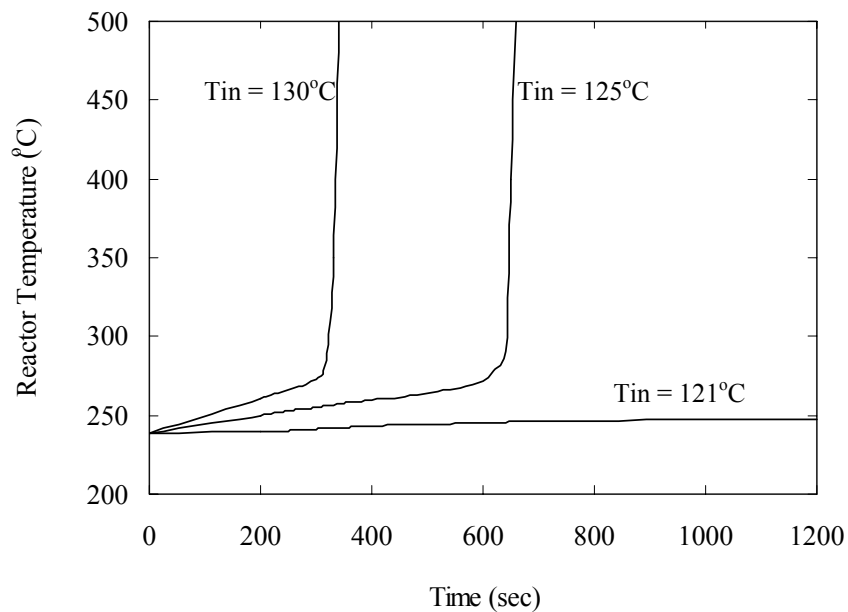
Figure 2.12 The reactor is subjected to different feed temperature disturbance.

2.5.4 The Effect of Feed Impurity

Zhang et al. (1996) presented that small amounts of impurities (e.g., acetylene) can be found in the reactor feed; they can decompose into free radicals and induce runaway reactions. Zhang and coworkers performed the influence of inlet acetylene concentration on the steady-state reactor temperature under both open-loop and closed-loop conditions. Without a controller, very small amounts of acetylene (0.13 ppm) can cause reactor runaway; but with just a simple P controller, steady-state operation can be achieved even at a much higher acetylene concentration (1.5 ppm).

2.6 Multiple Steady States and Bifurcation Analysis of LDPE CSTR-Separator-Recycle

For the CSTR-separator-recycle polymerization system, the stability of steady states had been studied by using a complex reaction mechanism as reported by Kiss et al. (2002). The mechanism considered is the initiation, propagation, termination through dispropertionation, chain transfer to monomer, and chain transfer to solvent. The stoichiometric model and kinetic parameters correspond to the isothermal LDPE process. A sharp separation between reactants and products at a separator was assumed. Two steady states existed in the system. Kiss and coworkers found that one of the steady states had zero conversion. At this steady state, the recycle flow rate was infinite, rendering it infeasible. The system generates the other feasible solution only when the Da or Damkohler number is greater than the critical value ($Da_{cr} = 320$) as shown in Figure 2.13. However, the polymerization reaction was an isothermal system and decomposition of ethylene was not considered. Therefore, further study on

non-isothermal reactors should be performed. As discussed previously, it was difficult to control the temperature of LDPE autoclave reactors because of its highly exothermic and adiabatic operation.
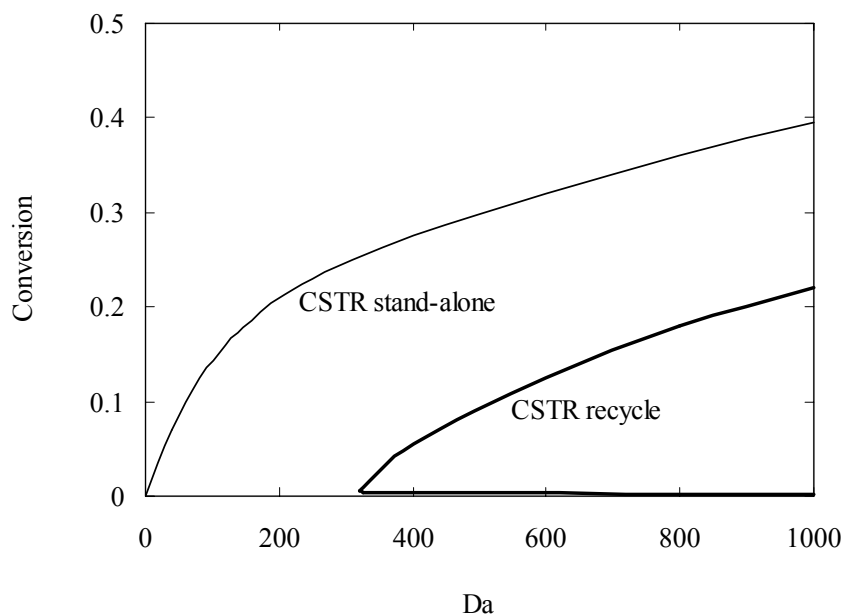
Figure 2.13 Steady-state of conversion is shown as a function of Damkohler number (*Da*) in a LDPE CSTR-separator-recycle polymerization system (Kiss et al., 2002).

2.7 Newton Method for a System of Non-linear Equations

Note that the methods and the corresponding MATLAB routines mentioned so far can handle only one scalar equation with respect to one scalar variable. In order to see how a system of equations can be solved numerically, we rewrite the set of algebraic equations

$$f_1(x_1, x_2, ..., x_n) = 0 \tag{2.31}$$

$$f_2(x_1, x_2, ..., x_n) = 0 \tag{2.32}$$

$$\vdots$$

$$f_n(x_1, x_2, ..., x_n) = 0 \tag{2.33}$$

by taking the Taylor series expansion up to first-order about some estimate point $(x_{1k}, x_{2k}, ..., x_{nk})$ as

$$f_1(x_1, x_2, ..., x_n) \cong f_1(x_{1k}, x_{2k}, ..., x_{nk}) + \frac{\partial f_1}{\partial x_1}\bigg|_{(x_{1k}, x_{2k}, ..., x_{nk})} (x_1 - x_{1k})$$

$$+ \frac{\partial f_1}{\partial x_2}\bigg|_{(x_{1k}, x_{2k}, ..., x_{nk})} (x_2 - x_{2k}) + ...$$

$$+ \frac{\partial f_1}{\partial x_n}\bigg|_{(x_{1k}, x_{2k}, ..., x_{nk})} (x_n - x_{nk}) = 0 \tag{2.34}$$

$$f_2(x_1, x_2, ..., x_n) \cong f_2(x_{1k}, x_{2k}, ..., x_{nk}) + \frac{\partial f_2}{\partial x_1}\bigg|_{(x_{1k}, x_{2k}, ..., x_{nk})} (x_1 - x_{1k})$$

$$+ \frac{\partial f_2}{\partial x_2}\bigg|_{(x_{1k}, x_{2k}, ..., x_{nk})} (x_2 - x_{2k}) + ...$$

$$+ \frac{\partial f_2}{\partial x_n}\bigg|_{(x_{1k}, x_{2k}, ..., x_{nk})} (x_n - x_{nk}) = 0 \tag{2.35}$$

$$\vdots$$

$$f_n(x_1, x_2, ..., x_n) \cong f_n(x_{1k}, x_{2k}, ..., x_{nk}) + \frac{\partial f_n}{\partial x_1}\bigg|_{(x_{1k}, x_{2k}, ..., x_{nk})} (x_1 - x_{1k})$$

$$+ \frac{\partial f_n}{\partial x_2}\bigg|_{(x_{1k}, x_{2k}, ..., x_{nk})} (x_2 - x_{2k}) + ...$$

$$+ \frac{\partial f_n}{\partial x_n}\bigg|_{(x_{1k}, x_{2k}, ..., x_{nk})} (x_n - x_{nk}) = 0 \tag{2.36}$$

This can be arranged into a matrix-vector form as

$$
\begin{bmatrix} f_1(x_1,x_2,...,x_n) \\ f_2(x_1,x_2,...,x_n) \\ \vdots \\ f_n(x_1,x_2,...,x_n) \end{bmatrix} \cong \begin{bmatrix} f_1(x_{1k},x_{2k},...,x_{nk}) \\ f_2(x_{1k},x_{2k},...,x_{nk}) \\ \vdots \\ f_n(x_{1k},x_{2k},...,x_{nk}) \end{bmatrix}
$$

$$
+ \begin{bmatrix} \dfrac{\partial f_1}{\partial x_1} & \dfrac{\partial f_1}{\partial x_2} & \cdots & \dfrac{\partial f_1}{\partial x_n} \\ \dfrac{\partial f_2}{\partial x_1} & \dfrac{\partial f_2}{\partial x_2} & \cdots & \dfrac{\partial f_2}{\partial x_n} \\ \vdots & & & \\ \dfrac{\partial f_n}{\partial x_1} & \dfrac{\partial f_n}{\partial x_2} & \cdots & \dfrac{\partial f_n}{\partial x_n} \end{bmatrix}_{(x_{1k},x_{2k},...,x_{nk})} \begin{bmatrix} x_1 - x_{1k} \\ x_2 - x_{2k} \\ \vdots \\ x_n - x_{nk} \end{bmatrix}
$$

$$
= \begin{bmatrix} 0 \\ 0 \\ \vdots \\ 0 \end{bmatrix}_{n\times 1} \tag{2.37}
$$

which we solve for $(x_1,x_2,..,x_n)$ to get the updated vector estimate

$$
\begin{bmatrix} x_{1,k+1} \\ x_{2,k+1} \\ \vdots \\ x_{n,k+1} \end{bmatrix} = \begin{bmatrix} x_{1k} \\ x_{2k} \\ \vdots \\ x_{nk} \end{bmatrix} - \begin{bmatrix} \dfrac{\partial f_1}{\partial x_1} & \dfrac{\partial f_1}{\partial x_2} & \cdots & \dfrac{\partial f_1}{\partial x_n} \\ \dfrac{\partial f_2}{\partial x_1} & \dfrac{\partial f_2}{\partial x_2} & \cdots & \dfrac{\partial f_2}{\partial x_n} \\ \vdots & & & \\ \dfrac{\partial f_n}{\partial x_1} & \dfrac{\partial f_n}{\partial x_2} & \cdots & \dfrac{\partial f_n}{\partial x_n} \end{bmatrix}_{(x_{1k},x_{2k},...,x_{nk})}^{-1} \begin{bmatrix} f_1(x_{1k},x_{2k},...,x_{nk}) \\ f_2(x_{1k},x_{2k},...,x_{nk}) \\ \vdots \\ fn(x_{1k},x_{2k},...,x_{nk}) \end{bmatrix} \tag{2.38}
$$

$$
X_{k+1} = X_k - J_k^{-1} f(X_k) \text{ with the Jacobian } J_k(m,n) = \begin{bmatrix} \dfrac{\partial f_m}{\partial x_n} \end{bmatrix}_{X_k}
$$

where the first derivative of a vector-valued function $f(X_k)$ with respect to a vector

$X = \begin{bmatrix} x_1 & x_2 & \cdots & x_n \end{bmatrix}^T$ is called the Jacobian of $f(X_k)$.

This is not much different from the Newton iterative formula and is cast into the MATLAB routine "newtons( )" that proposed by Yang et al. (2005) as can be seen in Appendix A.

2.8 Non-linear Analysis

A major difficulty in analyzing the response of non-linear processes is that they cannot be described by linear differential equations. A linear differential equation consists of terms each of which the variable or derivative must be of the first power. Many powerful and extensive linear analysis tools are available to the process engineer. These include tools for assessing performance and designing control systems base on linear systems theory. Consequently, the simple method to analyze the non-linear processes is to linearize them. In this thesis, the model equations of LDPE CSTR-separator-recycle system are non-linear. As a result, this section presents the technique known as *linearization* to approximate the response of non-linear systems with linear equation that can then be analyzed.

Let us consider the set of ODEs given by

$$\frac{dx_1}{dt} = f_1(t, x_1, x_2, x_3, \ldots, x_n) \tag{2.39}$$

$$\frac{dx_2}{dt} = f_2(t, x_1, x_2, x_3, \ldots, x_n) \tag{2.40}$$

$$\vdots$$

$$\frac{dx_n}{dt} = f_n(t, x_1, x_2, x_3, \ldots, x_n) \tag{2.41}$$

Linearization can be performed by expanding the right-hand sides as a multi-variable Taylor series about the steady state points (x_{js}). For Equation (2.39) to (2.41), a linearization yields:

$$\frac{dx_i}{dt} = f_i(x_s) + \sum_{j=1}^{n} \left.\frac{\partial f_i}{\partial x_j}\right|_{x_{js}} (x_j - x_{js}), \qquad i = 1, \ldots, n \tag{2.42}$$

Rearranging Equation (2.42) in a compact form, one obtains

$$\frac{d\bar{x}}{dt} = \sum_{j=1}^{n} \left.\frac{\partial f_i}{\partial x_j}\right|_{x_{js}} (\bar{x}_i), \qquad i = 1, \ldots, n \tag{2.43}$$

Rewriting Equation (2.43) in a matrix-vector form, we arrive at

$$\frac{d}{dt}\bar{x} = J\bar{x} \tag{2.44}$$

where J is the system Jacobian (matrix of partial derivatives) evaluated at steady state point x_s.

$$J = \begin{pmatrix} \dfrac{\partial f_1}{\partial x_1} & \dfrac{\partial f_1}{\partial x_2} & \cdots & \dfrac{\partial f_1}{\partial x_n} \\ \vdots & \vdots & \cdots & \vdots \\ \dfrac{\partial f_n}{\partial x_1} & \dfrac{\partial f_n}{\partial x_2} & \cdots & \dfrac{\partial f_n}{\partial x_n} \end{pmatrix}$$

(2.45)

The vector $\bar{x}$ is the state variables:

$$\bar{x} = \left(x_1 - x_{1s}, \ x_2 - x_{2s}, \ ..., \ x_n - x_{ns}\right)^T$$

(2.46)

Assuming that the Jacobian matrix J has distinct eigenvalues $\lambda_i, i = 1, ..., n$ and the eigenvectors are $v_i, i = 1, ..., n,$ the general solutions of the variational equation are in the form

$$x(t) = \sum_{i=1}^{n} c_i e^{\lambda_i t} + g(t)$$

(2.47)

It is the value of $e^{\lambda_i t}$ which characterizes the local response to perturbations about the particular solution $g(t)$.

There are two important cases related to the eigenvalues which illustrate the two major classes of problems to be encountered.

2.8.1 Unstable Case

Here, some λ_i are positive and large, hence the solution curves diverge. This is inherent instability. On the other hand, for stable steady states, the real part of all eigenvalues λ_i of the Jacobian $J(t)$ must be negative.

Some process engineering problems have this type of characteristic. For example, ethylene polymerization at high-pressure autoclave reactors can exhibit thermal runaway which leads to an unstable situation when a critical temperature in the reactor is reached (Zhang et al., 1996). Kiss et al. (2002) studied state multiplicity in CSTR-separator-recycle polymerization systems. They proved the stability of the multiple steady-state solution with dynamic simulation. As a result, the system is initially in the low-conversion state. At dimensionless time (τ) of 1000, the bifurcation parameter as Damkohler number Da is changed by 1% for a limited period of time. Depending on the disturbance direction, the high- or zero-conversion states are reached as it proves that the low-conversion state is unstable and as shown in Figure 2.14. Certain processes which have a control system installed can also exhibit instability due to unsatisfactory controller tuning or design.
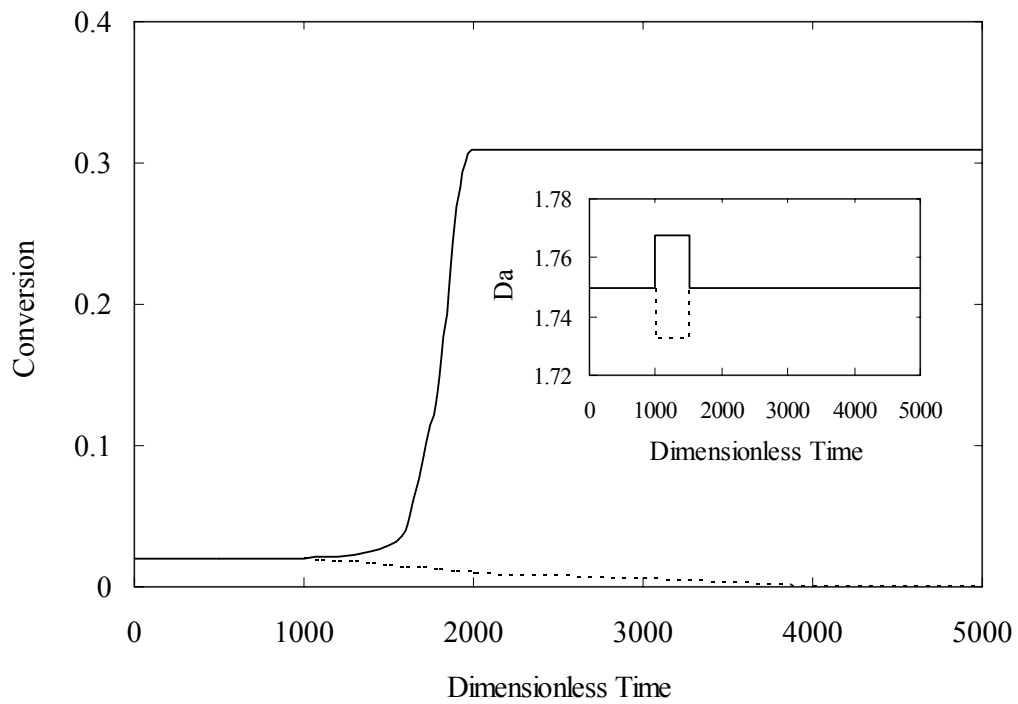
Figure 2.14 Dynamic response of the low-conversion unstable steady-state with

small disturbances (Kiss et al., 2002).

2.8.2 Stable Case

Here the λ_i have negative real parts; hence the solution curves obtained

from Equation (2.47) converge to the initial value before any disturbances take place.

2.9 Runge-Kutta Fehlberg

Manny practical problems in engineering and science require the solution of a system of simultaneous ordinary differential equations. Such systems may be represented generally as shown by equations (2.39) to (2.41). One of many methods that are more accurate predictions is Runge-Kutta Fehlberg.

For the present case, we use the following fourth-order estimate

$$x_{i,j+1} = x_{i,j} + \left(\frac{37}{378} k_{1,i} + \frac{250}{621} k_{3,i} + \frac{125}{594} k_{4,i} + \frac{512}{1771} k_{6,i} \right) h \tag{2.48}$$

along with the fifth-order formula:

$$x_{i,j+1} = x_{i,j} + \left(\frac{2825}{27648} k_{1,i} + \frac{18575}{48384} k_{3,i} + \frac{13525}{55296} k_{4,i} + \frac{277}{14336} k_{5,i} + \frac{1}{4} k_{6,i} \right) h \tag{2.49}$$

where

$$k_{1,i} = f\left(t_j, \ x_{i,j} \right)$$

$$k_{2,i} = f\left(t_j + \frac{1}{5} h, \ x_{i,j} + \frac{1}{5} k_{1,i} h \right)$$

$$k_{3,i} = f\left(t_j + \frac{3}{10} h, \ x_{i,j} + \frac{3}{40} k_{1,i} h + \frac{9}{40} k_{2,i} h \right)$$

$$k_{4,i} = f\left(t_j + \frac{3}{5} h, \ x_{i,j} + \frac{3}{10} k_{1,i} h - \frac{9}{10} k_{2,i} h + \frac{6}{5} k_{3,i} h \right)$$

$$k_{5,i} = f\left(t_j + h,\ x_{i,j} - \frac{11}{54}k_{1,i}h - \frac{5}{2}k_{2,i}h - \frac{70}{27}k_{3,i}h + \frac{35}{27}k_{4,i}h\right)$$

$$k_{6,i} = f\left(t_j + \frac{7}{8}h,\ x_{i,j} + \frac{1631}{55296}k_{1,i}h - \frac{175}{512}k_{2,i}h + \frac{575}{13824}k_{3,i}h\right.$$

$$\left. + \frac{44275}{110592}k_{4,i}h + \frac{253}{4096}k_{5,i}h\right)$$

Thus, the ODEs can be solved with Eq. (2.49) and the error estimated as the difference of the fifth- and fourth-order estimates. As might be expected, the standard MATLAB package has excellent capabilities for solving ODEs. The standard ODE solvers include two functions to implement the adaptive step-size Runge-Kutte Fehlberg method. There is ODE45, which uses fifth- and fourth-order formulas to attain high accuracy. An example as shown in Appendix B illustrates how it can be used to solve a system of ODEs.

CHAPTER III

MODELING AND SIMULATION

In this chapter, the strategy for detailed modeling of the CSTR-separator-recycle LDPE polymerization system in this thesis is presented. This information includes polymerization and ethylene decomposition kinetics, material, and energy balances of a reactor, a mixer, a compressor, a heat exchanger, and a separator. The rate constants of ethylene decomposition are estimated from the experimental data reported in literature (Watanabe et al., 1972). The dynamic and steady-state models are solved with MATLAB in order to study the bifurcation behavior of LDPE in stand-alone CSTR and CSTR-separator-recycle systems.

3.1 Process Description

A generic flow diagram of the LDPE process is shown schematically in Figure 3.1. Briefly, the fresh ethylene feed is mixed with the recycle ethylene stream before entering the primary compressor. This stream is then pressurized to the desired reactor pressure in the second compression stage. Polymerization of the monomer is initiated by addition of free-radical initiators (e.g., organic peroxides). The heat of reaction is usually removed by sensible heat because the thick reactor wall causes the low heat transfer rate. The polymer molecular weight is controlled by adjusting the reactor temperature and pressure and, optionally, by adding a chain-terminating agent. In this process, ethylene is both the reactant and the solvent (here monomer) for the polymer.

Due to the short reactor residence time (10-120 s), the monomer conversion is relatively low, between 10 and 30% by weight. The reactor effluent stream is depressurized across a pressure reduction valve down to 150-250 atm to allow separation of the product from the unreacted ethylene in a high-pressure separator (HPS). The overhead monomer rich stream is cooled and recycled back to the entrance of the secondary compressor whereas the bottom polymer-rich stream undergoes a second separation step at near atmospheric pressures in a low-pressure separator (LPS). The low-pressure gas is recycled to the entrance of the primary compressor from the LPS overhead. Most of the unreacted gas recycles continuously in this process. The byproducts are accumulated until the product qualities are outside the control limits. By that point, the operator will be notified to purge the recycled gas in order to maintain the purity of the reacting gas.
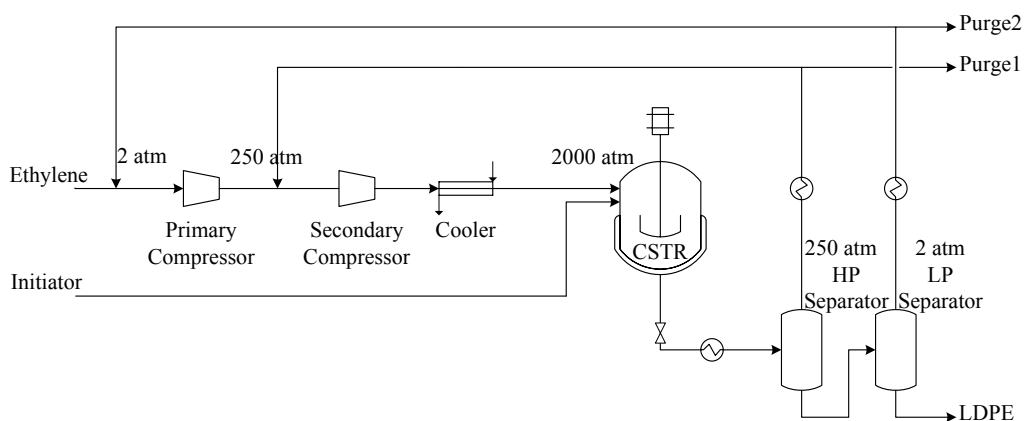
Figure 3.1 Process flow diagram of high-pressure LDPE

3.2 Model Assumptions

The system investigated in this thesis obeys the following assumptions:

(1)   Volume of the mixer, compressor, cooler, and separator are insignificant and are neglected.

(2)   Monomer feed at the primary mixer is 4 kg/s.

(3)   The initiator used is di-*tert*-butyl peroxide (DTBP).

(4)   Reactor volume value of 1,000 L (Zhang et al., 1996).

(5)   Autoclave LDPE polymerization reactor is assumed to be a non-isothermal adiabatic CSTR.

(6)   The LDPE reactor has very thick walls because the reactor is pressurized to around 2,000 atm. Because of this thickness and fast and highly exothermic reaction, the reactor can be reasonably modeled as an adiabatic reactor (Zhang et al., 1996).

(7)   The main sources of heat released are the exothermic propagation reaction and the exothermic ethylene decomposition.

(8)   The quasi-steady-state assumption for each of the radical concentrations is used.

(9)   The effect of delay on the behavior of the coupled CSTR-separator-recycle system is neglected.

(10)   Pressure will be assumed constant (Zhang et al., 1996).

(11)   The gel effect, caused by increasing polymer molecular weight, is neglected.

(12)   A sharp separation between reactants and products are assumed with constant product compositions (Kiss et al., 2002).

(13)   Mass and energy balances for mixer, compressor, cooler, and both

flash are assumed to be quasi-stationary.

3.3 Detailed Model of the CSTR

This study will not only include the standard initiation, propagation, and termination reactions for radical polymerization, but the free radical reactions that describe the decomposition of ethylene ultimately leading to a runaway will also be included. Although it is well known that other mechanisms, such as chain transfer to (monomer, agents, and polymer), β-scission, and back-biting, also contribute significantly to the weight- and number-distribution of polymer, those mechanisms have little effect on the total monomer conversion and stability of LDPE autoclave reactors; thus those mechanisms have not been included (Fox and Tsai, 1996). The multiple steady-state non-linear bifurcation analysis of a CSTR-separator-recycle for production of LDPE is performed. The main bifurcation parameters, inlet initiator concentration and feed temperature are included and their effects are discussed. The dynamic and steady-state simulations are conducted with MATLAB to predict conversion and temperature as a function of bifurcation parameters. Examples with and without decomposition and mass recycle will be compared.

3.3.1 Reaction Mechanism

There have been numerous publications on modeling of LDPE reactors (Chan et al., 1993; Marini and Georgakis, 1984; Topalis et al., 1996). All these authors confine themselves to polymerization and polymer molecular structure with the exception of Zhang et al. (1996). Zhang and coworkers combined polymerization with decomposition reactions on their model. The rate constants of ethylene

decomposition were evaluated based on ethylene decomposition kinetic scheme proposed by Watanabe et al. (1972). However, the rates of decomposition products were erroneous (see Chapter II).

To close this gap, an estimation of the kinetic parameters of ethylene decomposition was conducted in this thesis before the decomposition can be used for simulation.

3.3.1.1 Decomposition of Ethylene

There are many independent parameters to be determined for the full decomposition model and there are few experimental results available in the literature. Therefore, it is not feasible to determine all the rate constants from experimental data.

Because of this reason, a simplified decomposition kinetic scheme with a minimum number of independent kinetic parameters proposed by Watanabe et al. (1972) will be used. The simplified ethylene decomposition kinetic scheme is presented in Table 3.1.

Even with the simplified decomposition kinetic scheme, there are still many rate constants to be determined before the decomposition can be used for simulation.

There are four radicals involved in the simplified ethylene decomposition kinetic scheme, $C_2H_5\cdot$, $C_2H_3\cdot$, $CH_3\cdot$, and $H\cdot$. As in other reaction mechanisms, quasi-steady-state assumption (QSSA) can be applied to all radical.

Table 3.1 Ethylene decomposition mechanism

Reaction step	Chemical reaction
Initiation	$2C_2H_4 \xrightarrow{k_1} C_2H_3\cdot + C_2H_5\cdot$
Propagation	$C_2H_5\cdot \xleftrightarrow{k_2,k_2'} C_2H_4 + H\cdot$ $C_2H_5\cdot + C_2H_4 \xrightarrow{k_3} C_2H_6 + C_2H_3\cdot$ $H\cdot + C_2H_4 \xrightarrow{k_4} H_2 + C_2H_3\cdot$ $C_2H_3\cdot \xrightarrow{k_5} C + CH_3\cdot$ $CH_3\cdot + C_2H_4 \xrightarrow{k_6} CH_4 + C_2H_3\cdot$
Termination	$CH_3\cdot + CH_3\cdot \xrightarrow{k_7} C_2H_6$ $C_2H_3\cdot + CH_3\cdot \xrightarrow{k_8} C_2H_2 + CH_4$ $C_2H_3\cdot + C_2H_3\cdot \xrightarrow{k_9} C_2H_2 + C_2H_4$

Based on the elementary reaction listed in Table 3.1, the following equations are obtained.

$$\frac{d[C_2H_5\cdot]}{dt} = k_1[C_2H_4]^2 - k_2[C_2H_5\cdot] + k_2'[C_2H_4][H\cdot]$$

$$- k_3[C_2H_4][C_2H_5\cdot] = 0 \tag{3.1}$$

$$\frac{d[C_2H_3\cdot]}{dt} = k_1[C_2H_4]^2 + k_3[C_2H_4][C_2H_5\cdot] + k_4[C_2H_4][H\cdot]$$

$$- k_5[C_2H_3\cdot] + k_6[C_2H_4][CH_3\cdot]$$

$$- k_8[C_2H_3\cdot][CH_3\cdot] - 2k_9[C_2H_3\cdot]^2 = 0 \tag{3.2}$$

$$\frac{d[CH_3\cdot]}{dt} = k_5[C_2H_3\cdot] - k_6[C_2H_4][CH_3\cdot]$$

$$- 2k_7[CH_3\cdot]^2 - k_8[C_2H_3\cdot][CH_3\cdot] = 0 \qquad (3.3)$$

$$\frac{d[H\cdot]}{dt} = k_2[C_2H_5\cdot] - k_2'[C_2H_4][H\cdot] - k_4[C_2H_4][H\cdot] = 0 \qquad (3.4)$$

Rearranging equations (3.1) and (3.4), $[C_2H_5\cdot]$ and $[H\cdot]$ can be represented by

$$[C_2H_5\cdot] = \frac{k_1[C_2H_4]^2\left(k_2' + k_4\right)}{k_2k_4 + k_2'k_3[C_2H_4] + k_3k_4[C_2H_4]} \qquad (3.5)$$

$$[H\cdot] = \frac{k_1k_2[C_2H_4]}{k_2k_4 + k_2'k_3[C_2H_4] + k_3k_4[C_2H_4]} \qquad (3.6)$$

By combination of equations (3.2) and (3.3), we arrive at

$$k_1[C_2H_4]^2 - (k_7[CH_3\cdot]^2 + k_8[[C_2H_3\cdot][CH_3\cdot] + k_9[C_2H_3\cdot]^2) = 0 \qquad (3.7)$$

By assuming the rate constants of termination reactions are approximately the same value, k, since carbon and methane are the main products. If $[C_2H_3\cdot]$ is roughly equal to $[CH_3\cdot]$, equation (3.7) then becomes

$$[C_2H_3\cdot] = [CH_3\cdot] = \sqrt{\frac{k_1}{3k}}[C_2H_4] \qquad (3.8)$$

where $k = k_7 = k_8 = k_9$ (Watanabe et al., 1972)

The rate of consumption of ethylene through ethylene decomposition is represented by equation (3.9).

$$-\frac{d[C_2H_4]}{dt} = 2k_1[C_2H_4]^2 - k_2[C_2H_5\cdot] + k_2'[C_2H_4][H\cdot]$$

$$+ k_3[C_2H_4][H\cdot] + k_4[C_2H_4][H\cdot]$$

$$+ k_6[C_2H_4][CH_3\cdot] - k_9[C_2H_3\cdot]^2 \tag{3.9}$$

The substitution of equation (3.5), (3.6), and (3.8) into (3.9) yields

$$-\frac{d[C_2H_4]}{dt} = \left(2k_1 - \frac{k_1}{3} + k_6\sqrt{\frac{k_1}{3k}}\right)[C_2H_4]^2$$

$$+ \frac{k_1k_3[C_2H_4]^3(k_2' + k_4)}{k_2k_4 + k_3[C_2H_4](k_2' + k_4)} \tag{3.10}$$

Because k_2 is smaller than $k_2'[C_2H_4]$ as described above and k_2k_4 is much smaller than $k_3[C_2H_4](k_2' + k_4)$ (Watanabe et al., 1972), equation (3.10) then becomes;

$$-\frac{d[C_2H_4]}{dt} = \left(\frac{8}{3}k_1 + k_6\sqrt{\frac{k_1}{3k}}\right)[C_2H_4]^2 \tag{3.11}$$

The rates of formation of products can, thus, represented by the following equations.

$$\frac{d[C]}{dt} = k_5[C_2H_3\cdot] = \left(k_6\sqrt{\frac{k_1}{3k}}\right)[C_2H_4]^2 \tag{3.12}$$

$$\frac{d[CH_4]}{dt} = k_6[C_2H_4][CH_3\cdot] + k_8[C_2H_3\cdot][CH_3\cdot]$$

$$= \left(\frac{k_1}{3} + k_6\sqrt{\frac{k_1}{k}}\right)[C_2H_4]^2 \tag{3.13}$$

$$\frac{d[C_2H_6]}{dt} = k_3[C_2H_4][C_2H_5\cdot] + k_7[CH_3\cdot]^2 = \left(\frac{4}{3}k_1\right)[C_2H_4]^2 \tag{3.14}$$

$$\frac{d[C_2H_2]}{dt} = k_8[C_2H_3\cdot][CH_3\cdot] + k_9[C_2H_3\cdot]^2 = \left(\frac{2}{3}k_1\right)[C_2H_4]^2 \tag{3.15}$$

Consequently, the generation rate of decomposition products consist of two parts: $k_1[C_2H_4]^2$, corresponding to ethylene decomposition into radicals, and $k_6\sqrt{(k_1/k)}[C_2H_4]^2$, representing the consumption of ethylene through propagation steps. There are two independent rate constants required to be determined, k_1 and $k_6k^{-0.5}$, with this simplified decomposition scheme. These rate constants can be determined from two pieces of information, the crossing temperature of the decomposition reaction rate with the polymerization rate and the decomposition products distribution at a specified temperature. In this thesis, the crossing temperature will be chosen to be 310°C as proposed by Zhang et al. (1996) and is represented here in Figure 3.2. The decomposition product distributions were obtained from the average of the experimental results reported in Watanabe et al. (1972).
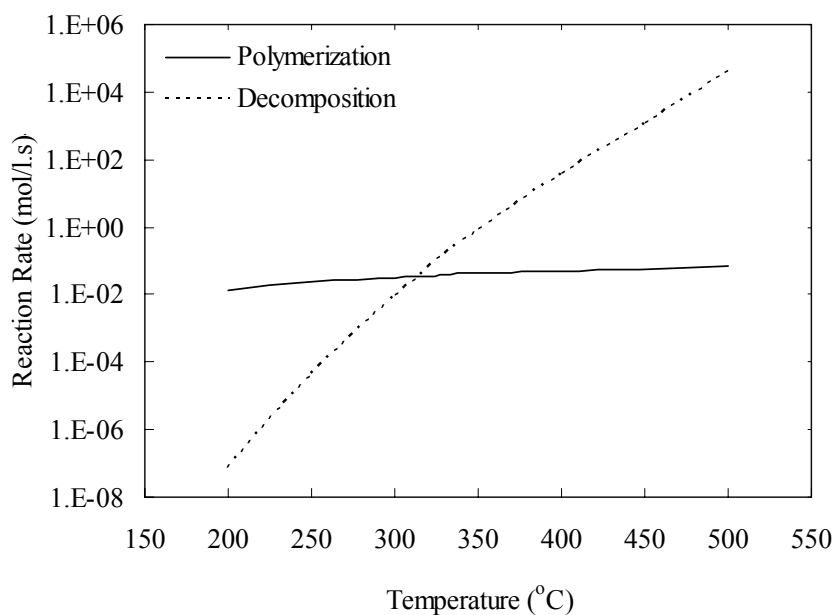
Figure 3.2 Polymerization and decomposition rates of ethylene are shown as

functions of temperature.

3.3.1.2 Polymerization

The kinetic model of LDPE polymerization is a form of free-radical addition polymerization with initiator and impurity break down to produce the radical ($R\cdot$) and the radical reacts with monomer (M) to produce growing polymer for propagation step. Dead polymer chains (P) are created in the termination step. All of these reactions are shown in Table 3.2.

Table 3.2 Simplified kinetics of free-radical polymerization

Reaction step		Chemical reaction
Initiation		$I \xrightarrow{fk_d} 2R\cdot$
		$2C_2H_2 \xrightarrow{gk_a} 2R\cdot$
Propagation		$M + R\cdot \xrightarrow{k_p} R\cdot$
Termination:	**By coupling**	$R\cdot + R\cdot \xrightarrow{k_{tc}} P$
	Spontaneous	$R\cdot + X \xrightarrow{k_{tx}} P$

From Table 3.2, the rate of formation of the free-radical $R\cdot$ formed by initiator and impurity are first considered. Because there will always be scavenging or recombining of the primary radicals, only a certain fraction of initiator (*f*) and of impurities *(g)* is successful in initiating polymer chains. As a result, with the QSSA for all free radicals, the total free-radical concentration is

$$[R\cdot] = \sqrt{\frac{fk_d[I] + gk_a[C_2H_2]^2}{k_t}} \tag{3.16}$$

where $k_t = k_{tc} + k_{td} + k_{tx} + k_{tsp}$

The long-chain approximation (LCA) is then utilized. Briefly, the assumption of LCA is that the rate of propagation is much greater than the rate of initiation. Consequently, the application of LCA yields simplified kinetics of free-radical polymerization

$$-r_M = k_p[M][R\cdot] \tag{3.17}$$

After substitution of $R\cdot$, the rate of disappearance of monomer (Zhang et al., 1996) is

$$-r_M = k_p[M]\sqrt{\frac{fk_d[I] + gk_a[C_2H_2]^2}{k_t}} \tag{3.18}$$

The reaction rate constants in the LDPE model will be calculated from a generalized Arrhenius form shown in equation (3.19)

$$k = k_0 \exp\left[-\frac{E_a}{RT} - \frac{V_a P}{RT}\right] \tag{3.19}$$

where k_0 is the preexponential factor, E_a is the activation energy, R is the gas constant, T is the absolute temperature, P is the absolute pressure, and V_a is the activation volume. The activation volume term is used to account for the effect of pressure on reaction rate for reactions occurring at high pressures.

The initiator being used in the plant and considered in the present study is di-*tert*-butyl peroxide (DTBP). The kinetic parameters for polymerization reaction are taken from Zhang et al. (1996) with little adjustments and are summarized in Table 3.3. The initiator decomposition efficiency f is 0.9 and 0.1 for the impurity (acetylene).

Table 3.3 Kinetic parameters (Zhang et al., 1996)

Rate constant	k_0 *(s^{-1}), **(L/gmol·s)	E_a (cal/gmol)	V_a (cal/atm·gmol)	Reference
k_{dDTBP}	*1.81x10^{16}	38,400	0.0605	Chen et al., 1976
k_{dC2H2}	*2.944x10^{10}	16,828	0.0	Gray et al., 1965
k_p	**1.14x10^{7}	7,091	-0.477	Chen et al., 1976
k_{tc}	**3.00x10^{9}	2,400	0.3147	Chen et al., 1976
ΔH_{poly}	-24,000 (cal/gmol)			Chen et al., 1976
ΔH_{decomp}	-30,200 (cal/gmol)			Huffman et al., 1974

3.3.2 Model Equations

The model is written in a general way such that different reaction media, outflow types, and thermal conditions can be modeled as special cases of the general model (Figure 3.1). The balance equations of the well-mixed tank reactor include;

•Material balances for monomer, polymer, decomposition products, and other non-polymer species.

•Energy balances on a reactor.

The mixture in the reactor is treated as single-phase mixture consisted of monomer, polymer, solvent (here monomer), and decomposition products considered to have significant physical properties. Other species, such as initiator, impurity, and inhibitor exist only in trace amounts and have negligible physical properties.

Component densities (ρ_k) and heat capacities (C_{pk}) of individual are polynomial functions of temperature and pressure (Chen et al., 1976; Orbey et al., 1998; Costas et al., 2002). The reacting mixture properties such as the reacting

mixture density (ρ) and the reacting mixture heat capacity (C_p) are calculated from individual-component physical properties assuming zero volume changes of mixing.

$$\frac{1}{\rho} = \sum_{k=1}^{N} \frac{W_k}{\rho_k} \tag{3.20}$$

$$C_p = \sum_{k=1}^{N} W_k C_{p\,k} \tag{3.21}$$

where W_k is the weight fraction of individual-component k, N is number of components with significant volume contributions.

A total material balance around the reactor yields

$$\frac{d(V_{out}\rho_{out})}{dt} = Q_{in}\rho_{in} - Q_{out}\rho_{out} \tag{3.22}$$

where V_{out} is the volume of reaction mixture, Q_{in} is the inlet volumetric flow rate, Q_{out} is the outlet volumetric flow rate, ρ_{in} is the inlet reacting mixture density, ρ_{out} is the outlet reacting mixture density.

The fraction conversion to polymer X_p is defined as the fraction of monomer units being converted into polymer over the total amount of monomer units in the reactor, which includes monomers M, decomposition products Di, and polymers P:

$$X_p = \frac{[P]}{[M]+[P]+[D_i]} \tag{3.23}$$

3.3.2.1 Total Mass Balance Equation

The total material balance around the reactor is given by:

$$\frac{dV_{out}}{dt} = -Q_{out} + \frac{(Q_{in}\rho_{in})}{\rho_{out}} - V_{out}\rho_{out}\frac{\partial P_{out}}{\partial t}\sum_{k=1}^{N}\frac{W_{k,out}}{\rho_{k,out}^2}\frac{\partial \rho_{k,out}}{\partial P_{out}}$$

$$+ V_{out}\rho_{out}\sum_{k=1}^{N}\frac{1}{\rho_{k,out}}\frac{dW_{k,out}}{dt} - V_{out}\rho_{out}\frac{\partial T_{out}}{\partial t}\sum_{k=1}^{N}\frac{W_{k,out}}{\rho_{k,out}^2}\frac{\partial \rho_{k,out}}{\partial T_{out}} \qquad (3.24)$$

3.3.2.2 Component Mass Balance Equations

The balance for monomer in the reactor is:

$$\frac{dW_{M,out}}{dt} = \frac{Q_{in}\rho_{in}}{V_{out}\rho_{out}}\left(W_{M,in} - W_{M,out}\right) - \frac{MW_M(-R_p - R_d)}{\rho_{out}} \qquad (3.25)$$

The balances for other non-polymer species in the reactor are:

$$\frac{dW_{I,out}}{dt} = \frac{Q_{in}\rho_{in}}{V_{out}\rho_{out}}\left(W_{I,in} - W_{I,out}\right) - fk_{d_I}W_{I,out} \qquad (3.26)$$

$$\frac{dW_{D_i,out}}{dt} = \frac{Q_{in}\rho_{in}}{V_{out}\rho_{out}}\left(W_{D_i,in} - W_{D_i,out}\right) + \frac{MW_{D_i}R_{W_{D_I}}^k}{\rho_{out}} \qquad (3.27)$$

$$\frac{dW_{X,out}}{dt} = \frac{Q_{in}\rho_{in}}{V_{out}\rho_{out}}\left(W_{X,in} - W_{X,out}\right) - k_{tx}W_{X,out} \qquad (3.28)$$

3.3.2.3 Energy Balance Equation

The total energy balance around the reactor is:

$$\frac{dT_{out}}{dt} = \frac{Q_{in}\rho_{in}(e_{in} - e_{out}) + E_{input} + V_{out}(R_p\Delta H_{poly} + R_d\Delta H_{decomp})}{V_{out}\rho_{out}c_{p,out} + c}$$

(3.29)

Where c is the reactor wall heat capacity and e is the enthalpy of reaction mixture per unit mass:

$$e = \int_{T_{ref}}^{T} c_p dT$$

(3.30)

3.4 Peripheral Units

The mathematical models for the peripheral units (mixer, compressors, and cooler) are derived from balance equations for mass and energy. For simplicity, it is assumed that the separation in the flash units is ideal, only the monomer and the modifier are recycled, and only the product (polymer) is withdrawn from the plant. It is assumed, that the heat capacity and density of modifier is the same as those of ethylene. All volumes are well mixed and for all model equations of the peripheral units the pseudo-steady state approach is used. The ideal controllers that keep the controlled variables at the desired set point are assumed; hence, the temperatures in the recycle lines are assumed constant.

3.4.1 Mixer

In the plant there are several units for mixing different streams, e.g. mixing fresh ethylene with the recycle from the low pressure separator, or the injection of new initiator into the reactor tube. For all of these units, the volumes of

these units are small in comparison with the flow terms. Thus, the different fluxes mix instantaneously, meaning that the mixer is modelled as a continuous stirred tank reactor with infinitely small volume. Hence these systems can be described solely by algebraic equations. Therefore all mixers in the plant are described by algebraic mass, component and energy balance.

$$0 = Q_{out}\rho_{out} - \sum_{j=1}^{J} Q_{in,j}\rho_{in,j} \tag{3.31}$$

$$0 = Q_{out}\rho_{out}W_{i,out} - \sum_{j=1}^{J} Q_{in,j}\rho_{in,j}W_{i,in,j} \tag{3.32}$$

$$0 = T_{out}Q_{out}\rho_{out} - \sum_{j=1}^{J} Q_{in,j}\rho_{in,j}T_{in,j} \tag{3.33}$$

3.4.2 Compressor

It is assumed that both compressors in the plant consist of one stage for an isentropic system.

$$0 = Q_{out}\rho_{out} - Q_{in}\rho_{in} \tag{3.34}$$

$$0 = Q_{out}\rho_{out}W_{i,out} - Q_{in}\rho_{in}W_{i,in} \tag{3.35}$$

$$0 = \frac{-Q_{in}\rho_{in}\left(\int_{T_f}^{T_{out}} C_{p,out}dT - \int_{T_f}^{T_{in}} C_{p,in}dT\right) - Ws}{V_{out}\rho_{out}C_{p,out}} \tag{3.36}$$

3.4.3 Heat Exchanger

The total mass balance, components mass balance, and energy balanced are obtained

$$0 = Q_{out}\rho_{out} - Q_{in}\rho_{in} \tag{3.37}$$

$$0 = Q_{out}\rho_{out}W_{i,out} - Q_{in}\rho_{in}W_{i,in} \qquad \forall \, i = 1, ..., N \tag{3.38}$$

$$0 = \frac{Q_{in}\rho_{in}\int\limits_{T_{in}}^{T_{out}} C_{p,out}dT + Q_k}{V_{out}\rho_{out}C_{p,out}} \tag{3.39}$$

3.4.4 Separator

To describe the high-pressure flash unit, the composition of the outlet streams is assumed constant. All polymer and about 10% of unreacted monomer and ethylene decomposition products are separated and fed to the low-pressure separator unit (Orbey et al., 1998). So the global mass balance and components mass balance are shown as the following equations.

$$0 = 0.9\big(Q_{in}\rho_{in} - Q_{P,in}\rho_{P,in}\big)_{out1}$$
$$+ \big[0.1\big(Q_{in}\rho_{in} - Q_{P,in}\rho_{P,in}\big) + Q_{P,in}\rho_{P,in}\big]_{out2} - Q_{in}\rho_{in} \tag{3.40}$$

$$0 = 0.9\big(Q_{in}\rho_{in} - Q_{P,in}\rho_{P,in}\big)W_{i,out1}$$
$$+ 0.1\big(Q_{in}\rho_{in} - Q_{P,in}\rho_{P,in}\big)W_{i,out2} - Q_{in}\rho_{in}W_{i,in} \tag{3.41}$$

where equations (3.41) and (3.43) are component balance for *M* and *Di*.

The low-pressure flash is modeled to separate ideally the polymer P from the mixture of unreacted monomer M and ethylene decomposition products Di, hence all polymer is withdrawn from the plant. So the model equations for this unit read

$$0 = \left(Q_M\rho_M + Q_{Di}\rho_{Di}\right)_{out1} + Q_{P,out2}\rho_{P,out2} - Q_{in}\rho_{in}, \tag{3.42}$$

$$0 = \left(Q_M\rho_M + Q_{Di}\rho_{Di}\right)_{out1}W_{i,out1} - Q_{in}\rho_{in}W_{i,in}, \tag{3.43}$$

the two flashes are temperature controlled, so that separation temperature = constant.

3.5 Simulation Method

This thesis focuses on bifurcation behavior of multiple steady-state in CSTR-separator-recycle LDPE polymerizations and the steady-state model is obtained by performing steady-state material and energy balances. The steady-state model is solved numerically with Newton and the steady-state solutions are presented on bifurcation diagram. The stable steady states are identified from the values of the eigenvalues of the linearized unsteady state model (Topalis et al., 1996); if the real parts of all eigenvalues are negative, the steady state is the stable steady state. In addition, the simulation conditions that are investigated in this thesis are shown in Table 2.1.

For dynamic simulation, the unsteady state model was first derived. Then, the full set of modeling equations, which are a set of differential algebraic equations, are solved by method of fourth-order Runge-Kutta-Fehlberg in MATLAB (ODE45).

Table 3.4 Simulation conditions

Bifurcation parameter	Stand-alone CSTR	CSTR-separator-recycle											
	With ethylene decomposition	With ethylene decomposition but without acetylene decomposition				Without ethylene and acetylene decomposition				With ethylene and acetylene decomposition			
		Mass recycle ratio (re)				Mass recycle ratio (re)				Mass recycle ratio (re)			
		0	0.20	0.50	0.70	0	0.20	0.50	0.70	0	0.20	0.50	0.70
Feed temperature	at $W_{I,feed}$ = 7.5 ppm, residence time = 75 s	at $W_{I,feed}$ = 7.5 ppm				at $W_{I,feed}$ = 7.5 ppm				at $W_{I,feed}$ = 7.5 ppm			
Residence time	at $W_{I,feed}$ = 7.5 ppm, T_{feed} = 30°C												
Works load for primary compressor (W_{s1}) and secondary compressor (W_{s2})		at $W_{I,feed}$ = 7.5 ppm, T_{feed} = 30°C											
Removal heat from cooler (Q_k)		at $W_{I,feed}$ = 7.5 ppm, T_{feed} = 30°C											
Inlet initiator concentration		at T_{feed} = 30°C								at T_{feed} = 30°C			

CHAPTER IV

SIMULATION RESULTS AND DISCUSSION

Continuation analysis of the reactor offers important information regarding to multiple steady states and their stability. Many results were published on continuation analysis of the LDPE stand-alone autoclave reactors (Chan et al., 1993; Marini and Georgakis, 1984; Topalis et al., 1996). However, in all of those results only polymerization mechanisms are considered in their models, which significantly limited the predictive power of their models. Zhang et al. (1996) combined polymerization and ethylene decomposition reactions on their model for stand-alone reactor assuming the adiabatic autoclave is well mixed. Nevertheless, there is no analysis on the behavior of a adiabatic reactor-separator-recycle system that ethylene decomposition is included in the model. Consequently, three operating condition variables; feed temperature, residence time and inlet initiator concentration, and their effects on reactor's behavior are investigated in this thesis. The effect of heat and the presence of ethylene and acetylene decomposition are both included in the model where the stability of steady states on bifurcation diagrams is investigated. The observations presented here can be used to avoid runaway phenomena or instability in a CSTR-separator-recycle LDPE polymerization system.

4.1 Parameter Estimation

Zhang et al. (1996) combined polymerization with decomposition reactions on their model. Their rate constants of ethylene decomposition were evaluated based on ethylene decomposition kinetic scheme proposed by Watanabe et al. (1972). They reported that the generation rate of decomposition products consist of two parts: $k_1[C_2H_4]^2,$ corresponding to ethylene decomposition into radicals, and $k_6\sqrt{(k_1/k)}[C_2H_4]^2$, representing the consumption of ethylene through propagation steps. There are two independent rate constants required to be determined, k_1 and $k_6k^{-0.5}$, with this simplified decomposition scheme. These rate constants were determined from two pieces of information, the crossing temperature of 310°C of the decomposition reaction rate with the polymerization rate (Marini and Georgakis, 1984a; Bonsel and Luft, 1995) and the decomposition products distribution at a specified temperature (Watanabe et al., 1972). However, their rates of ethylene decomposition products were erroneous with inconsistent stoichiometric coefficients. To overcome this shortcoming, a consistent rate of ethylene decomposition is first derived and the kinetic parameters are estimated from the crossing temperature and decomposition product distribution. The kinetic scheme used here is based on the scheme originally proposed by Watanabe et al. (1972). The rate constants for our and result from Zhang and coworkers are listed in Table 4.1.

Table 4.1 Kinetic parameters for ethylene decomposition

Rate constant	k_0 (l/gmol·s)	E_a (cal/gmol)	V_a (cal/atm·gmol)	Reference
k_1	6.004×10^{19}	65,000	-0.1937	This study
$k_6 k^{-0.5}$	1.587×10^{20}	65,000	0.32185	This study
k_1	4.003×10^{19}	65,000	-0.1937	Zhang et al., 1996
$k_6 k^{-0.5}$	1.587×10^{20}	65,000	0.32185	Zhang et al., 1996

Figure 4.1 compares the consumption rate of ethylene and the generation rate of decomposition products as functions of ethylene. The results from the present model are compared with the simulation results from Zhang et al. (1996) at the same conditions. The simulation results from Zhang et el. (1996) are compared with experimental results from Watanabe et al. (1972) as shown in Figure 4.2, and good agreement was observed for the cases of methane and carbon. The predicted rate of ethylene decomposition resulting from Zhang et al. (1996) is smaller than the measured rate presented by Watanabe et al. (1972), especially at high pressure. Generally, our derived model yields the increased rate of ethylene decomposition when compared with model of Zhang et al. (1996).
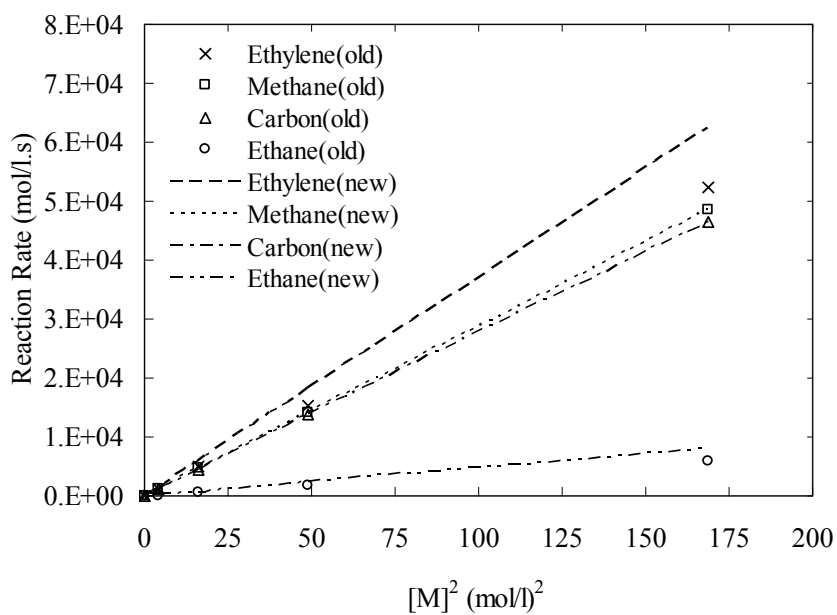
Figure 4.1 The consumption rate of ethylene and the production rate of decomposition

decomposition products as functions of ethylene concentration are

compared between this work (new) and simulation results from

Zhang et al., 1996 (old).
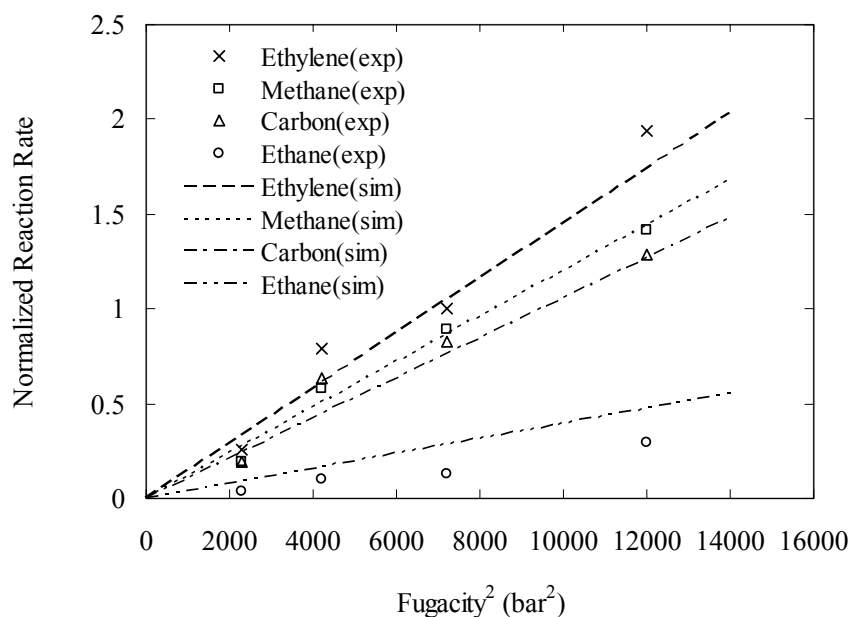
Figure 4.2 The consumption rate of ethylene and the production rate of decomposition

products as functions of ethylene fugacity are compared between

simulation results from Zhang et al. (1996) and experimental results from

Watanabe et al. (1972).

4.2 Model Validation

First of all, our model is validated by comparing the numerical results to those

presented in Zhang et al. (1996). Figure 4.3 shows the effect of feed temperature for a

stand-alone CSTR system with comparing between our model and a model of Zhang

et al. (1996). From Figure 4.3, it is obvious that the small differences in both model

appear when the reactor temperatures is above $230^{\circ}C$; our results are lower than the

result of Zhang et al. (1996) since the present decomposition rate is lower than the

decomposition rate of Zhang et al. (1996) as shown in Figure 4.4. When the

temperature is lower than $230^{\circ}C$, the polymerization dominates; thus, there is no

difference in this temperature range. Furthermore, the polymerization and decomposition rates for both models cross at approximately 310°C. This observation agrees with those of Marini and Georgakis (1984) and Bonsel and Luft (1995) in which it is generally accepted that ethylene decomposition is faster than polymerization above 300°C.

Figure 4.3 The bifurcation diagram of feed temperature on reactor temperature

when ethylene decomposition reactions is included in the model.

Comparison between this model and the model of Zhang et al. (1996)

for stand-alone CSTR with constant heat capacity of ethylene. Dash

line refers to unstable branch and solid line refers to stable branch.
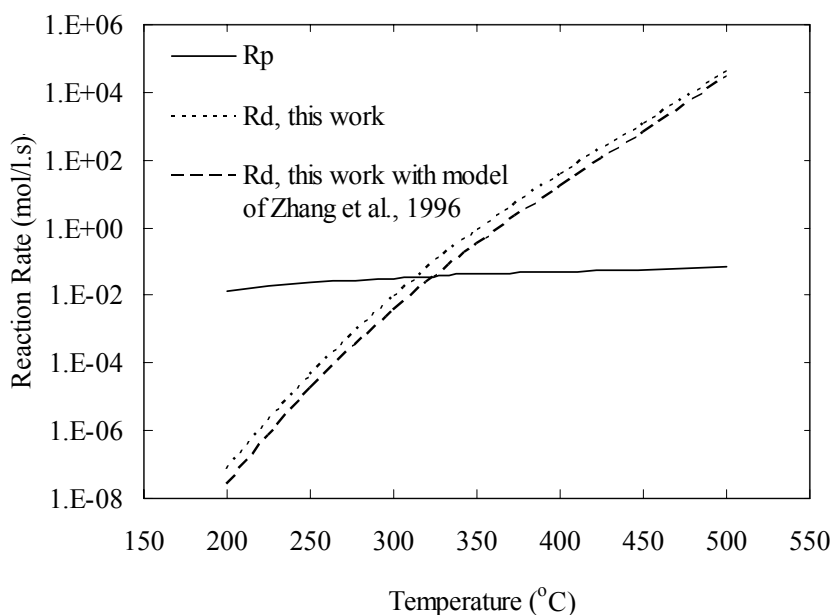
Figure 4.4 Polymerization and decomposition rates of ethylene are shown as
function of temperature comparison between our model and a
model of Zhang et al. (1996).

Since the assumption of constant heat capacity was used by Zhang and
coworkers, the comparison of our model (with heat capacity of ethylene as a function
of temperature and pressure) and Zhang et al. (1996) is made in order to investigate
the effect of variable heat capacity. The simulation results of Zhang and coworkers
were obtained with the component densities and heat capacities as polynomial
functions of reactor temperature and pressure but constant heat capacity of ethylene
(0.518 cal/g·K). Figure 4.5 and 4.6 show the steady-state of reactor temperature as a
function of feed temperature and residence time with variable heat capacity for stand-
alone CSTR. From those figures, it is obvious that the heat capacity of ethylene
should not be the constant when one models a LDPE polymerization reactor.
Therefore, the specific heat of ethylene as a function of reactor temperature and

pressure are used throughout this thesis. Nevertheless, the reactor is unstable over a wide range of feed temperature for both models but the middle stable branch of our numerical results exists at the higher feed temperature and residence time due to the relaxation of the assumption. For both simulation results, the feed and product temperature of the lower stable steady states are similar indicating very low conversion.
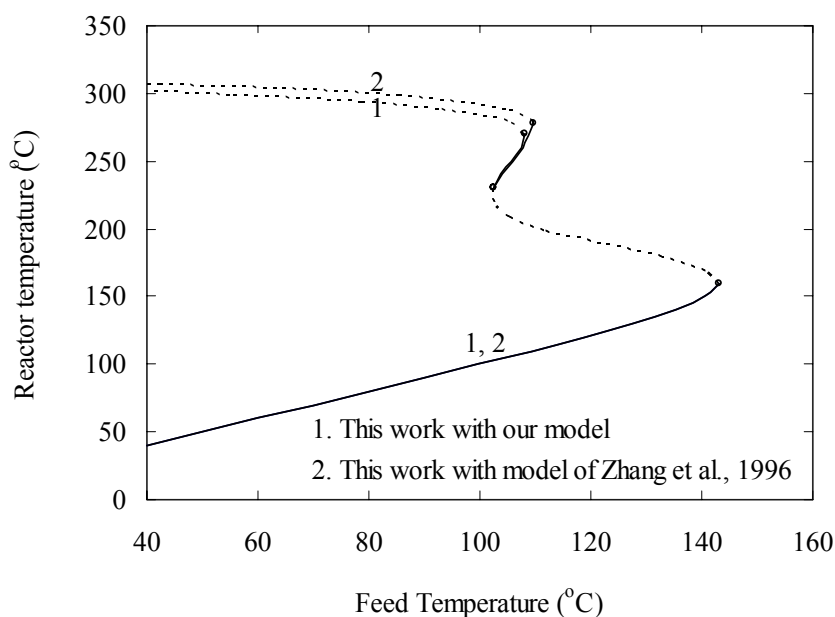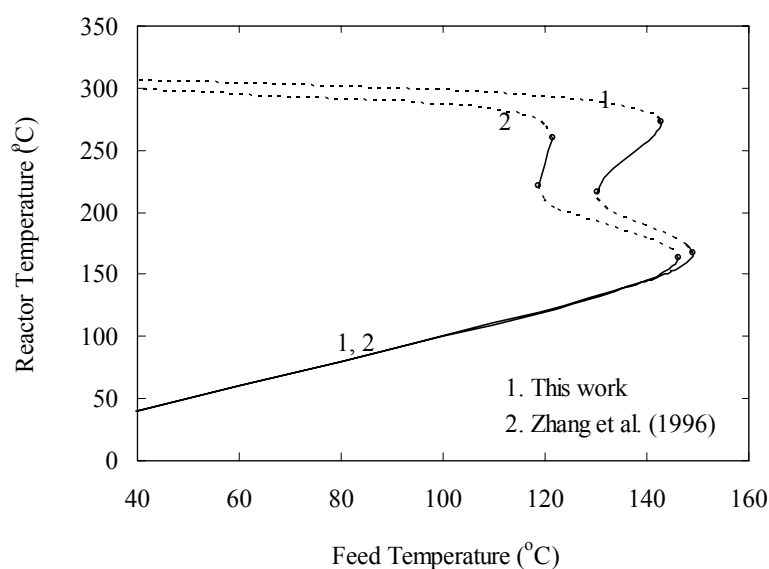

Figure 4.5 The bifurcation diagram of feed temperature on reactor temperature when ethylene decomposition reactions is included in the model. Comparison between this work (variable ethylene heat capacity) and result from Zhang et al. (1996) (constant ethylene heat capacity).
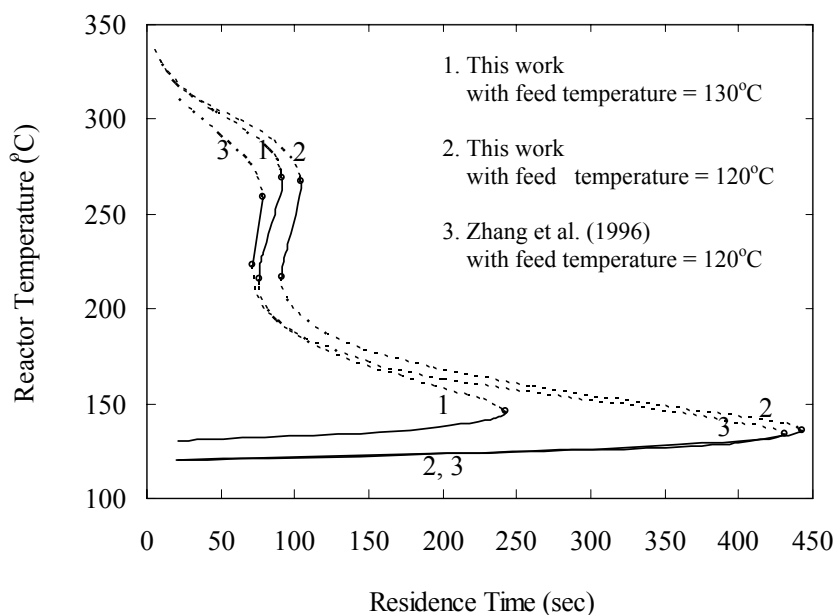
Figure 4.6 The bifurcation diagram of residence time on reactor temperature when ethylene decomposition reactions is included in the model. Comparison between this work (variable ethylene heat capacity) and result from Zhang et al. (1996) (constant ethylene heat capacity).

4.3 Effect of Ethylene Decomposition

Because the decomposition reactions occur over a very small time interval (Huffman et al., 1974), there is no practical way to control the high temperature and pressure in the reactor once the decomposition reactions have started. Thus, it is common for LDPE reactors to be equipped with relief valves that open at a specified upper pressure limit. Many attempts on modeling of LDPE stand-alone autoclave (Chan et al., 1993; Marini and Georgakis, 1984; Topalis et al., 1996) can be found and there is an attempt on modeling of CSTR-separator-recycled (Kiss et al., 2002). However, most of these results deal with only polymerization and polymer molecular

structure due to the lack of a fundamental understanding of the decomposition reactions. Descriptions of typical decomposition phenomena can be found elsewhere (Zhang et al., 1996; Watanabe et al., 1972). As a result, it is the objectives of this research to investigate the effect of ethylene decomposition by comparing the results of the model that ethylene is included with the one that ethylene is not included.

The reactor can be kept below a certain critical temperature, the decomposition can, in principle, be avoided. However, as shown later, it is not easy to maintain a steady reaction temperature due to a fast reaction rate, a short residence time, and no external cooling. Local areas of high temperature or hot spots can also be caused by imperfect mixing and can propagate through the reactor and result in a global decomposition. Figure 4.7, 4.8, 4.9, and 4.10 compare the effects of variations in feed temperature on reactor temperature when ethylene decomposition is included or excluded in the model with recycle and without recycle, respectively. As a result, when ethylene decomposition is included in the model, there are three stable (upper, middle, lower) and two unstable (upper, lower) branches appeared, represented by solid and dashed lines, respectively. In Figure 4.7-4.10, a circle point on the line is called a "fold bifurcation point" or a "transcritical bifurcation point". When the decomposition reactions are not included in the model, the reactor temperature continuation diagram has the typical S-shape, which is similar to the simulation result from Zhang et al. (1996). However, the upper branch of the continuation diagram is completely different when the decomposition reactions are included. The reactor temperature in upper unstable branch with decomposition reaction included increases as the feed temperature increases. At the temperature on the upper stable branch, the ethylene starts to decompose and the decomposition reactions become the dominant

reaction; there appears an upper stable steady state. With ample amount of monomer available for decomposing into free radicals, there is no need for additional initiator to sustain the high-reactor temperature steady state. The calculated upper steady state of $3,300^{\circ}C$ agrees the adiabatic temperature rise corresponding to complete ethylene decomposition. Additionally, these results suggest the importance of considering both decomposition and polymerization kinetics in performing process analysis, design, and control. In this study, the focus is on the four lower branches since these branches are in the normal operating ranges.

Figure 4.7 The steady-state reactor temperature is shown as a function of feed temperature at the primary mixer when ethylene decomposition are included (1) or excluded (2) for system without recycle at initiator feed concentration of 7.5 ppm.

Figure 4.8 The steady-state reactor temperature is shown as a function of feed

temperature at the reactor when ethylene decomposition are

included (1) or excluded (2) for system without recycle at

initiator feed concentration of 7.5 ppm.
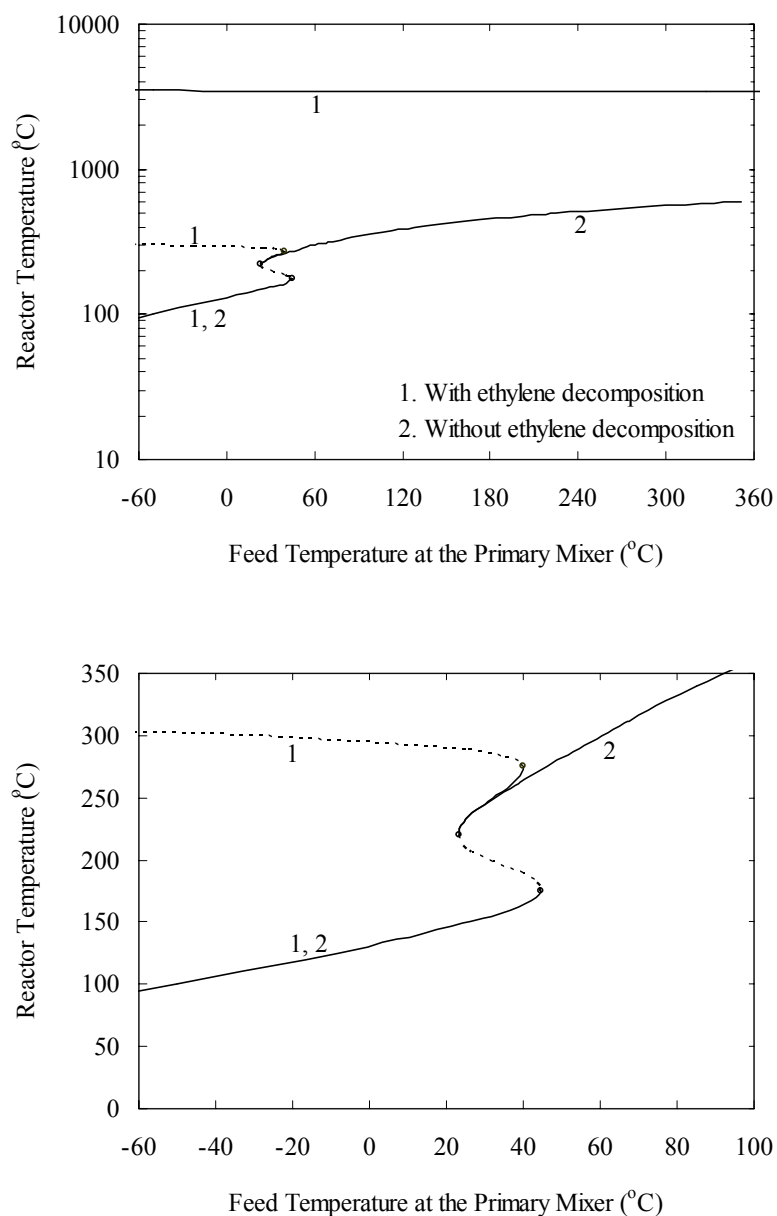
Figure 4.9 The steady-state reactor temperature is shown as a function of feed

temperature at the primary mixer when ethylene decomposition are

included (1) or excluded (2) for system with recycle at initiator

feed concentration of 7.5 ppm.

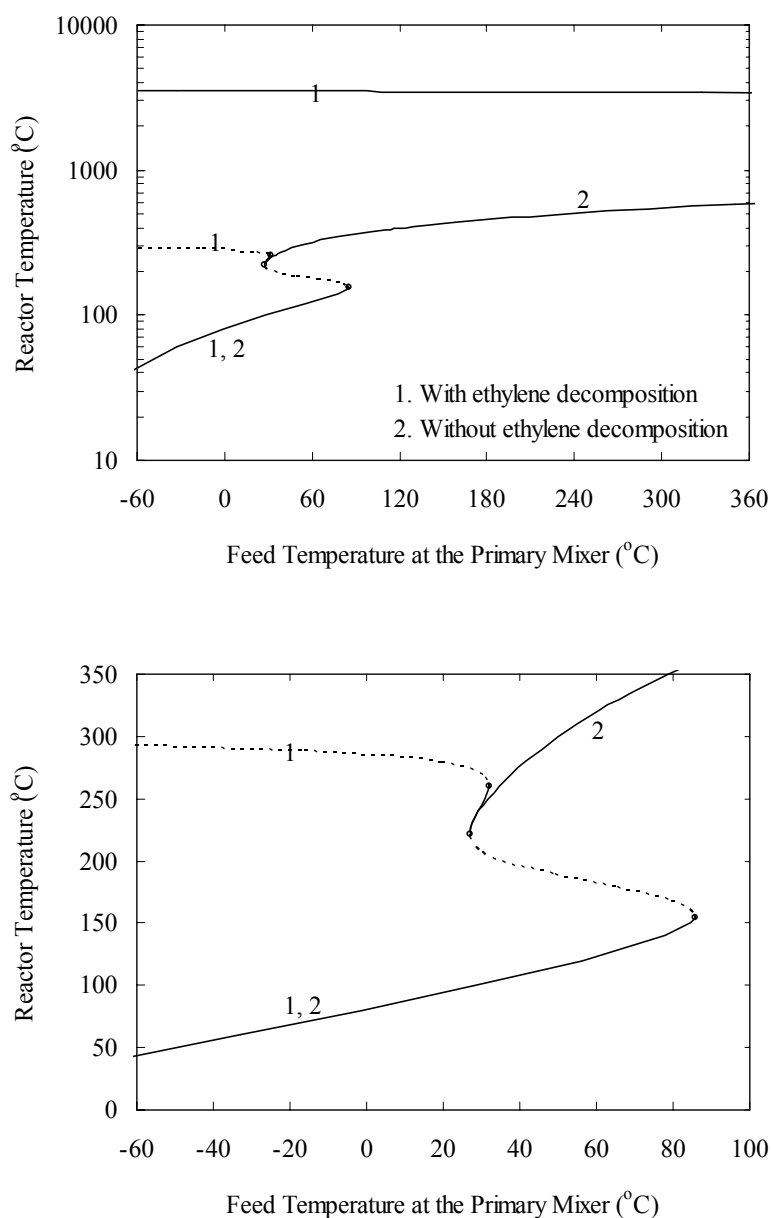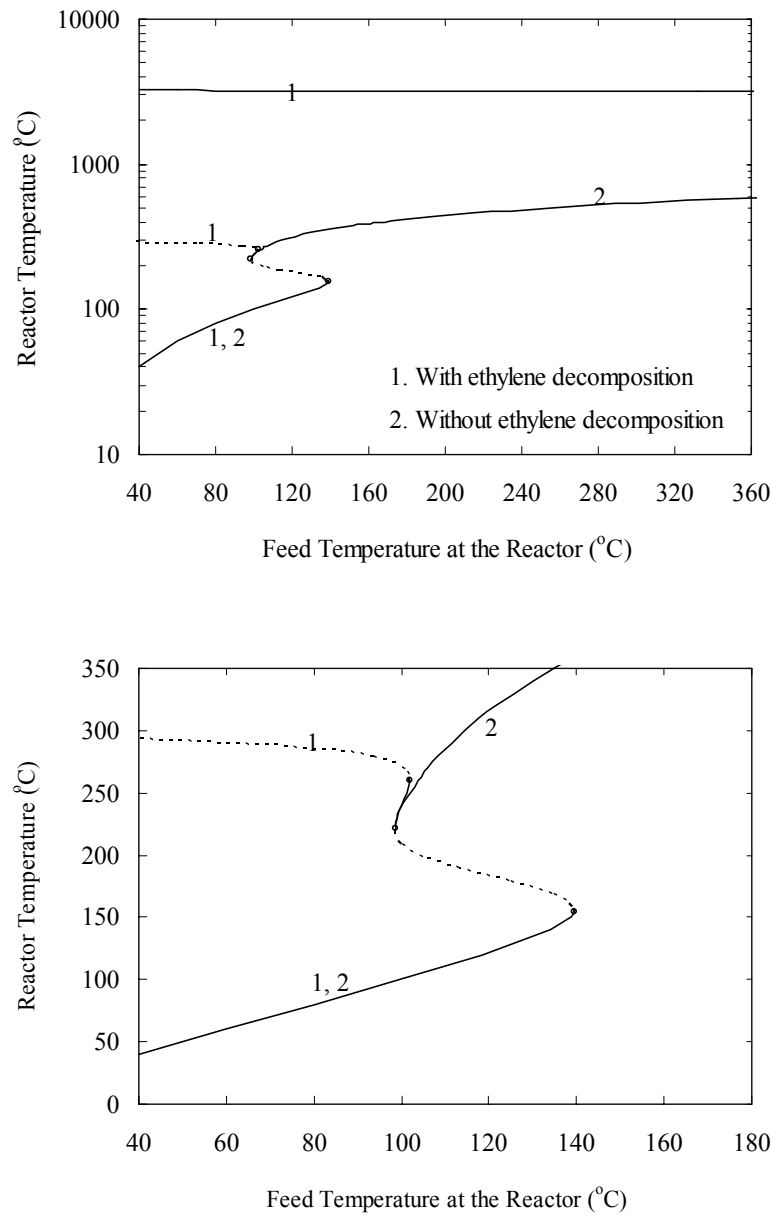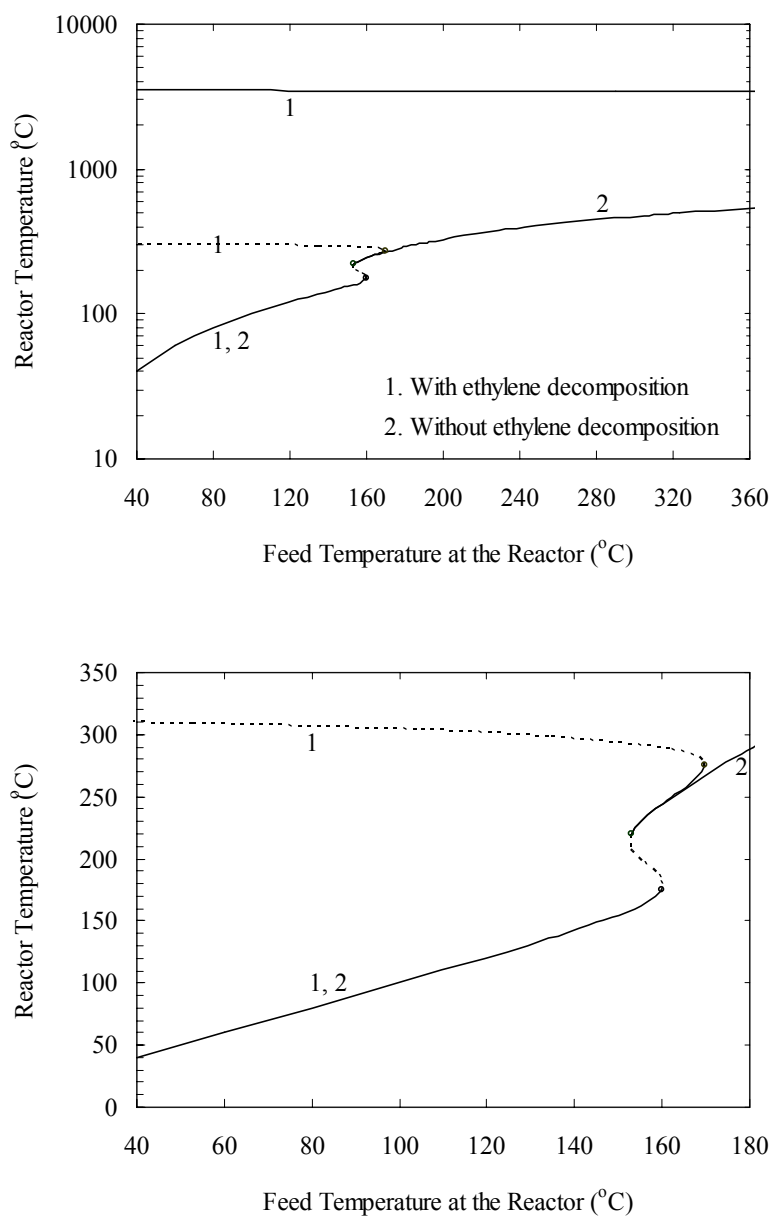**Figure 4.10** The steady-state reactor temperature is shown as a function of feed temperature at the reactor when ethylene decomposition reactions are included (1) or excluded (2) for system with recycle at initiator feed concentration of 7.5 ppm.

Because a design at an unstable steady state without a feedback controller should be avoided in practice, it is of interest to recognize such conditions. In identifying stability steady-state, the technique proposed by Topalis et al. (1996) in which the eigenvalues of the Jacobian matrix of the system are calculated and analyzed for the stable-unstable steady-state; if all real part of the eigenvalues are negative, the steady state is stable. In order to prove the validity of the eigenvalue technique, the eigenvalue of the unstable steady-state is evaluated and the result is compared with the numerical results obtained from the unsteady state model as shown in Figure 4.11 and 4.12 for no recycle and with recycle, respectively. As a result, the steady-state reactor temperature is set initially at $190^{o}C$. At 10,000 sec, the feed temperature at primary mixer is changed for a limited period of time. Depending on the disturbance direction, runaway reaction or lower reactor temperature are reached; it proves that at the reactor temperature of $190^{o}C$ is unstable steady-state. Since the reactor is adiabatic, the negative sign of eigenvalues are both necessary and sufficient stability conditions. A similar technical was used to prove the stability of steady-state solution by Kiss et al. (2002). Additionally, Figure 4.13 shows decomposition products' distribution during the runaway reaction for no recycle. The decomposition products' distribution is in good agreement with experimental observations (Watanabe et al., 1972). Carbon, methane, acetylene, and ethane are the major decomposition products.
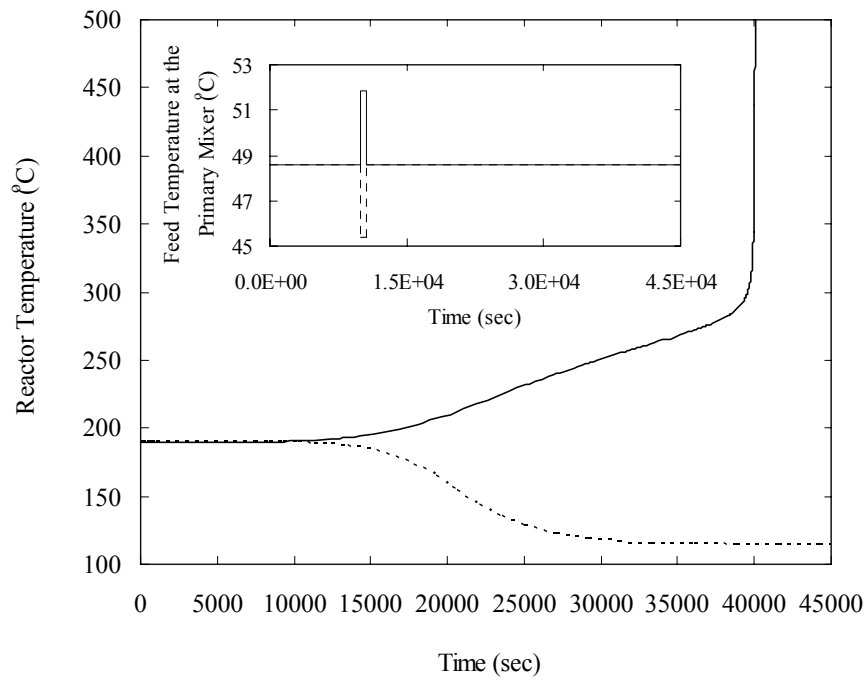
Figure 4.11 Dynamic responses of unstable steady state at reactor temperature of

190°C without recycled to a feed temperature at the primary mixer

disturbance when ethylene decomposition reactions are included.
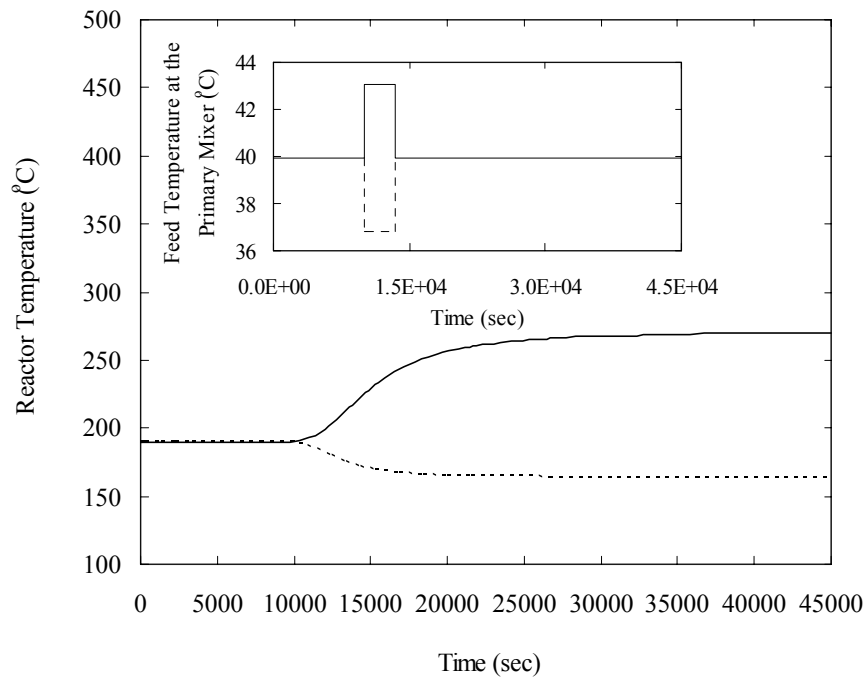
Figure 4.12 Dynamic responses of unstable steady state at reactor temperature of

190°C with recycle to a feed temperature at the primary mixer

disturbance when ethylene decomposition reactions are included.
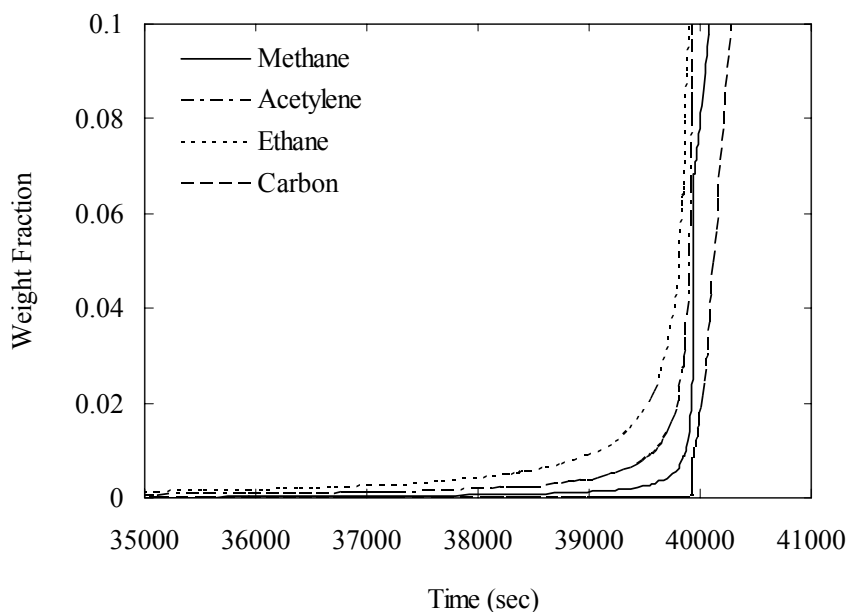
Figure 4.13 Decomposition product distribution during a runaway reaction without

recycle.

With recycle, the feedback due to the material recycles has much higher

impact on the solution. The presence of such a feedback can lead to instability and

multiple steady states as previously pointed out by Kiss et al. (2002). As a practical

application example, LDPE in a continuous stirred tank stand-alone reactor and

reactor-separator-recycle system were considered. Kiss et al. (2002) reported that one

steady state for stand-alone reactor existed and two steady states with lower stable

branches occurred for a reactor-separator-recycle system while our results are

different. The main reason for the difference is the assumption of isothermal

assumption and the negligence of decomposition in their work. Because of the thick

wall of LDPE autoclave due to high pressure and highly exothermic polymerization

and decomposition reactions, an adiabatic reactor is unlikely. Consequently, the

model developed in this thesis is the better alternative.

4.4 Works and Heat

Works load for primary and secondary compressors and heat removal of the cooler at feed temperature at primary mixer of 30°C and initiator feed concentration of 7.5 ppm are calculated in order to study possibility of the model.

The stability analysis is carried out to predict the removal heat from the cooler before feed at the reactor corresponds to the multiple steady states as shown in Figure 4.14. When the recycle ratio (re) increases, the lower stable steady state moves toward the right. On the other hand, the middle stable reactor temperature increases with increasing recycle ratio. It should be pointed out that that the desired operating temperature is the middle stable branch because of acceptable conversion; however, the slope of the curve at the middle stable branch indicates that these steady states are poor robustness to disturbances. Thus, even with a good control system, one could very easily drop to the lower stable steady state where the reaction ceases, or be carried away towards an upper stable steady state where decomposition occurs. For the middle stable branch, the reactor temperature in the ranges from 225 to 260°C, 220 to 265°C, 215 to 270°C, and 210 to 275°C with recycle ratio of 0, 0.20, 0.50, and 0.70, respectively. The heat at the same branch is from 199 to 210 kcal/s, 205 to 223 kcal/s, 191 to 246 kcal/s, and 128 to 258 kcal/s with recycle ratio of 0, 0.20, 0.50, and 0.70, respectively. In addition, Figure 4.15 and 4.16 show the work load for the primary compressor and secondary compressor with corresponding to the heat of the cooler. For the middle stable branch, the work for the primary compressor is in the ranges from 80.3 to 80.4 kcal/s, 85 to 85.5 kcal/s, and 92.4 to 94.5 kcal/s with recycle ratio of 0.20, 0.50, and 0.70 respectively while the work is constant at 78.6 kcal/s without recycle. As the same branch, the work for the secondary compressor is

constant at 242 kcal/s for no recycled while it is in the ranges from 293 to 296 kcal/s,

437 to 452 kcal/s, and 666 to 729 kcal/s are occurred with recycle ratio of 0.20, 0.50,

and 0.70 respectively.
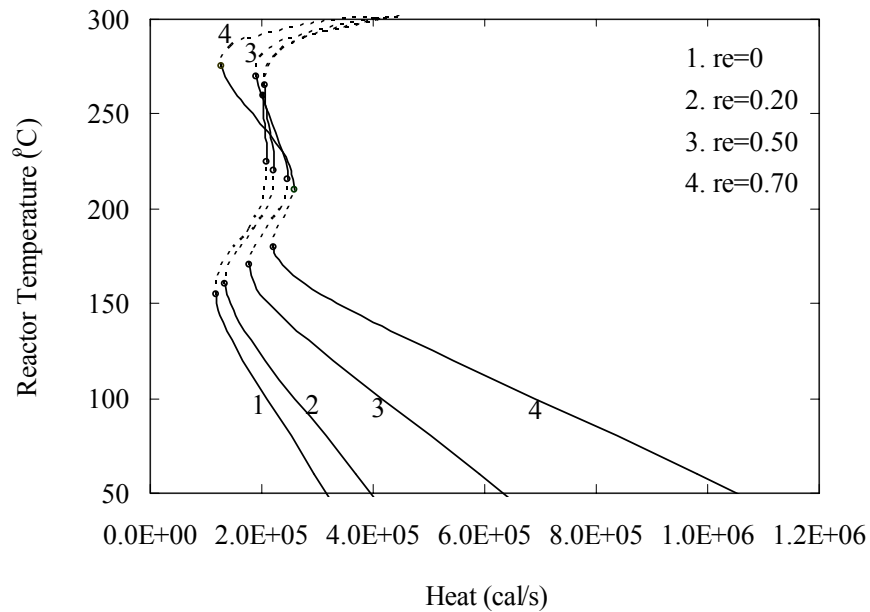
Figure 4.14 The steady-state reactor temperature is shown as a function of removal

heat from the cooler before feed at the reactor for constant of feed

temperature at the primary mixer of 30^oC and initiator feed

concentration of 7.5 ppm.
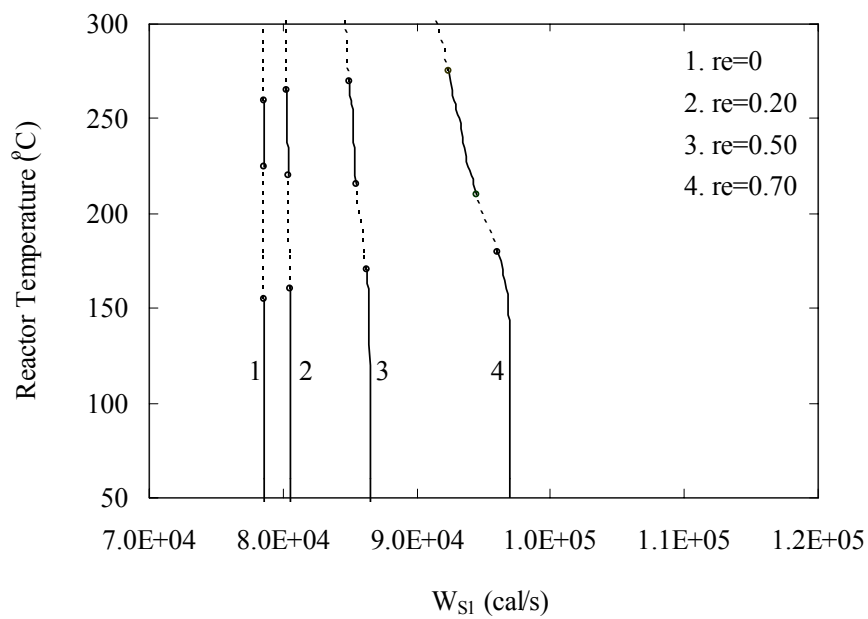
Figure 4.15 The steady-state reactor temperature is shown as a function of work load into the primary compressor for constant of feed temperature at the primary mixer of 30°C and initiator feed concentration of 7.5 ppm.
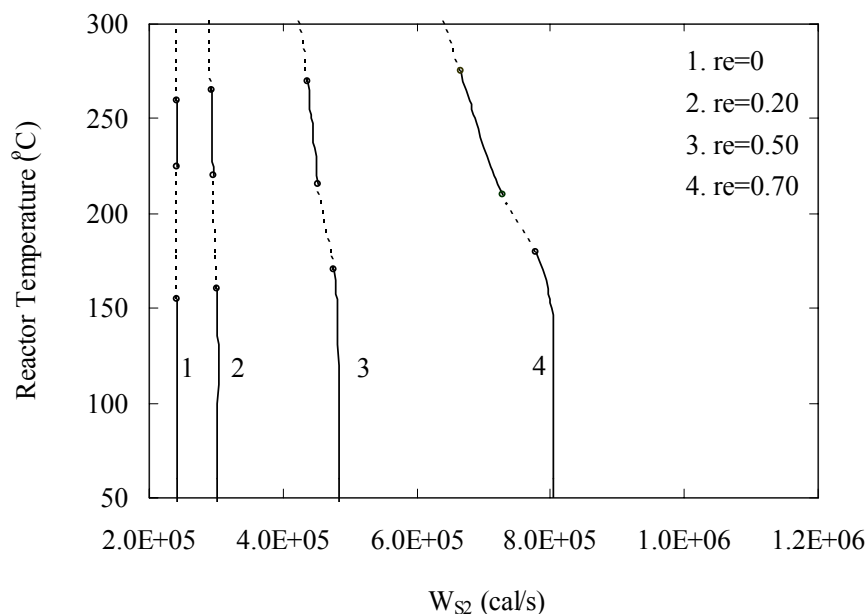
Figure 4.16 The steady-state reactor temperature is shown as a function of work load into the secondary compressor for constant of feed temperature at the primary mixer of $30^{\circ}C$ and initiator feed concentration of 7.5 ppm.

4.5 Ethylene and Acetylene Decomposition with Recycle

In this thesis, the focus is on the bifurcation behavior of a LDPE CSTR-separator-recycle polymerization system for an adiabatic non-isothermal CSTR in the presence of ethylene decomposition. From Watanabe et al. (1972), the cracking of ethylene at low conversion, carbon, methane, acetylene, and ethane would be present. Then, Zhang et al. (1996) reported that small amounts of impurities (e.g., acetylene), which can be found in monomer feed, can decompose into free radicals and induce runaway reaction. They modeled LDPE stand-alone CSTR by including both ethylene and acetylene decomposition in their model and performed the influence of inlet acetylene concentration on the steady-state reactor temperature. Furthermore, the

acetylene would be in the recycle stream; hence, the model of LDPE CSTR-separator-recycle system when ethylene and acetylene decomposition are considered with recycle are investigated.

The effect of ethylene and acetylene decompositions with recycle ratio of 0.20, 0.50, and 0.70 are shown in Figure 4.17, 4.18, and 4.19, respectively. These curves show the effect of feed temperature on the reactor temperature in comparison to the case of without recycle (line 1). As stated in the legend, the ethylene decomposition is considered with 0% of acetylene is separation and the decomposition of acetylene is neglected which index by line number 2. Both ethylene and acetylene decompositions are considered that indicating by line number 3, 4, and 5 for 100%, 95%, and 0% of acetylene separation with respectively. As a results, when both ethylene and acetylene decomposition is considered, the effect becomes more significant. The acetylene decomposition would unstabilize the reactor and the undesirable results occur. For example, the middle stable steady state disappeared completely even at low recycle ratio (0.20). It should be noted that this observation agreed with the conclusions discussed by Zhang et al. (1996) where the impurity of acetylene is in the feed. Because of the significance effect of acetylene decomposition in the presence of recycle, further investigation on the effect of better separator, in which acetylene can be separated from the recycle stream, on the bifurcation of the systems was investigated. From the investigation, it has found that the high efficiency (100%) of acetylene separation yields the much improved results with the middle stable steady states. However, low efficiency acetylene separation (even at 95%) could not remediate the problems.
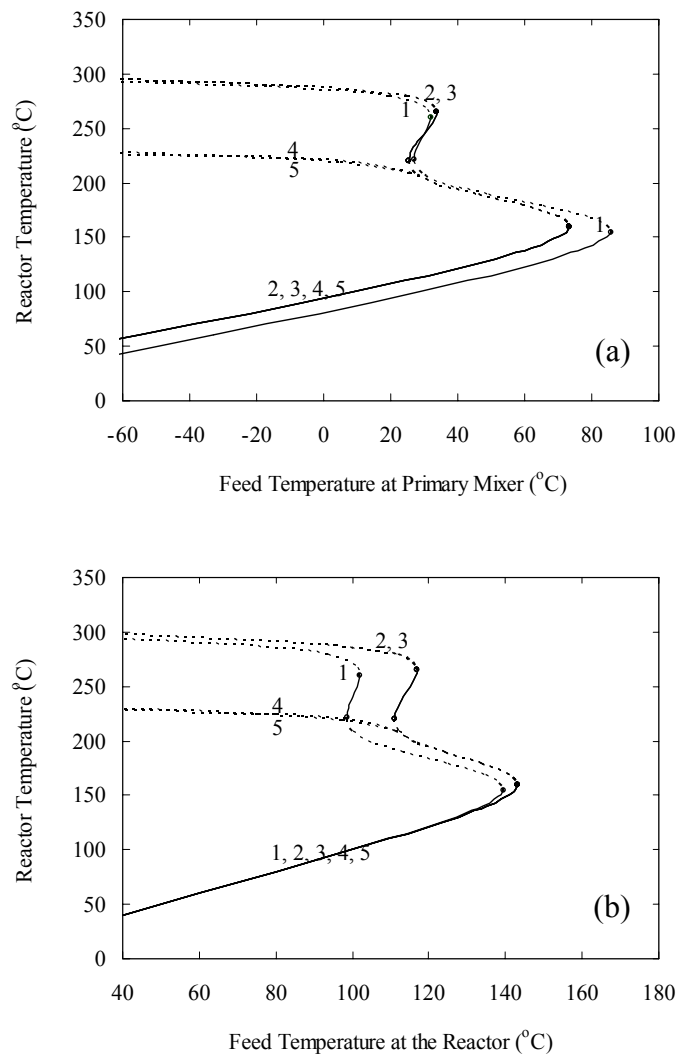
1. No recycled

2. 0% acetylene separation without acetylene decomposition

3. 100% acetylene separation

4. 95% acetylene separation with acetylene decomposition

5. 0% acetylene separation with acetylene decomposition

Figure 4.17 The bifurcation diagram of (a) feed temperature at primary mixer and

(b) feed temperature at the reactor on reactor temperature when ethylene

decomposition reactions are included with and without the effect of

acetylene decomposition for recycle ratio of 0.20.
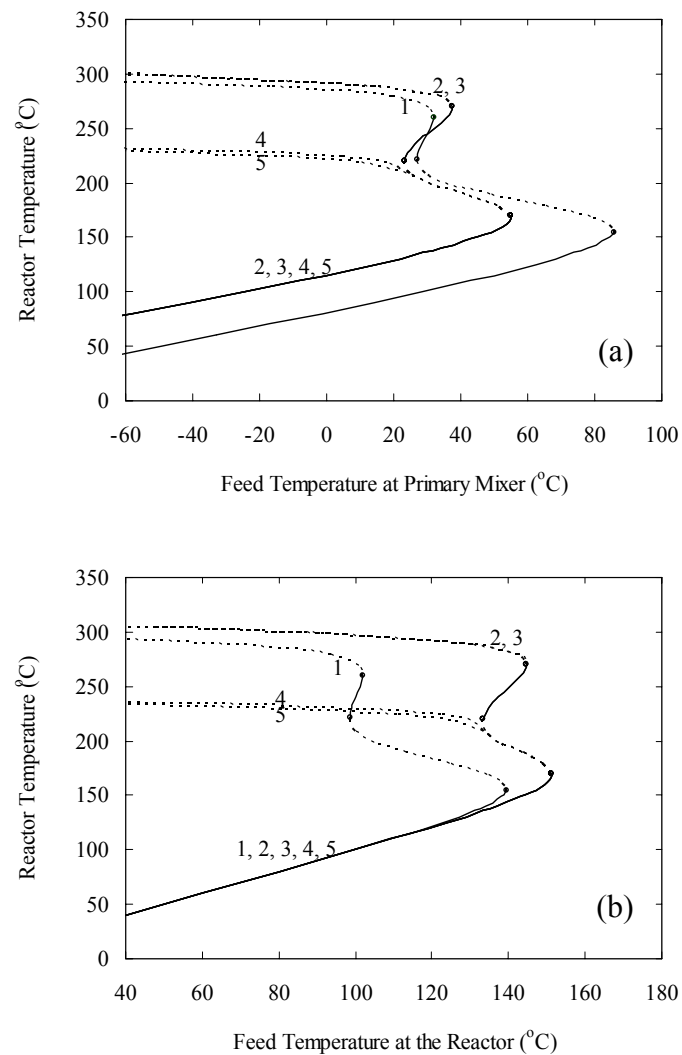
1. No recycled

2. 0% acetylene separation without acetylene decomposition

3. 100% acetylene separation

4. 95% acetylene separation with acetylene decomposition

5. 0% acetylene separation with acetylene decomposition

Figure 4.18 The bifurcation diagram of (a) feed temperature at primary mixer and

(b) feed temperature at the reactor on reactor temperature when ethylene

decomposition reactions are included with and without the effect of

acetylene decomposition are compared for recycle ratio of 0.50.
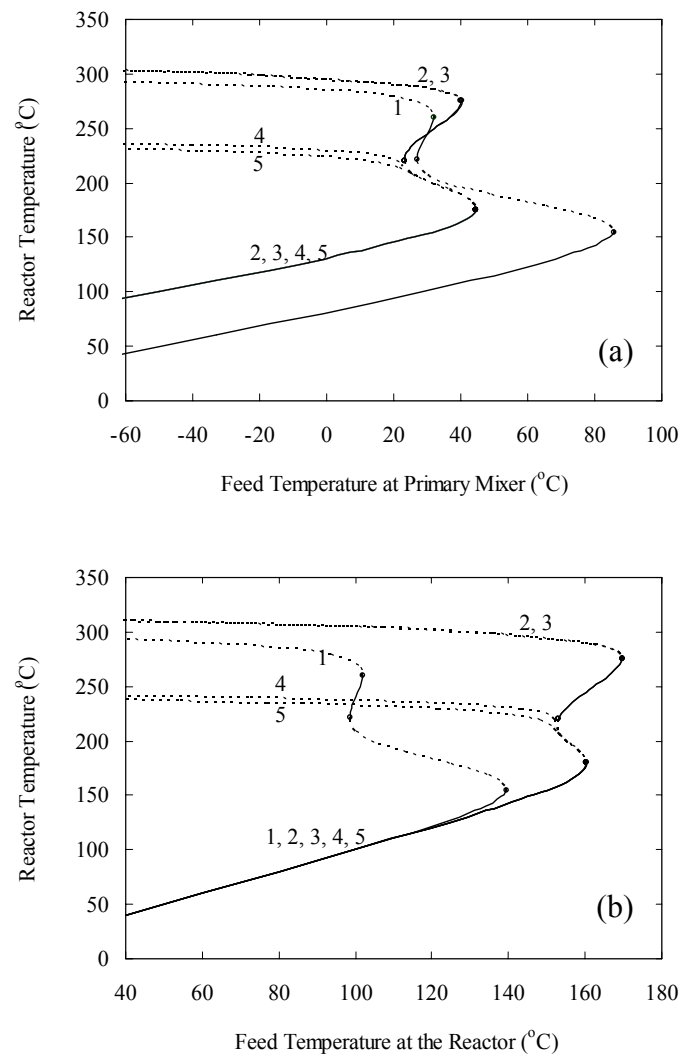
1. No recycled

2. 0% acetylene separation without acetylene decomposition

3. 100% acetylene separation

4. 95% acetylene separation with acetylene decomposition

5. 0% acetylene separation with acetylene decomposition

Figure 4.19 The bifurcation diagram of (a) feed temperature at primary mixer and

(b) feed temperature at the reactor on reactor temperature when ethylene

decomposition reactions are included with and without the effect of

acetylene decomposition are compared for recycle ratio of 0.70.

4.6 The Effect of Bifurcation Parameters

High-pressure free radical polymerization of ethylene in autoclaves is an important process that is widely used in industries. Because of the high operation pressure and the large heat of polymerization, difficulties are encountered in the design and in the operation of the reactor. Hence, the precise selection of the operating conditions such as feed temperature and feed initiator concentration is essential in the economic process operation. In this regard, it is important to analyze the steady states characteristic of the reactor in relationship with the change of various operating conditions by using appropriate mathematical model.

4.6.1 Feed Temperature

The feed temperature can have an effect on the reactor stability behavior of the system. The effect of feed temperature on the reactor temperature and overall conversions when the ethylene decomposition is considered, 0% of acetylene is separated and the decomposition of acetylene is neglected at initiator feed concentration of 7.5 ppm are shown in Figure 4.20, 4.21, and 4.22. Because of Arrhenius, increasing the feed temperature has the beneficial effect of allowing much higher degrees of monomer conversion and conversion to polymer at middle stable branch. With the higher recycle ratio, the wider middle stable branch appears with a longer feed temperature range. For example the middle stable reactor temperature is in the range of 220 to 260°C for no recycle case and 220 to 265°C, 220 to 270°C, and 220 to 275°C for the cases of recycle ratio values of 0.20, 0.50, and 0.70, respectively. In addition, the middle stable exist at a range of feed temperature at primary mixer from 27 to 32°C, 25 to 34°C, 23 to 37°C, and 23 to 40°C for recycle ratio of 0, 0.20, 0.50, and 0.70 respectively. As the recycle ratio increases, the conversion to polymer

at the middle stable branch is higher. Therefore, the higher overall conversion could be obtained in an economically reasonable region of operation commercial plant. The middle stable branch is the normal operating branch and the conversions in this branch is from 10 to 13% for no recycle case and 11 to 15%, 13 to 20%, and 16 to 25% for the cases of recycle ratio values of 0.20, 0.50, and 0.70, respectively. For lower stable branch, when the recycle ratios increase, a range of feed temperature at the primary mixer is slightly smaller but a range of feed temperature at the reactor is slightly larger. At higher reactor temperatures, decomposition products are produced more and polymer selectivity for middle stable and upper unstable branches decrease as shown in Figure 4.23.

Figure 4.20 Steady-state reactor temperature is shown as a function of (a) feed temperature at primary mixer and (b) feed temperature at the reactor when ethylene decomposition reactions are included, 0% acetylene separation and without the effect of acetylene decomposition at initiator feed concentration of 7.5 ppm.

Figure 4.21 Steady-state monomer conversion is shown as a function of (a) feed temperature at primary mixer and (b) feed temperature at the reactor when ethylene decomposition reactions are included, 0% acetylene separation and without the effect of acetylene decomposition at initiator feed concentration of 7.5 ppm.

Figure 4.22 Steady-state conversion to polymer is shown as a function of (a) feed temperature at primary mixer and (b) feed temperature at the reactor when ethylene decomposition reactions are included, 0% acetylene separation and without the effect of acetylene decomposition at initiator feed concentration of 7.5 ppm.
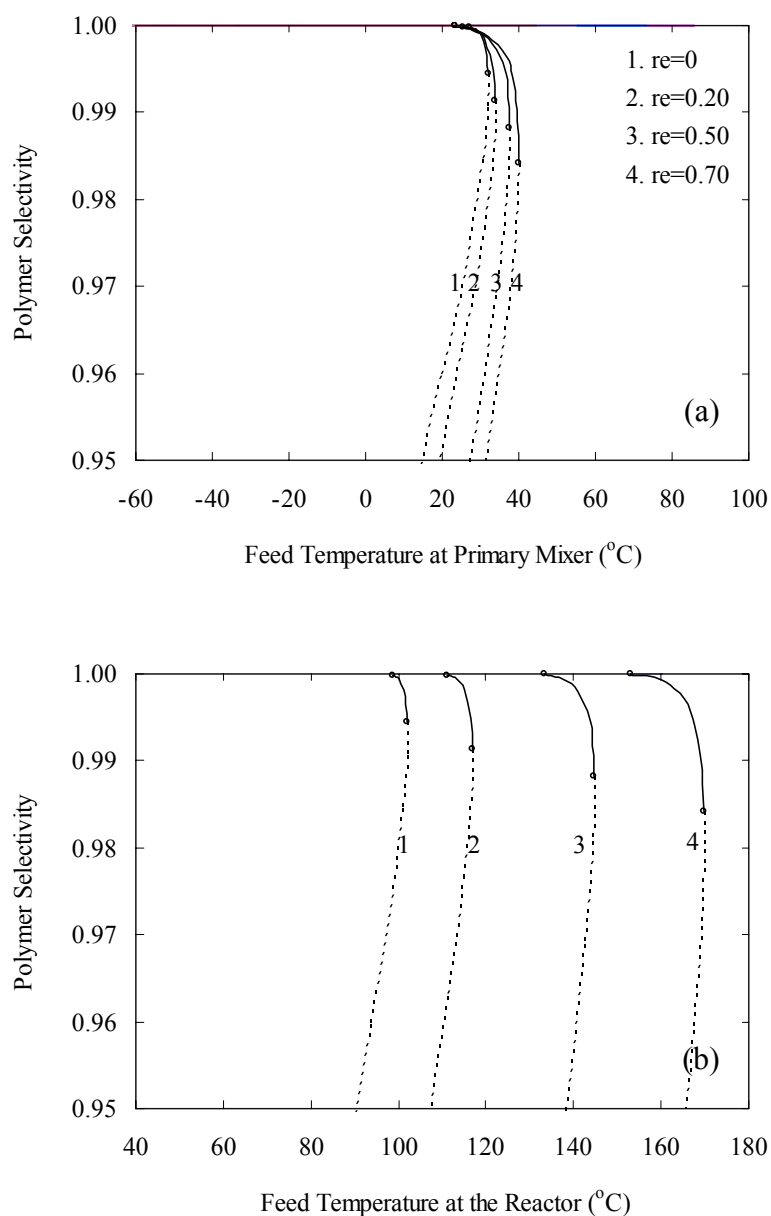
Figure 4.23 Polymer selectivity is shown as a function of (a) feed temperature at primary mixer and (b) feed temperature at the reactor when ethylene decomposition reactions are included, 0% acetylene separation and without the effect of acetylene decomposition at initiator feed concentration of 7.5 ppm.

When the effect of both ethylene and acetylene decomposition with 0% acetylene separation is investigated as shown in Figure 4.24, 4.25, and 4.26, there are two steady state branches with one lower stable branch. The lower stable branch is similar to the behavior of without the acetylene decomposition because very small amount of decomposition products are produced at this temperature. For this case, there is no middle stable branch because acetylene produced from ethylene decomposition at the temperatures in middle stable branch is recycled and induce the runaway reactor which Zhang et al. (1996) has reported when acetylene is present in the feed.
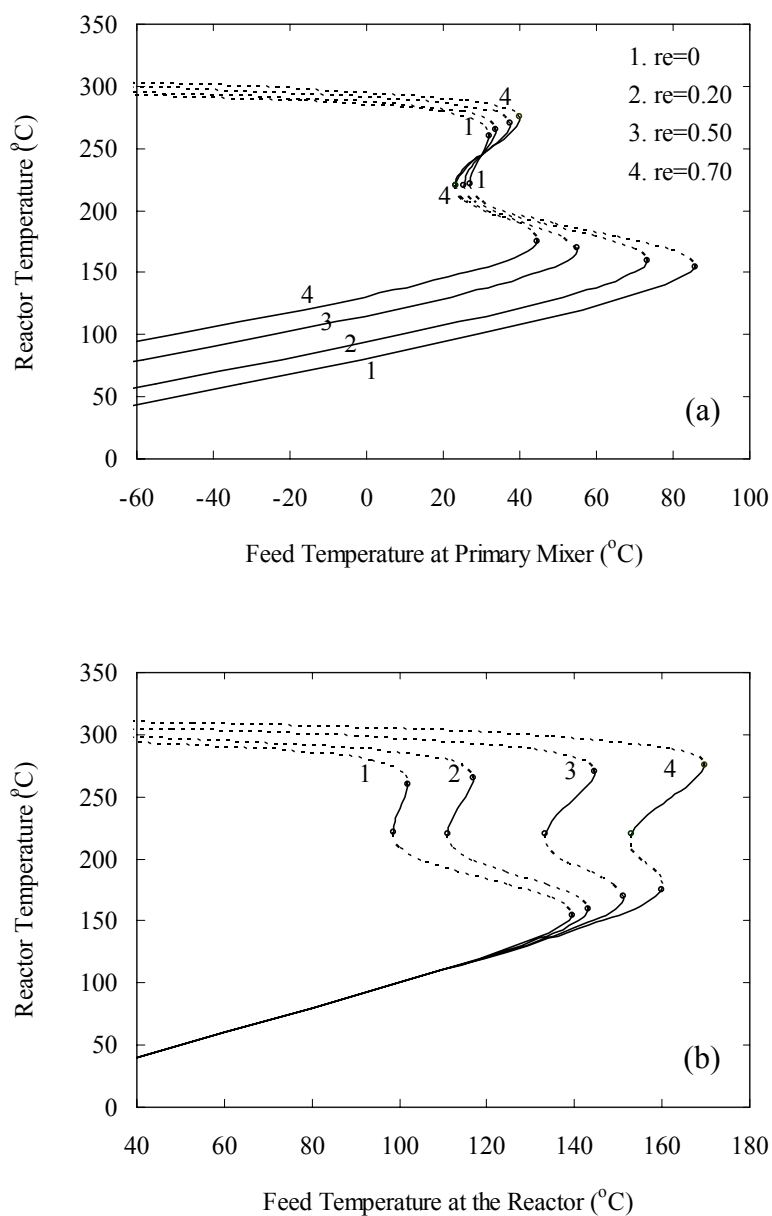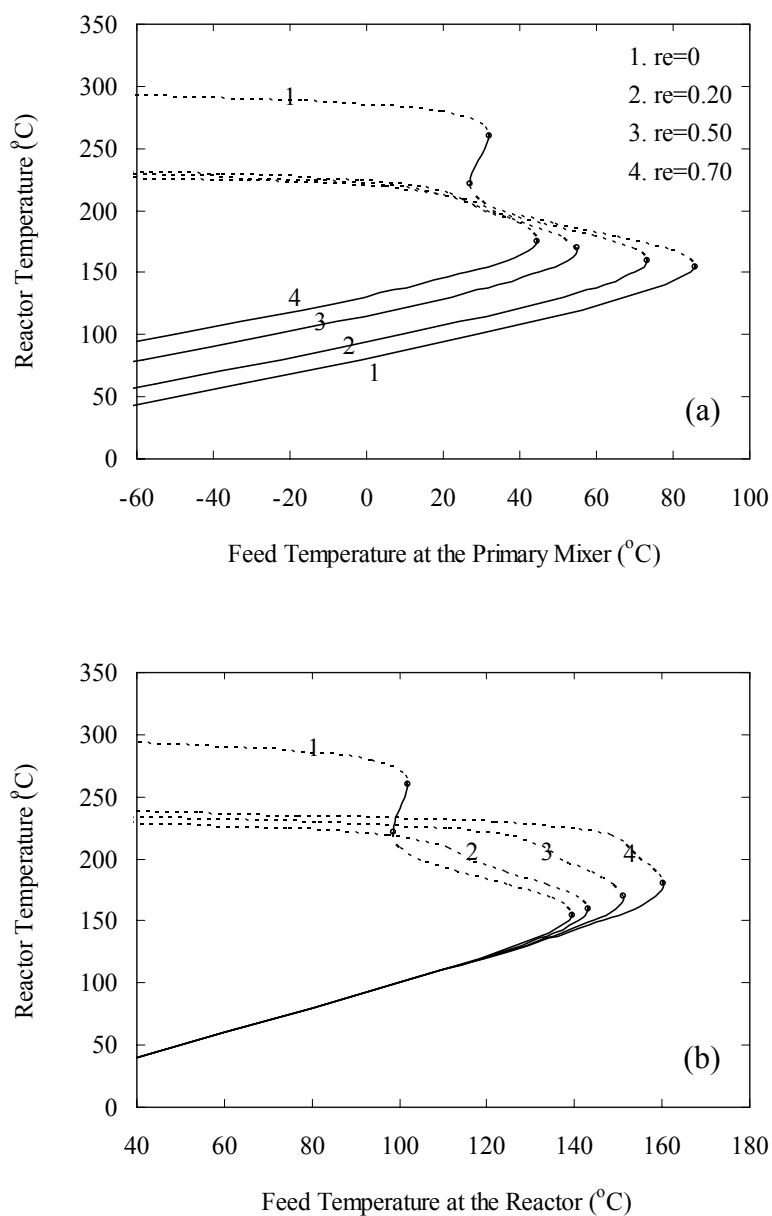
Figure 4.24 Steady-state reactor temperature is shown as a function of (a) feed temperature at primary mixer and (b) feed temperature at the reactor with ethylene decomposition reactions included, 0% acetylene separation and with the effect of acetylene decomposition at initiator feed concentration of 7.5 ppm.
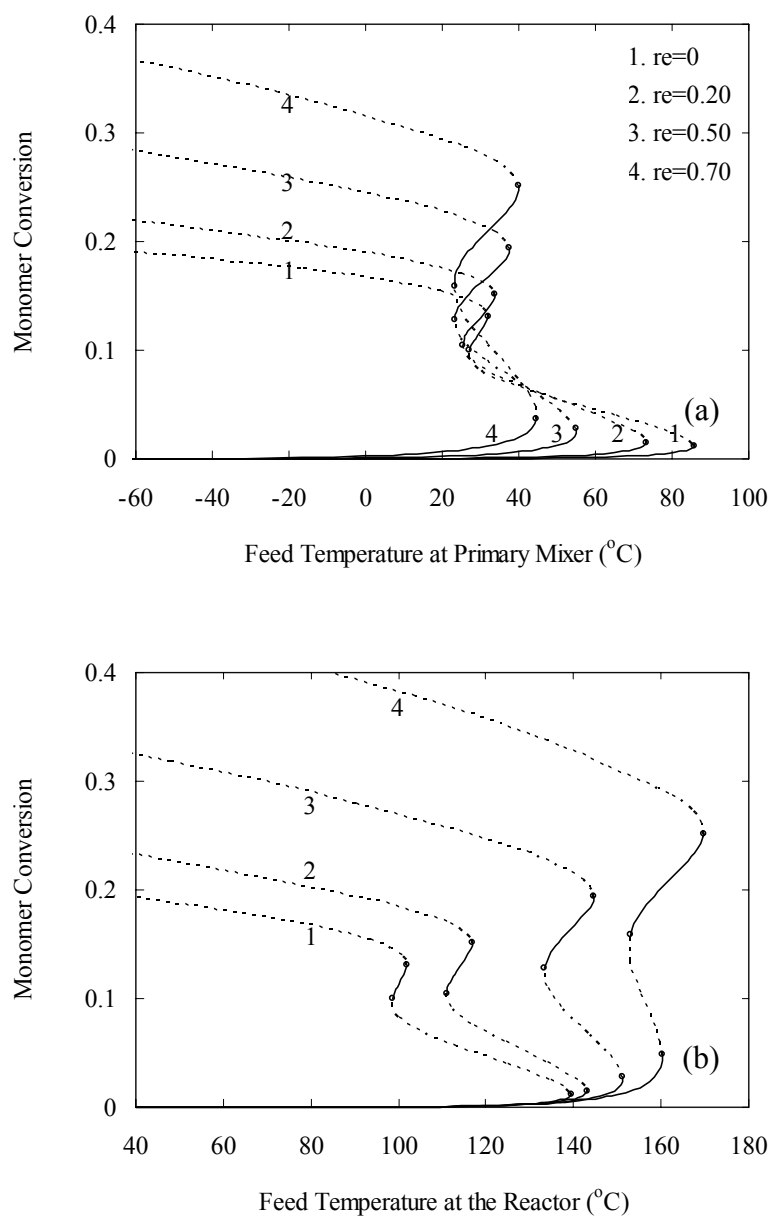
Figure 4.25 Steady-state monomer conversion is shown as a function of (a) feed temperature at primary mixer and (b) feed temperature at the reactor with ethylene decomposition reactions included, 0% acetylene separation and with the effect of acetylene decomposition at initiator feed concentration of 7.5 ppm.
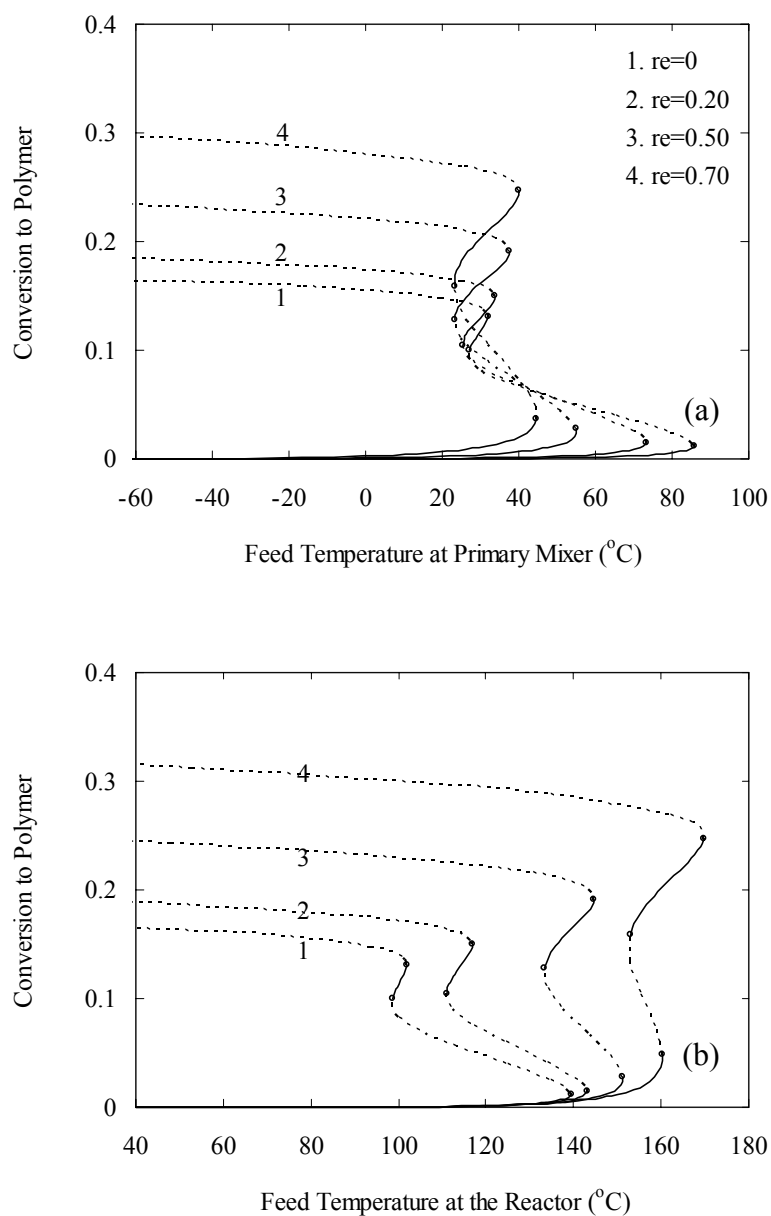
Figure 4.26 Steady-state conversion to polymer is shown as a function of (a) feed
temperature at primary mixer and (b) feed temperature at the reactor
with ethylene decomposition reactions included, 0% acetylene
separation and with the effect of acetylene decomposition at initiator
feed concentration of 7.5 ppm.

The only way to remove the heat in the LDPE CSTR is by the cold inlet stream. In addition, the conversion is a function of this temperature difference. To obtain higher conversions, the steady-state reactor temperature must be higher, indicating that the inlet stream must be colder to remove the excess heat. However, increasing reactor temperature moves the reactor close to the unstable boundary. In practice, designs near the transcritical bifurcation points are dangerous, since changing operating conditions or uncertain design parameters can lead to a behavior that is different from the expected one. A reactor design close to the transcrical bifurcation is unlikely, because the overall conversion would have a lower value or runaway reaction. So, it should be operated at reactor temperature of 245°C for the case of acetylene separation about 100% that can be obtained middle stable steady-state and high conversion.

4.6.2 Inlet Initiator Concentration

Due to the adiabatic nature of the LDPE autoclave, inlet initiator is the main operation variable used to control the reactor temperature. Figure 4.27, 4.28, and 4.29 show the reactor temperature, monomer conversion, and conversion to polymer respectively as a function of inlet initiator concentration at various recycle ratio, 100% of acetylene recycle and at feed temperature at primary mixer of 30°C when ethylene decomposition is considered; but acetylene decomposition is not considered. The initiator used is di-*tert*-butyl peroxide (DTBP). As can be seen in Figure 4.27, the increase in recycle ratio causes the decrease in the lower stable steady-state reactor temperature but the range of the middle stable steady state increases. For example the middle stable reactor temperature is in the ranges of 222 to 263°C, 219 to 265°C, 218 to 271°C, and 218 to 272°C for recycle ratio of 0, 0.20, 0.50, and 0.70, respectively.

Furthermore, the middle stable exist at a range of inlet initiator concentration from 7.3 to 7.6 ppm, 7.1 to 7.8 ppm, 6.8 to 8.1 ppm, and 6.7 to 8.3 ppm for recycle ratio of 0, 0.20, 0.50, and 0.70 respectively. As shown in Figure 4.28 and 4.29, the lower stable branch for all recycle ratios correspond to monomer conversion and conversion to polymer values below 3% while the middle stable branch is the normal operating branch and covers conversions in the range of 9 to 14% for no recycle case and 10 to 15%, 12 to 20%, and 15 to 26% for the cases of recycle ratio of 0.20, 0.50, and 0.70, respectively. The upper unstable branch is characterized by increasing consumption of monomer by decomposition reactions. It is along this branch that conversion to polymer reaches a peak and drops to zero as the decomposition products become more and more abundant. This unstable branch represents the transition to a final stable branch that appears at a much higher reactor temperature and corresponds to complete reactor runaway. The polymer selectivity relative to these branches is also presented and shown in Figure 4.30.

Figure 4.27 Steady-state reactor temperature is shown as a function of initiator feed
concentration with ethylene decomposition reactions included, 0%
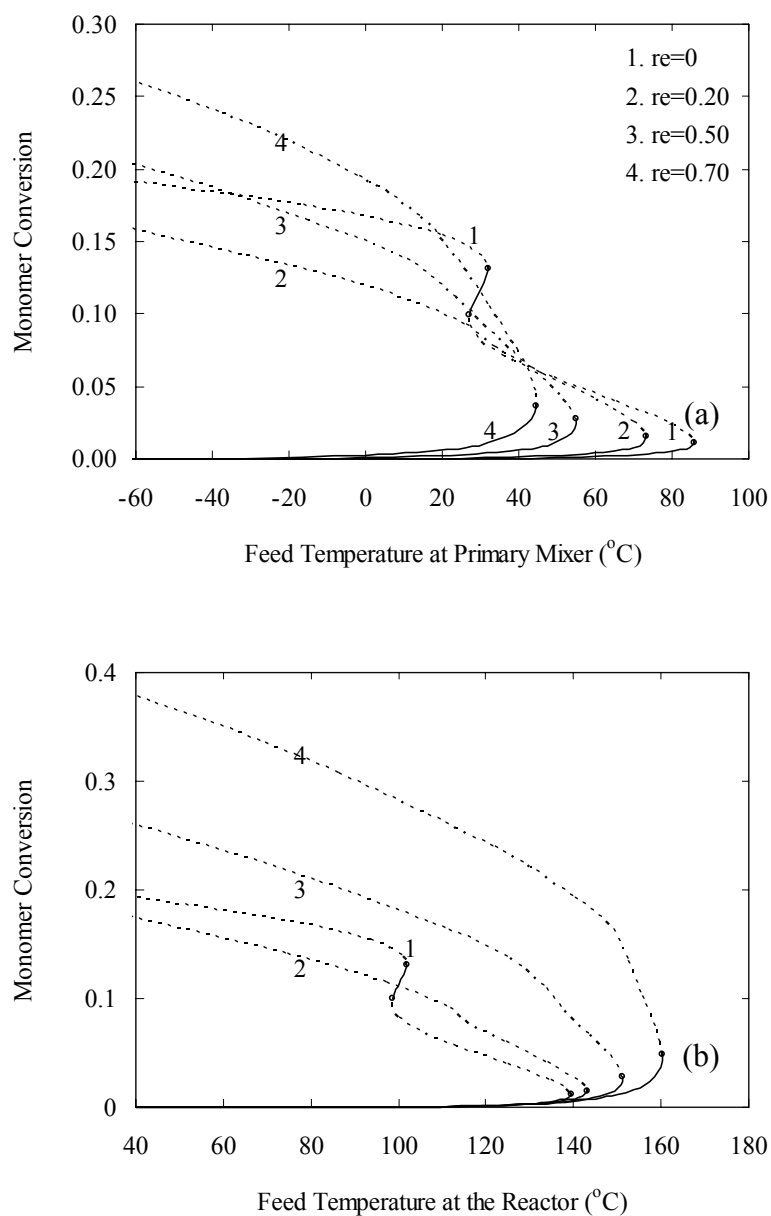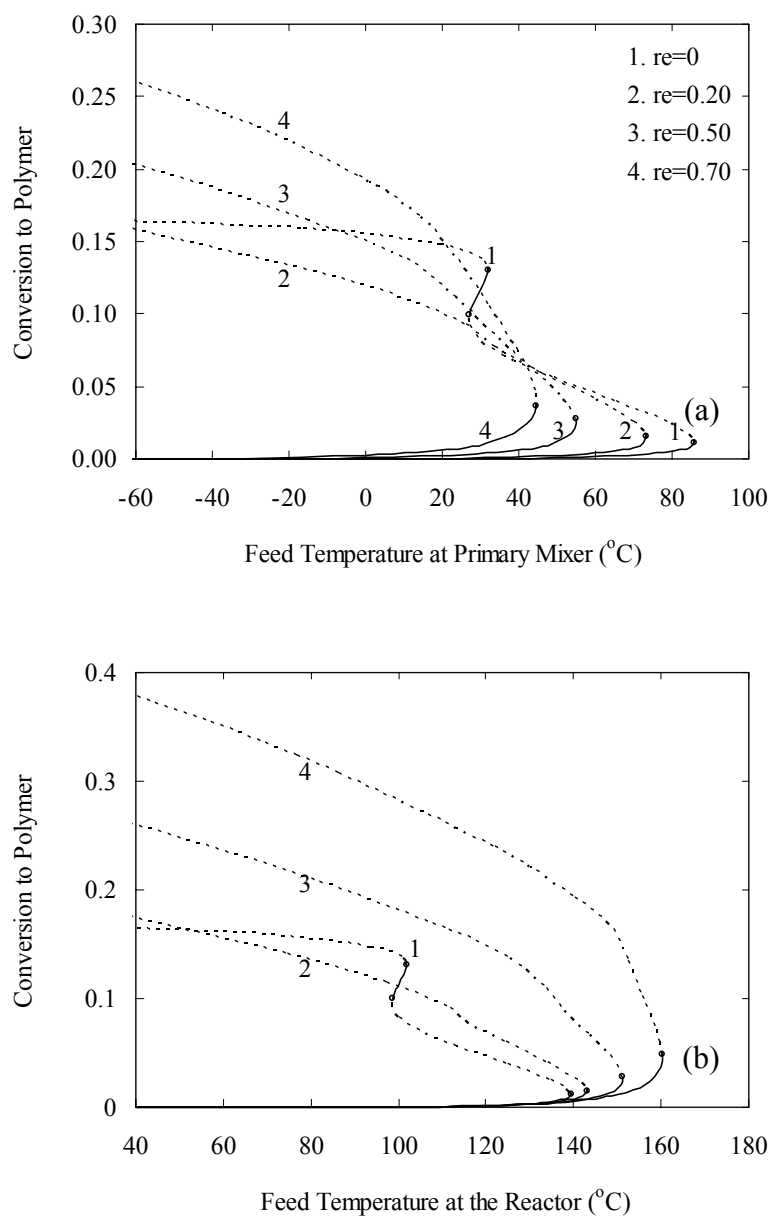acetylene separation and without the effect of acetylene decomposition
at feed temperature at primary mixer of $30^{\circ}C$.

Figure 4.28 Steady-state monomer conversion is shown as a function of initiator

feed concentration with ethylene decomposition reactions included,

0% acetylene separation and without the effect of acetylene

decomposition at feed temperature at primary mixer of 30°C.
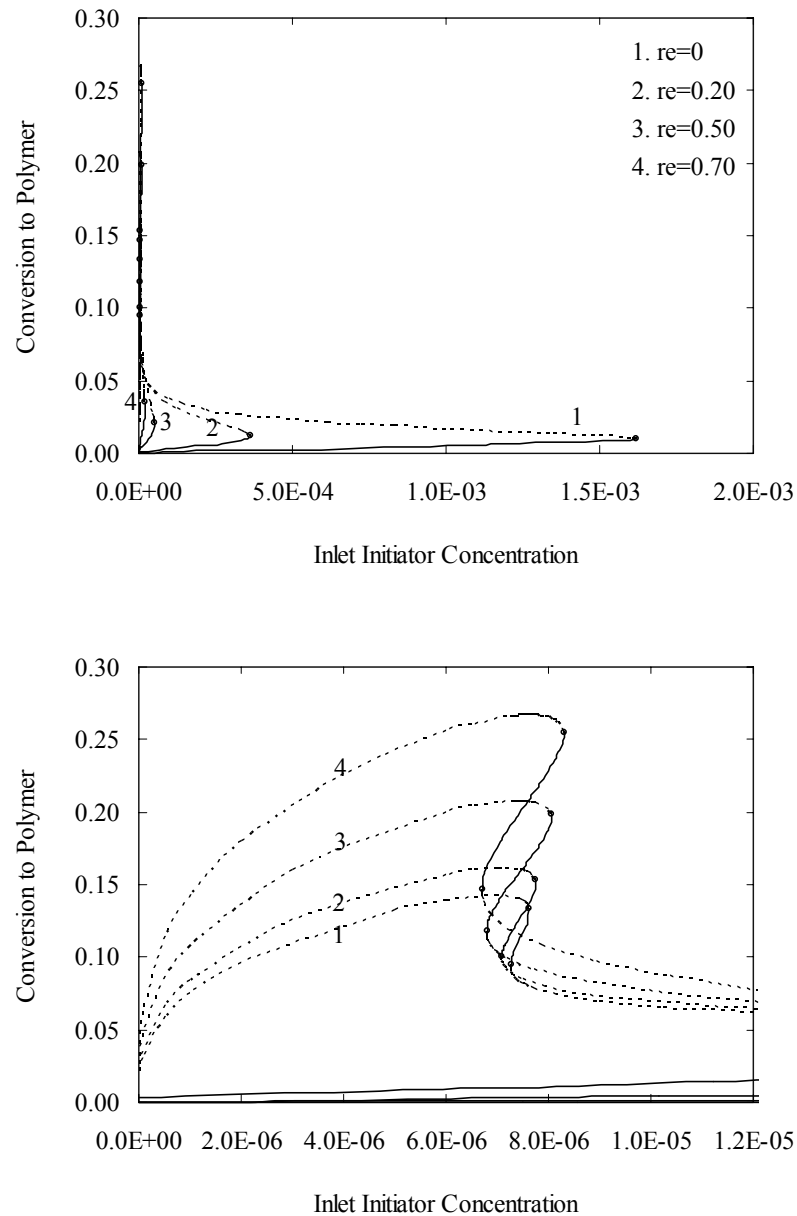
Figure 4.29 Steady-state conversion to polymer is shown as a function of initiator

feed concentration with ethylene decomposition reactions included,

0% acetylene separation and without the effect of acetylene

decomposition at feed temperature at primary mixer of 30°C.
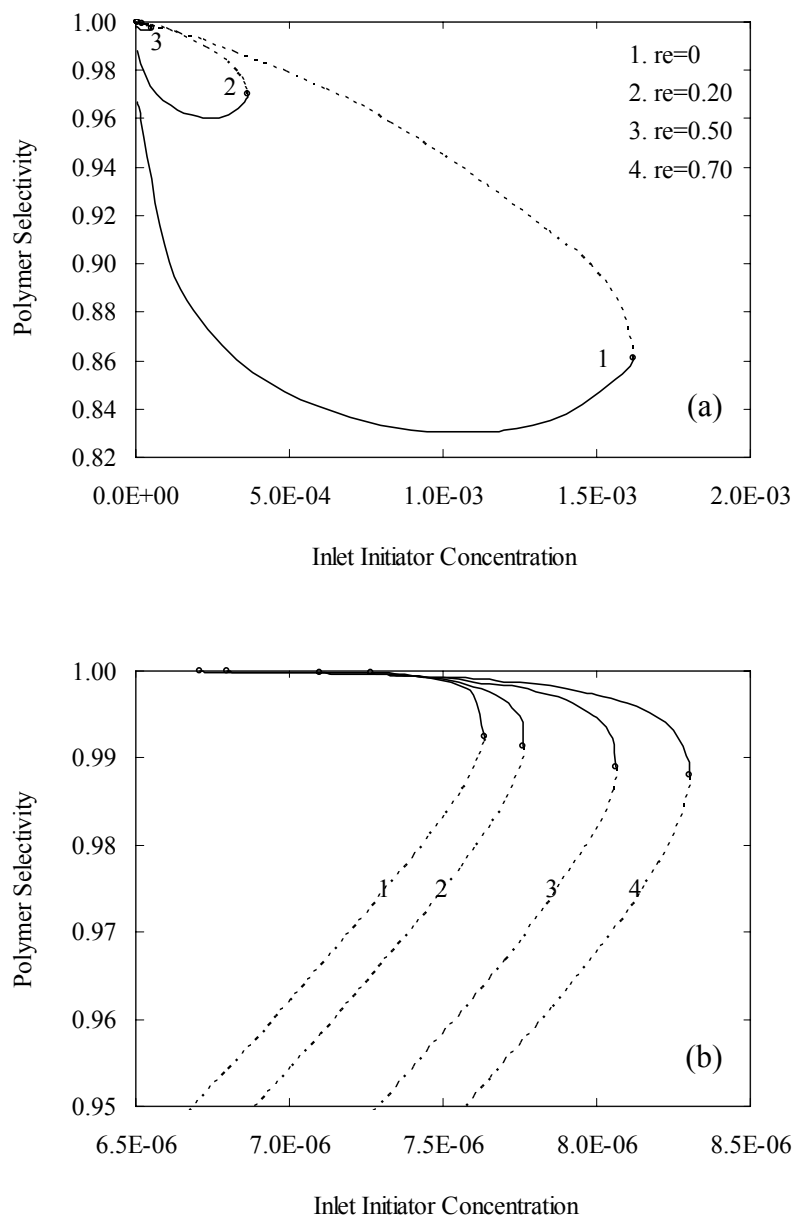
Figure 4.30 Polymer selectivity is shown as a function of initiator feed concentration with ethylene decomposition reactions included, 0% acetylene separation and without the effect of acetylene decomposition at feed temperature at primary mixer of 30°C. (a) For lower stable and lower unstable branches, (b) for middle stable and upper unstable branches.

In order to obtain the better knowledge on the system, the steady-state of reactor temperature, monomer conversion, and conversion to polymer with ethylene and acetylene decompositions and 0% of acetylene separation is considered as a function of inlet initiator concentration are shown in Figure 4.31, 4.32 and 4.33 respectively. There are an unstable branch at higher reactor temperatures and a lower stable branch at lower reactor temperatures. The behavior of the lower stable branch is similar to the behavior of without acetylene decomposition because very small amount of decomposition products are generated at low reactor temperature. At higher reactor temperatures, more acetylene is produced and recycled back to the inlet of the reactor, decompose into free-radical and induce runaway reactions. From these observations, it can be concluded that the middle stable branch can reappear if all acetylene can be separated from the recycle stream.
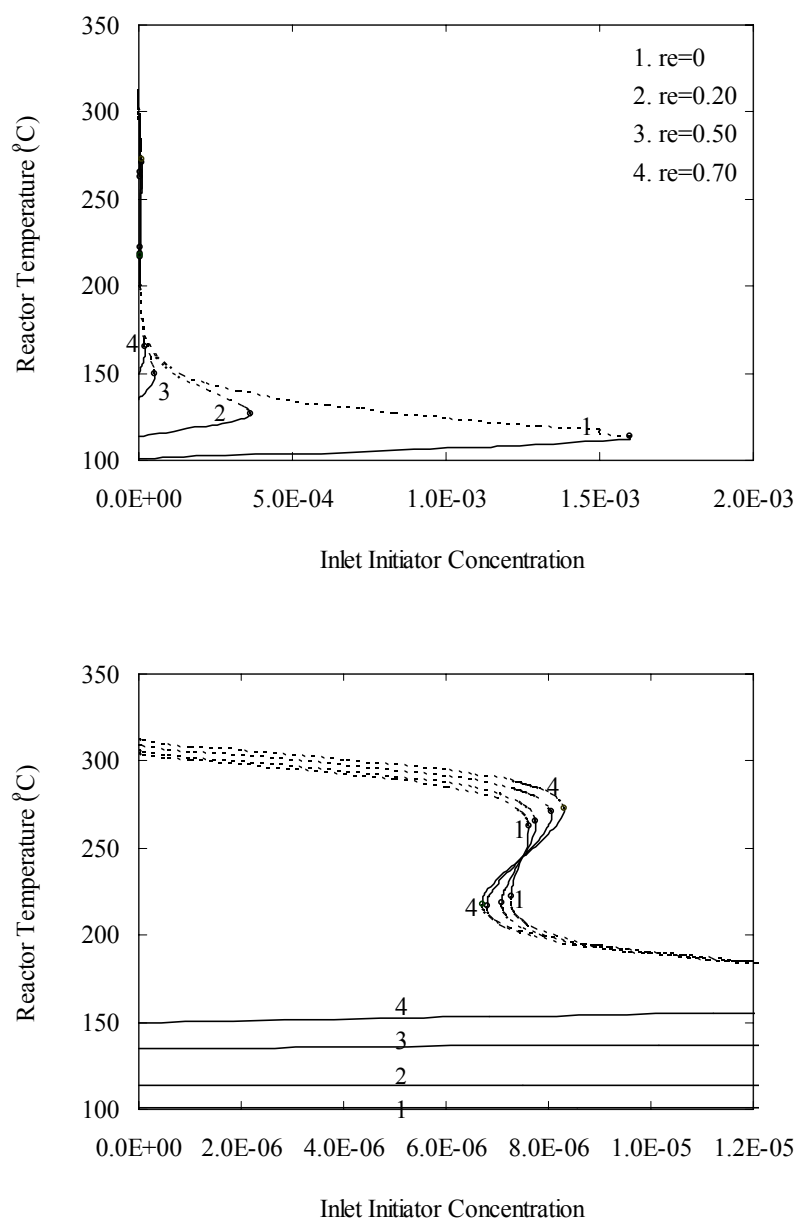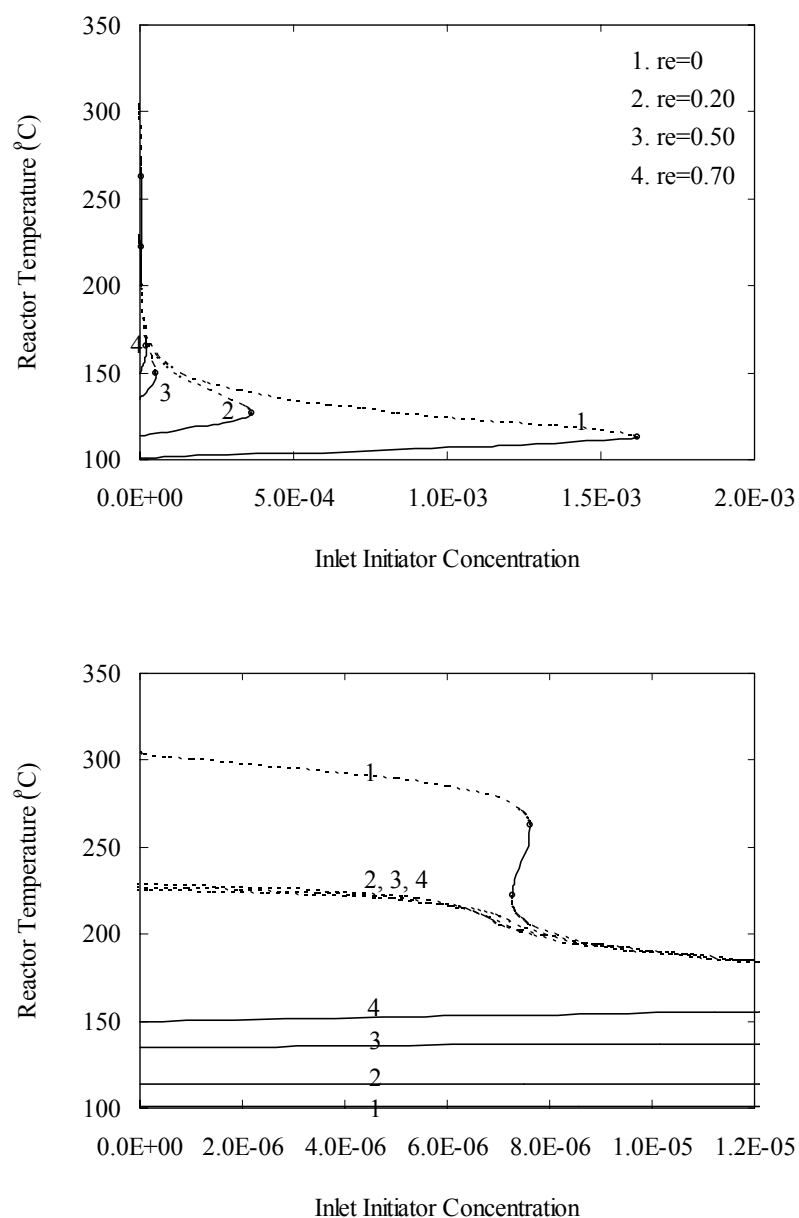
Figure 4.31 Steady-state reactor temperature is shown as a function of initiator feed concentration with ethylene decomposition reactions included, 0% acetylene separation and with the effect of acetylene decomposition at feed temperature at primary mixer of 30°C.
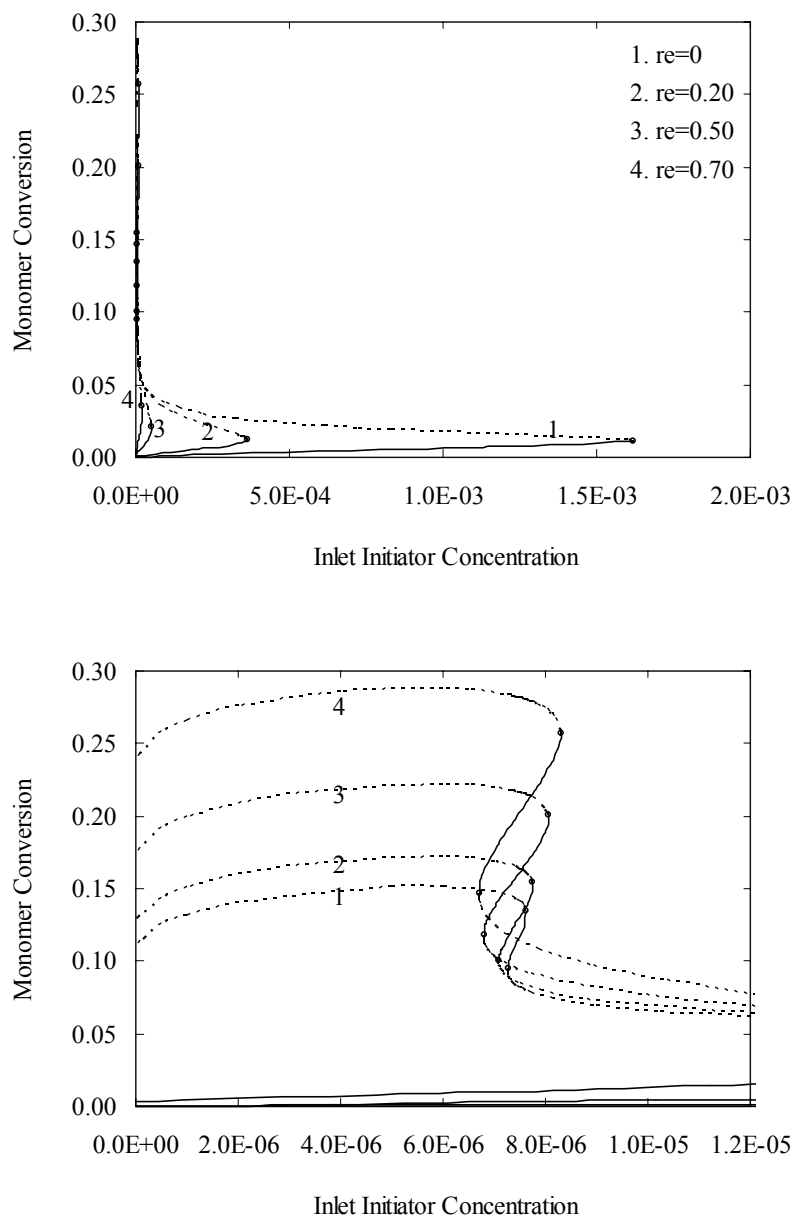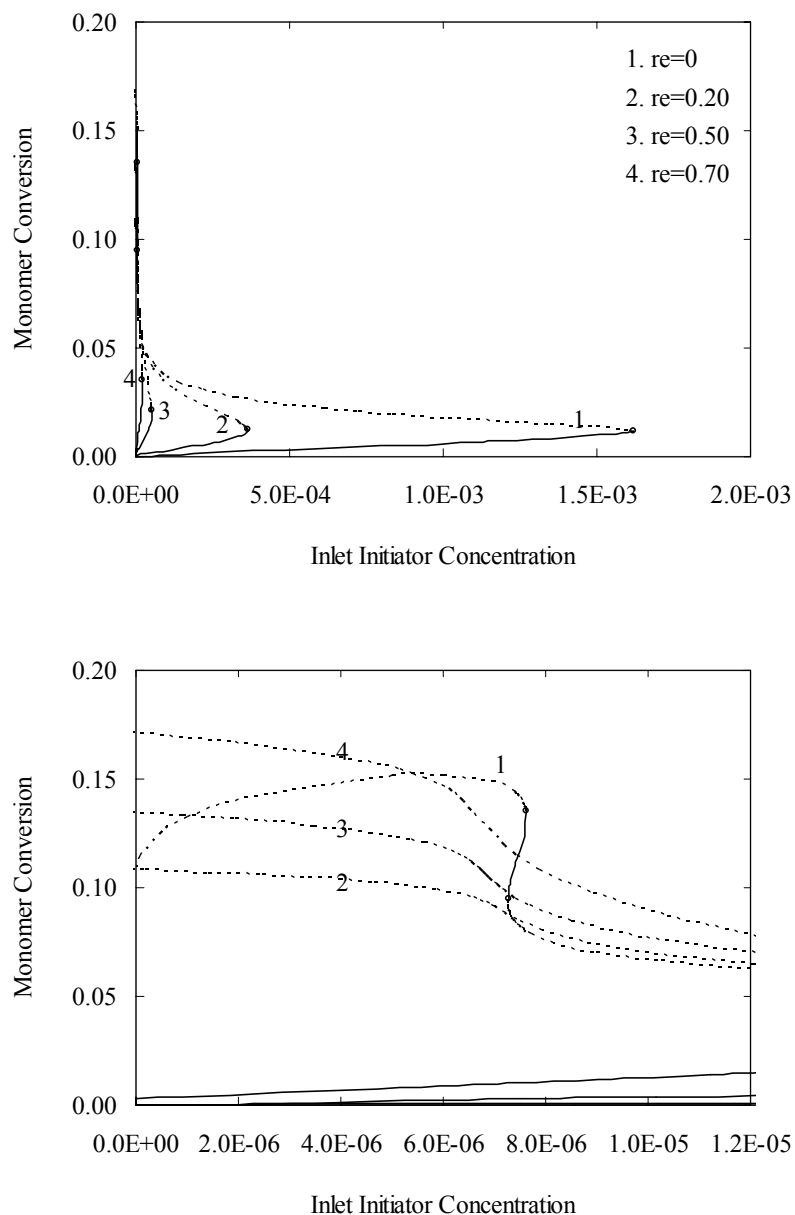
Figure 4.32 Steady-state monomer conversion is shown as a function of initiator

feed concentration with ethylene decomposition reactions included,

0% acetylene separation and with the effect of acetylene

decomposition at feed temperature at primary mixer of 30°C.
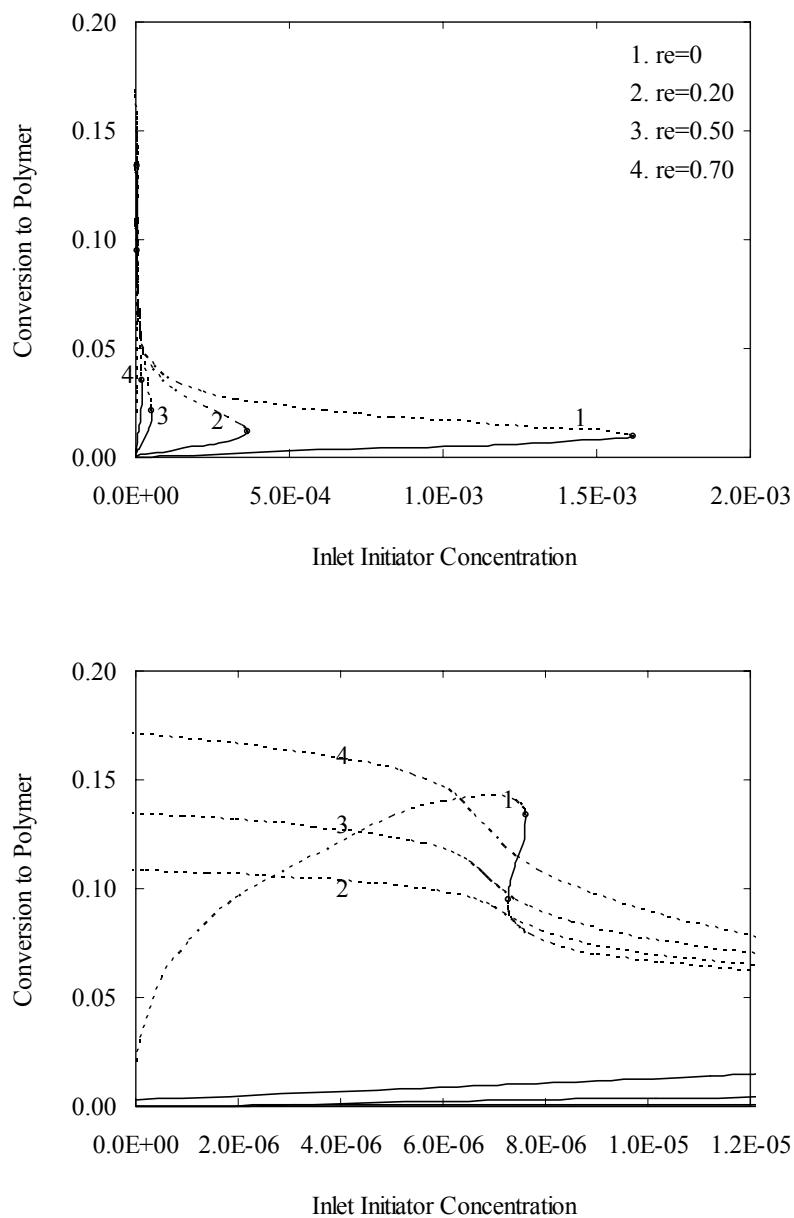
Figure 4.33 Steady-state conversion to polymer is shown as a function of initiator

feed concentration with ethylene decomposition reactions included,

0% acetylene separation and with the effect of acetylene

decomposition at feed temperature at primary mixer of $30^{\circ}C$.

The bifurcation behavior of inlet initiator concentration and feed temperature on the system are similar and good agreement is observed with the simulation results from Zhang et al. (1996). During LDPE production, it is often necessary to change the reactor operating conditions to produce a different grade polymer. The reactor stability may become an important issue during this transition period since reactor temperature can significantly affect the polymer molecular structure and subsequently the physical properties. Increasing recycle ratio can yield the larger area of stable steady-state because the reactor temperature range at the steady states is wider. Consequently, operating at high recycle ratio can produce a variety of different polymer. However, at higher recycle ratio, larger amount of acetylene would be produced and this phenomenon could lead to the disappearance of middle stable branch. Nevertheless, this would not be a problem if all acetylene is separated from the recycle.

CHAPTER V

CONCLUSIONS AND RECOMMENDATIONS

5.1 Conclusions

A comprehensive mathematical model of an industrial LDPE plant is developed to analyze the non-linear behavior when ethylene and acetylene decomposition kinetics are considered. The effect of bifurcation parameters such as feed temperature, residence time, and inlet initiator concentration on reactor temperature and overall conversion are also investigated. The plant consists of the CSTR, mixers, compressors, heat exchangers, and separator. The overall model formulation comprises the differential and algebraic equations. The steady-state model is solved numerically with Newton and the reactor behavior is examined by constructing the bifurcation diagram. For dynamic simulation, the unsteady state modeling equation as a set of differential algebraic equations are solved by method of fourth-order Runge-Kutta-Fehlberg in MATLAB. The validity of the eigenvalue technique in which the eigenvalue is calculated and analyzed for the stability steady-state solution is proved with the numerical solution obtained from the unsteady state model.

5.1.1 Parameters estimation

The kinetic parameters for polymerization and decomposition reaction are taken from the literature. The rate constants of ethylene decomposition were evaluated based on ethylene decomposition kinetic scheme proposed by the other

researchers. However, the rates equations for decomposition products proposed in literature were erroneous. To overcome this obstacle, an estimation of the kinetic parameters for ethylene decomposition is conducted in this thesis. The results from the present model are compared with the experimental results, and the good agreement is observed.

5.1.2 Model Validation

The present model is validated by comparing to the model of Zhang et al. (1996). It has been found that good agreement is observed by studying the bifurcation behavior of feed temperature and residence time on the reactor for stand-alone CSTR.

5.1.3 Effect of Ethylene Decomposition

Inclusion of ethylene decomposition reactions in the model is important. It can be seen that a maximum of five steady states are possible with three stable (upper, middle, lower) branches and two unstable (upper, lower) branches when the ethylene decomposition reactions is included. The middle stable branch is the desired operating conditions because of its stability and acceptable conversion.

5.1.4 Ethylene and Acetylene Decomposition with Recycle

At low conversion, carbon, methane, ethane and acetylene would be present as the product of ethylene decomposition (Watanabe et al., 1972). The ethylene with its impurities, acetylene and other gases, can be recycled to the feed. Because Zhang and coworkers reported that acetylene can decompose into free radicals and induce runaway reaction, the model with both ethylene and acetylene decomposition is developed and solved numerically. It can be seen that when both ethylene and acetylene decomposition is considered, the effect becomes more

significant. The acetylene decomposition would unstabilize the reactor and the undersirable results occur; the middle stable steady state disappeared completely even at low recycle ratio (0.20). From further investigation, it is found that the high efficiency (100%) of acetylene separation yields the much improved bifurcation, middle stable steady states. However, low efficiency acetylene separation (even at 95%) could not remediate the problems.

5.1.5 The Effect of Bifurcation Parameters

During LDPE production, it is often necessary to change the reactor operating conditions to produce the different grade polymer since reactor temperature can significantly affect the polymer molecular structure and subsequently the physical properties. As the recycle ratio increases, the range of reactor temperature at the stable steady-state of is wider. Consequently, operating at high recycle ratio can produce various different grade polymer and adequately high overall conversion. However, at high recycle ratio operation, higher amount of acetylene can be sometime produced and this can lead to the disappearance of middle stable branch. There would not be any problems if all acetylene can be efficiently separated and there is no impurity in the feed.

The reactor bifurcation behavior at different inlet initiator concentration and different feed temperature are similar and good agreement with the simulation results reported by Zhang et al. (1996) is reached. Additionally, middle stable steady state branch can be obtained if a proper control system is in place. The reactor temperature and the overall conversions as the function of operating parameters (e.g., feed temperature at primary mixer and inlet initiator concentration) for the middle stable branch are shown in Table 5.1. It found that the reactor temperature and overall

conversions could be obtained in an economical reasonable region of operation commercial plant.

Table 5.1 Ranges of the middle stable steady state branch of bifurcation parameters on the reactor temperature and overall conversions.

Mass recycle ratio	Reactor temperature (^{o}C)	Overall monomer conversion (%)	Overall conversion to polymer (%)	Feed temperature at primary mixer (^{o}C)	Inlet initiator concentration (ppm)
0	220-260	10-13	10-13	27-32	7.5
0.2	220-265	11-15	11-15	25-34	7.5
0.5	220-270	13-20	13-20	23-37	7.5
0.7	220-275	16-25	16-25	23-40	7.5
0	222-263	9-14	9-14	30	7.3-7.6
0.2	219-265	10-15	10-15	30	7.1-7.8
0.5	218-271	12-20	12-20	30	6.8-8.1
0.7	218-272	15-26	15-26	30	6.7-8.3

A numerical bifurcation and stability analysis are performed to predict the region of stable operation and indicate safe operating limits for certain variables at typical conditions. The models are useful for the design of optimal reactor operating conditions and reactor controls to obtain maximum polymer productivity.

5.2 Recommendations

5.2.1 In this thesis, both the polymerization and decomposition reactions were modeled and the bifurcation behavior of the reactor temperature and overall conversion were investigated. Commonly, LDPE operation at high temperature has only a small stable region without feedback control (Zhang et al., 1996); therefore, a feedback controller was used to regulate reactor temperature for stand-alone reactor by manipulating the inlet concentration of initiator. The future research should focus on analyzing a feedback controller of LDPE CSTR-separator-recycle in order to obtain stable operation at high temperature.

5.2.2 Although it is well known that other mechanisms, such as chain transfer to (monomer, agents, and polymer), β-scission, and back-biting, also contribute significantly to the weight- and number-distribution of polymer (Hutchinson and Fuller, 1998), those mechanisms have little or no net effect on the total monomer conversion (Fox and Tsai, 1996) and thus have not been included in this thesis. Therefore, the future attempt on combining the other mechanisms with the model should be beneficial for prediction of physical properties of polymer.

5.2.3 The reactor operates adiabatically at relatively high temperature and at extremely high pressure. Because of the high rate of reaction under these conditions, the reactor residence times must be kept very short to limit the temperature rise in the reactor and the reactor cannot practically be assumed perfectly mixed. The coupling of the current model with the effect of imperfect mixing should be useful.

REFERENCES

Albert, J. and Luft, G. (1998). Runaway phenomena in the ethylene/vinylacetate copolymerization under high pressure. **Chem. Eng. & Proc.** 37: 55-59.

Auger, J. and Nguyen, L. (2001). Using polymer characterization techniques to predict LDPE resin suitability for extruded foam applications. **Journal of Cellular Plastics.** 37(6): 485-499.

Bonsel, H. and Luft, G. (1995). Safety studies on the explosive degradation of compressed ethene. **Chem. Ing. Tech.** 67: 862.

Busch, M. and van Boxtel, H. C. M. (1998). Modeling of kinetics and polymer properties in high-pressure free-radical polymerizations. **DECHEMA Monogr**. 134: 49-59.

Chan, W., Gloor, P. E., and Hamielec, A. E. (1993). A kinetic model for olefin polymerization in high pressure autoclave reactors. **AIChE J.** 39: 111-126.

Chen, C. H., Vermeychuk, J. G., Howell, J. A., and Ehrlich, P. (1976). Computer model for tubular high-pressure polyethylene reactor. **AIChE J.** 22(3): 463-469.

Costas, P. B., Ramanathan, S., and Brown, J. (2002). Physical properties, reactor modeling, and polymerization kinetics in the low-density polyethylene tubular process. **Ind. Eng. Chem. Res.** 41: 1017-1030.

Doedel, E. (1986). **AUTO: Software for Continuation and Bifurcation Problems in Ordinary Differential Equations**. Tech. Rep., Caltech, Pasadena.

Doedel, E., Champneys, A. R., Fairgrieve, T. F., Kuznetsov, Y. A., Sandstede, B., and Wang, X. (1997). **AUTO 97: Continuation and bifurcation software for ordinary differential equations–user's guide**. Montreal, Concordia University.

Ehrlich, P. and Mortimer, G. A. (1970). Fundamentals of the free-radical polymerization of ethylene. **Adv. Polym. Sci.** 7: 386-448.

Fogler, H. S. (1999). **Elements of Chemical Reaction Engineering**. Prentice Hall International Series in the Physical and Chemical Engineering Sciences, 3ed.

Fox, R. O. and Tsai K. (1996). PDF modeling of turbulent-mixing effects on initiator efficiency in a tubular LDPE reactor. **AIChE J.** 42(10): 2926-2939.

Freitas Filho, I. P., Biscaia JR E. C., and Pinto, J. C. (1994). Steady-state multiplicity in continuous bulk polymerization reactors–a general approach. **Chem. Eng. Sci.** 49: 3745-3755.

Gemassmer, A. M. (1978). Autoclave process for the high pressure polymerization of ethylene. **Erdol Kohle-Erdgas-petrochem**. 31: 221.

Häfele, M., Kienle, A., Boll, M., Schmidt, C.-U., and Schwibach, M. (2005). Dynamic simulation of a tubular reactor for the production of low-density polyethylene using adaptive method of lines. **Journal of Computational and Applied Mathematics**. 183: 288-300.

Häfele, M., Kienle, A., Boll, M., and Schmidt, C.-U. (2006). Modeling and analysis of a plant for the production of low density polyethylene. **Computers and Chemical Engineering**. 31: 51-65.

Ham, J. Y. and Rhee, H.-K. (1996). Modeling and control of an LDPE autoclave reactor. **J. Proc. Cont.** 6(4): 241-246.

Hamer, J. W., Akramov, T. A., and Ray, W. H. (1981). The dynamic behavior of continuous polymerization reactors–II. nonisothermal solution homopolymerization and copolymerization in a CSTR. **Chem. Eng. Sci.** 36: 1897-1914.

Hutchinson, R. A. and Fuller, R. E. (1998). Modeling and measurement of high pressure ethylene polymerization long-chain branching and molecular weight distributions. **DECHEMA Monogr.** 134: 35–47.

Kiss, A. A., Bildea, C. S., Dimian, A. C., andIedema, P. D. (2002). State multiplicity in CSTR-separator-recycle polymerization systems. **Chem. Eng. Sci.** 57: 535-546.

Kuznetov, Y. A. (1998). **Content-Integrated Environment for Analysis of Dynamical Systems**. Moscow.

Kwag, B. G. and Choi, K. Y. (1994). Effect of initiator characteristic on high-pressure ethylene polymerization in autoclave reactors. **Ind. Eng. Chem. Res.** 33: 211-217.

Lee, L., Ham, J. Y., Chang, K. S., Kim J. Y., and Rhee, H.-K. (1999). Analysis of an LDPE compact autoclave reactor by two-cell model with backflow. **Polym. Eng. & Sci.** 39: 1279-1290.

López-Negrete de la Fuente, R., Lopez-Rubio, J., Flores-Tlacuahuac, A., and Saldivar-Guerra, E. (2006). Steady-state multiplicity behavior analysis of a high-impact polystyrene continuous stirred tank reactor using a bifunctional initiator. **Ind. Eng. Chem. Res.** 45: 1689-1707.

Marini, L. and Georgakis, C. (1984). Low-density polyethylene vessel reactors part I: steady state and dynamic modeling. **AIChE J.** 30: 401-408.

Melo, P. A., Sampaio, J. G., Biscaia Jr., E. C., and Pinto, J. C. (2001). Periodic oscillations in continuous free-radical solution polymerization reactors–a general approach. **Chem. Eng. Sci.** 59: 3469-3482.

Orbey, H., Costas, P. B., and Chen, C.-C. (1998). Equation of state modeling of phase equilibrium in the low-density polyethylene process: the Sanchez-Lacombe, statistical associating fluid theory, and polymer-Soave-Redlich-Kwong equations of state. **Ind. Eng. Chem. Res.** 37: 4481-4491.

Pinto, J. C. (1995). The dynamic behavior of continuous solution polymerization reactors–a full bifurcation analysis of a full scale copolymerization reactor. **Chem. Eng. Sci.** 50: 3455-3475.

Pinto, J. C. and Ray, W. H. (1995a). The dynamic behavior of continuous solution polymerization reactors–vii. Experimental study of a copolymerization reactor. **Chem. Eng. Sci.** 50: 715-736.

Pinto, J. C. and Ray, W. H. (1995b). The dynamic behavior of continuous solution Ppolymerization reactors–viii. A full bifurcation analysis of a lab scale copolymerization reactor. **Chem. Eng. Sci.** 50: 1041.

Pushpavanam, S., and Kienle, A. (2001). Nonlinear behavior of an ideal reactor separator network with mass recycle. **Chem. Eng. Sci.** 56: 2837-2849.

Ray, W. H. and Villa, C. M. (2000). Nonlinear dynamics found in polymerization processes–a review. **Chem. Eng. Sci.** 55: 275-290.

Read, N. K., Zhang, S. X., and Ray, W. H. (1997). Simulations of a LDPE reactor using computational fluid dynamics. **AIChE J.** 43(1): 104-117.

Russo, L. P. and Bequette, B. W. (1998). Operability of chemical reactors: multiplicity behavior of a jacketed styrene polymerization reactor. **Chem. Eng. Sci.** 53: 27-45.

Schmidt, A. D., Clinch, A. B., and Ray, W. H. (1984). The dynamic behavior of continuous polymerization reactors–iii. An experimental study of multiple steady states in solution polymerization. **Chem. Eng. Sci.** 39: 419.

Teymour, F. and Ray, W. H. (1989). The Dynamic behavior of continuous solution polymerization reactors–iv. Dynamic stability and bifurcation analysis of an experimental reactor. **Chem. Eng. Sci.** 44: 1967-1982.

Topalis, E., Pladis, P., and Kiparissides, C. (1996). Dynamic modeling and steady-state multiplicity in high pressure multizone LDPE autoclaves. **Chem. Eng. Sci.** 51: 2461-2470.

Verazaluce-García, J. C., Flores-Tlacuahuac, A., and Saldívar-Guerra, E. (2000). Steady-state nonlinear bifurcation analysis of a high-impact polystyrene continuous stirred tank reactor. **Ind. Eng. Chem. Res.** 39: 1972-1979.

Watanabe, H., Kurihara, K., and Takehisa, M. (1972). The explosive decomposition of ethylene**. Pro. Pacific Chemical Engineering Congress (PACHEC), AIChE, New York**, p. 225-232.

Whiteley, K. S., Heggs, T. G., Koch, H., Mawer, R. L., and Immel, W. (1998). **Ullmann's Encyclopedia of Industrial Chemistry, chapter Polyolefins-Polyethylene**. WILEYVCH, D-69451 Weinheim, Germany, sixth edition.

Yang, W. Y., Cao, W., Chung, T-S., and Morris, J. (2005). **Applied Numerical Methods Using MATLAB**. Jhon Wiley & Sons, Inc.

Zhang, S. X., Read, N. K., and Ray, W. H. (1996). Runaway phenomena in low-density polyethylene autoclave reactor. **AIChE J.** 42: 2911-2925.

Zhang, S. X. and Ray, W. H. (1997). Modeling of imperfect mixing and its effects on polymer properties. **AIChE J.** 43: 1265-1277.

APPENDIX A

NEWTON METHOD MATLAB ROUTINE

NEWTON METHOD MATLAB ROUTINE

The MATLAB routine for Newton method for a system of non-linear equations (Yang et al., 2005)

```
function [x,fx,xx] = newtons(f,x0,TolX,MaxIter,varargin)
%newtons.m to solve a set of nonlinear eqs f1(x)=0, f2(x)=0,..
%input:   f  =1^st-order vector ftn equivalent to a set of equations
%          x0= the initial guess of the solution
%      TolX = the upper limit of |x(k) - x(k − 1)|
% MaxIter  = the maximum # of iteration
%output:  x  = the point which the algorithm has reached
%          fx   = f(x(last))
%          xx   = the history of x
h = 1e-6; TolFun = eps; EPS = 1e-9;
fx = feval(f,x0,varargin{:});
Nf = length(fx); Nx = length(x0);
if  Nf ~= Nx, error('Incompatible dimensions of f and x0!'); end
if  nargin < 4, MaxIter = 100; end
if  nargin < 3, TolX = EPS; end
xx(1,:) = x0(:). ';  %Initialize the solution as the initial row vector
```

```
%fx0 = norm(fx);                                    %(1)

for k = 1:  MaxIter

   dx = -jacob(f,xx(k,:),h,varargin{:})\fx(:);   %-[dfdx]^-1*fx

   %for l = 1:3 %damping to avoid divergence       %(2)

   %dx = dx/2;                                      %(3)

   xx(k + 1,:) = xx(k,:) + dx.';

   fx = feval(f,xx(k + 1,:),varargin{:}); fxn = norm(fx);

   % if  fxn < fx0, break; end                      %(4)

   %end                                             %(5)

   if fxn < TolFun | norm(dx) < TolX, break; end

   %fx0 = fxn;                                      %(6)

end

x = xx(k + 1,:);

if  k == MaxIter, fprintf('The best in %d iterations\n',MaxIter), end

function g = jacob(f,x,h,varargin) %Jacobian of f(x)

if nargin < 3, h = 1e-6; end

h2 =2*h; N = length(x); x = x(:).'; I = eye(N);

for  n = 1:N

   g(:,n) = (feval(f,x + I(n,:)*h,varargin{:}) ...

            -feval(f,x - I(n,:)*h,varargin{:}))'/h2;

end
```

For example, let's use this routine to solve the following system of non-linear equations

$$x_1^2 + 4x_2^2 = 5 \tag{A.1}$$

$$2x_1^2 - 2x_1 - 3x_2 = 2.5 \tag{A.2}$$

In order to so, we should first rewrite these equations into a form like Eqs. (2.31-2.33) as

$$f_1(x_1, x_2) = x_1^2 + 4x_2^2 - 5 = 0 \tag{A.3}$$

$$f_2(x_1, x_2) = 2x_1^2 - 2x_1 - 3x_2 - 2.5 = 0 \tag{A.4}$$

and convert it into a MATLAB function defined in an M-file, say, "f_kom1.m" as follows.

```
function y = f_kom1(x)
y(1) = x(1)*x(1)+4*x(2)*x(2)-5;
y(2) = 2*x(1)*x(1)-2*x(1)-3*x(2)-2.5;
```

Then, we type the following statements into the MATLAB command window:

```
>>x0 = [0.8 0.2]; x = newtons(@f_kom1, x0) %initial guess [0.8 0.2]
x = 2.0000    0.5000
```

APPENDIX B

USING MATLAB FOR ODEs

USING MATLAB FOR ODEs

Explore how MATLAB can be used to solve the following set of non-linear

ODEs from t = 0 to 20:

$$\frac{dx_1}{dt} = 1.2x_1 - 0.6x_1x_2 \qquad\qquad (B.1)$$

$$\frac{dx_2}{dt} = -0.8x_2 + 0.3x_1x_2 \qquad\qquad (B.2)$$

where $x_1 = 2$ and $x_2 = 1$ at $t = 0$.

before obtaining a solution with MATLAB, you must use a text processor to create an

M-file containing the right-hand side of the ODEs. This M-file will then be accessed

by the ODE solver [where $x_1 = x(1)$ and $x_2 = x(2)$]:

---

function dx = f_kom2(t, x)

dx=zeros(2,1);

dx(1) = 1.2*x(1)-0.6*x(1)*x(2);

dx(2) = -0.8*x(2)+0.3*x(1)*x(2);

---

we stored this M-file under the name: f_kom2.m.

Next, start up MATLAB, and enter the following commands to specify the

integration range and the initial conditions:

\>\> tspan = [0 20];

\>\> x0 = [2, 1];

the solver can then be invoked by

\>\>[t, x] = ode45(@f_kom2, tspan, x0);

This command will then solve the differential equations in f_kom2.m over the range defined by tspan using the initial conditions found in x0. The results can be displayed by simply typing

\>\> plot(t, x)
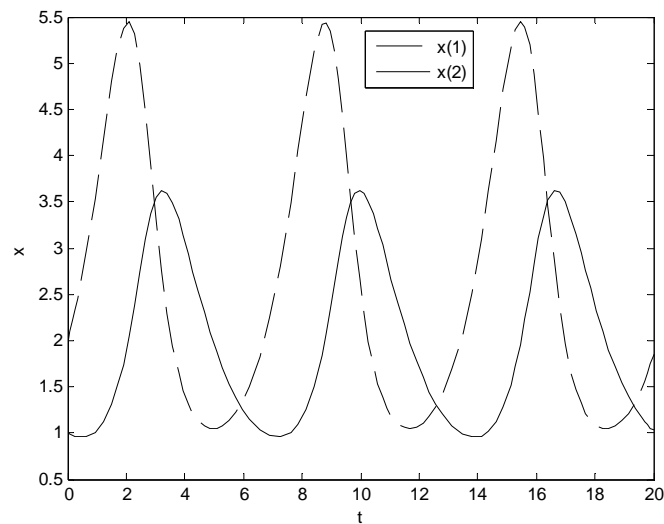
which yield Figure A.1.

Figure B.1 Solution of a set of ODEs with MATLAB.

BIOGRAPHY

Mr. Nikom Klomkliang was born on Saturday the 6th of March 1982, in Nongbua Sub-District, Thatoom District, Surin Province of Thailand. He started his primary education at Bannongbua Mitraphap 85 Primary School, Nongbua Sub-District, Thatoom District, Surin Province of Thailand in 1989 where he completed his primary education in 1995. Between 1995-2001, he studied at Thatoom Prachasermwith High School, Thatoom District, Surin Province of Thailand for his secondary education. He then moved to the famous Suranaree University of Technology (SUT) for his university education. During his bachelor degree study, he participated in the Cooperative Education Program for four months in the field of chemical engineering at the organization of Thai Citric Acid Co., Ltd. with topic of the monitoring resins saturated points and decreasing water usage in ion-exchange regeneration. In 2005, he graduated with a bachelor degree in chemical engineering from SUT. After his graduation, he has received scholarship for a research assistant at SUT to study for the master degree in chemical engineering at SUT since 2005.